UNIVERSITY OF CALIFORNIA
SANTA CRUZ

ENERGETICS OF REST AND LOCOMOTION IN DIVING MARINE MAMMALS:

NOVEL METRICS FOR PREDICTING THE VULNERABILITY OF THREATENED CETACEAN, PINNIPED, AND SIRENIAN SPECIES

A dissertation submitted in partial satisfaction
of the requirements for the degree of

DOCTOR OF PHILOSOPHY

in

ECOLOGY AND EVOLUTIONARY BIOLOGY

By
Jason Solouki Wolcott John

September 2020

The Dissertation of Jason S. John
is approved:

_____
Professor Terrie M. Williams, Chair

_____
Professor Peter T. Raimondi

_____
Professor Daniel P. Costa

_____
Professor Ari S. Friedlaender

_____
Quentin Williams
Vice Provost and Dean of Graduate Studies

TABLE OF CONTENTS

LIST OF TABLES

LIST OF FIGURES

ABSTRACT

Energetics of rest and locomotion in diving marine mammals:

Novel metrics for predicting the vulnerability of threatened cetacean, pinniped, and sirenian species

By Jason S. John

Each year, marine mammals are exposed to increasing levels of anthropogenic disturbance. Some disturbances, such as boat strikes and entanglement, directly impact animals through injuries and mortality events. However, indirect effects from disturbances including over-fishing, noise and environmental pollution, declining sea ice cover, and changes in coastal habitats can have significant, though less apparent, impacts as well. These can affect both individuals and populations through declining prey availability, decreased reproductive and juvenile success, declines in body-condition, and increased mortality. Unfortunately, as a result of their cryptic lifestyle, it is difficult to measure the impact of these disturbances on many marine mammal species or predict how they will affect individuals or populations in the future. A better understanding of both maintenance and locomotor energetic demands for these species is needed to quantify the impacts of these disturbances, model the future effects, and predict the capacity of these species to adapt or respond.

Using open-flow respirometry and submersible accelerometers, I undertook a comparative physiological study examining four marine mammal species from three different groups. In **Chapter 1**, I studied the interaction between maintenance and

locomotor costs in two coastal marine mammal species living in tropical and subtropical environments, West Indian manatees and Hawaiian monk seals. Although these warm water species exhibited a lower resting metabolic rate (RMR) than their cold-water relatives, I found that this does not confer an energetic advantage during locomotion for these species due to decreased metabolic variability. In **Chapter 2**, I measured RMR and locomotor costs in beluga whales as the first step towards creating a population consequences of disturbance model to aid conservation of the Cook Inlet beluga whale population. Despite variation in previous metabolic measurements of this species, the measured RMR in this study was consistent with the predicted value for similarly sized marine mammals. Analysis of locomotor costs also demonstrated a marked decrease in aerobic dive limit resulting from high speed swims commonly observed in marine mammals following disturbance. In **Chapter 3**, I examined and compared the relationships between locomotor metrics and the energetic cost of submerged swimming in Atlantic bottlenose dolphins, beluga whales, and West Indian manatees. This defined predictive relationships between oxygen consumption and multiple accelerometer metrics for continued collection of physiological data in both the study species and similar species in the wild.

Ultimately, these chapters provide novel information regarding the interaction between maintenance and locomotor costs in diving marine mammals, determined energetic costs to aid in the conservation of an endangered marine mammal population, and calibrated techniques that will allow future physiological study of marine mammals in the wild.

ACKNOWLEDGEMENTS

Throughout the course of this dissertation, I have been incredibly fortunate to work with a group of truly amazing people. First, I have to thank my graduate advisor, Terrie Williams, for taking a chance and bringing me into the lab. I am eternally grateful for the opportunities and experiences you have given me over the last 6 years. From my first time visiting the lab and meeting Puka and Primo (and all of my future human lab mates) to my first time stepping off the plane in Antarctica, your excitement and passion for "Science!" has been infectious and is a constant reminder of how fortunate I am to do this work. You have challenged me to look beyond the project at hand to think about the bigger picture, and you have taught me so much about being a scientist, educator, and advocate for the incredible animals we work with.

I am also grateful to my dissertation committee for all of your help in designing, modifying, adapting, and producing this dissertation. Pete Raimondi, I could not have navigated my way through comprehensive exams, dissertation committees, or (possibly most of all) statistics, without your help and guidance. Thank you for always being available to talk and provide advice. Even during the challenges our world has faced in the last few months, you have repeatedly taken the time to help me and I am grateful beyond words. Dan Costa, whether it was teaching me about the marine sloth during comprehensive exams or helping me understand pinniped evolution, your expertise in marine mammals has been an invaluable help in working with the many species in this study. Ari Friedlaender, as one of the first researchers Terrie introduced me to from outside the lab, you set the tone for collaboration that exemplifies this field. From

sharing data for comparison to showing me how these instruments are deployed in the field, you helped me design a study that will hopefully go far beyond this dissertation. Thank you all for your incredible insight and guidance.

This research would not have been possible without the trainers and volunteers at the Long Marine Laboratory, Mote Marine Laboratory and Aquarium, and the Georgia Aquarium. Traci Kendall, Beau Richter, Kat Boerner, Laura Denum, Dennis Christen, Katherine Flammer, thank you for leading the charge and keeping everything moving in the right direction day after day through training, troubleshooting, equipment building (and occasionally repair), teaching, planning, and so much more. I was constantly in awe of your knowledge, creativity, and compassion, and working with all of you was a highlight of my graduate career. The work you and your teams did went far beyond incredible and is directly responsible for the success of this research and the conservation applications in the future.

As fortunate as I have been to meet so many wonderful individuals over the last six years, I can honestly say that the ones I am the most grateful to are the amazing animals I had the privilege of working with. Puka, Primo, Kekoa, Hugh, Buffet, Maple, Qinu, Nunavik, Donley, and Rain, thank you for teaching us about yourselves and inspiring us each day. Working with you was, without questions, THE highlight of my graduate career and I am forever grateful to every one of you.

Over the last six years, my lab mates have been amazing teachers, research partners, and, most importantly, friends through the journey that is grad school. Traci

Kendall and Beau Richter, thank you for teaching, guiding, and working with me through some of the more “adventurous” moments of this crazy adventure. I learned so much from both of you and had an incredible time along the way! Along with Dr. Anthony Pagano, Dr. Nicole Thometz, Dr. Caleb Bryce, Dr. Shawn Noren, Dr. Robin Dunkin, Jessie Kendall-Barr, Lillian Carswell, Emily Nazario, and Doc Watson, I could not have asked for a better lab to be part of. Whether it was Nicole helping me figure out how to measure manatee respiration, Anthony helping me understand accelerometry, or every one of my lab mates helping me with everything from research to teaching, studying for comprehensive exams, grant applications, travel, and navigating conferences, they helped get me through every step and keep moving forward. In addition to my lab mates, I could not have survived grad school without the other incredible friends I’ve made along the way. Chris Law, Karen Tanner, Logan Palin, Luis Hückstädt, Rachel Holser, and Theresa Keates, thank you for making everything from the hours in the office to our Friday breaks so much fun.

I am also grateful to all of the faculty and staff both in and out of the EEB department for their help and guidance. Sarah Arantza Amador, Stephanie Zakarian, Judy Straub, and Debby Inferrera helped guide me through the maze that is grad school. Dr. Rita Mehta, Dr. Luis Hückstädt, Dr. Birgitte McDonald, Dr. Paul Ponganis, Dr. Cassondra Williams, Dr. Allyson Hindle, Dr. Randy Davis, and Dr. Lee Fuiman helped me learn and grow through teaching opportunities, field research, lab experience, and countless conversations about research, teaching, and life as a scientist.

The journey to this dissertation started a long time before graduate school, and I was fortunate to have two incredible teachers who really started me on this path. KJN Joe Soltis taught me from a young age that we should never stop being students. He instilled in me the drive to continuously improve and learn. To this day, KJN Joe continues to lead by example in showing that when it comes to learning, there is no end to the journey. Dr. Tracy Ruscetti first opened the world of research science to me as an undergrad. Dr Ruscetti showed me how exciting research could be, gave me the extra push I needed when I became complacent, and still teaches me something new every time we talk. I am incredibly lucky to still have these two remarkable teachers to learn from, and even more grateful to have them as friends.

Thank you to my family for being my constant friends and supporters. Mom, Dad, Alex, Mona, John, Eli, Joe, Sam, Daniel, Tracy, Martha, Terry, Kristy, Scott, Lauren, and Todd, thank you for supporting me when I chose to go back to school. Thank you, Mom and Dad, for being my first teachers and role models, and for constantly supporting and encouraging me through this journey. Thank you all for your messages and calls when I had to be away from home for months at a time and thank you for your patience as I would disappear into studying or research for weeks. I love you all and could not ask for a better family.

Finally, and most importantly, thank you Tamara Ford John, for everything. Your love, support, and encouragement mean the world to me. Thank you for standing by my side through all of the crazy ups and downs of the last eight years. Thank you for supporting me every day from applying to grad school through writing this

dissertation. Thank you for answering midnight calls from Antarctica and figuring out how to change our vacations when research travel was delayed. Thank you for letting me take over the table for three months when I was studying for comps and for getting me out of the house for our nightly walks down to the harbor. You are the love of my life, my partner, and my best friend. I am so grateful to be your husband and could not have done any of this without you.

INTRODUCTION

Metabolic energy is the primary currency of fitness for all living organisms (Brown et al., 2004). Balancing energy intake and use dictates an individual's ability to acquire food, reproduce, thermoregulate, and move through the environment, among other factors essential for survival (Costa, 1991; Costa and Maresh, 2017; Lockyer, 2007; Nagy, 2001; Nagy et al., 1999; Williams, 1999). As such, understanding the energy budget in wild animals can provide critical insight into the processes that affect the health of both individuals and populations (Costa, 2012; Tyack, 2008; Villegas-Amtmann et al., 2015; Wright et al., 2011). Despite the central importance of these physiological processes, measuring energy requirements or use in free-ranging, wild animals is often difficult. For marine mammals in particular, understanding the energy budget is a significant challenge due in part to cryptic behaviors, isolated habitats, and the environmental extremes they experience during dives. Many of these species are also exposed to increasing levels of anthropogenic disturbance as a result of commercial shipping and fishing, development, pollution, and resource exploration (Costa, 2012; Kendall et al., 2013; Lotze et al., 2017; McHuron et al., 2017; Pirotta et al., 2019; Williams et al., 2017a). Understanding energy need and expenditure in marine mammals is essential to recognizing their role in the environment and predicting the impact of these disturbances (Hunt et al., 2013; NMFS, 2016; Williams et al., 2014).

Maintenance and locomotion represent two of the most energetically costly physiological demands for marine mammals (Davis, 2014; Gallivan et al., 1983; Noren et al., 1999; Whittow, 1987; Williams et al., 1999a). Maintenance costs are reflected in

an individual's resting metabolic rate (RMR) and include the basic physiological costs associated with survival such as maintaining blood flow, cellular respiration, digestion, and thermoregulation (Davis, 2019; Ponganis, 2015). For most marine mammals, RMR is markedly elevated over values for terrestrial mammals due to the increased maintenance costs associated with living in the marine environment (Davis, 2019; Williams et al., 2001). Increased energy investment in both metabolic (i.e. heat production) and morphological (i.e. blubber, fur) thermoregulation is one of the primary drivers of this increase (Castellini, 2009; Whittow, 1987). In comparison, some marine mammal species found in tropical or sub-tropical climates exhibit lower RMRs (Davis, 2019). While this might be an adaptation to compensate for either the warmer temperature or lower productivity in the environment, it is unknown how these lower RMRs might impact locomotor costs in warm water species. As locomotor costs are a measure of the energy expended during movement, understanding the interaction between RMR and these costs is essential to examining the energy budget and predicting how it is affected by environmental or behavioral changes.

In addition to understanding the interaction between RMR and locomotion, measurements of these energetic costs are essential variables for bioenergetic modeling of both individuals and populations (Bejarano et al., 2017; Costa and Maresh, 2017; Costa et al., 2016; Gallagher et al., 2017; Maresh et al., 2014; McHuron et al., 2017; McHuron et al., 2018; New et al., 2013a; Otani et al., 2001; Pirotta et al., 2018a; Pirotta et al., 2018b; Villegas-Amtmann et al., 2015; Williams et al., 2017b; Williams et al., 2017a). Bioenergetic models can be used to calculate energy expenditure over extended

periods and determine prey consumption requirements. These quantitative measurements help define the factors driving population dynamics and can be used to inform management and conservation decisions (Hays et al., 2019; Noren, 2010; Rechsteiner et al., 2013). In threatened or endangered species these measurements are critical to understanding the impacts of disturbance or environmental changes on population health.

While direct measurement of locomotor costs is ideal for accurately defining the energy budget, it is not possible for many marine mammal species as a result of size (i.e. sperm whale, *Physeter macrocephalus*), cryptic lifestyle (i.e. *Ziphiidae* family), or extreme population depletion (i.e. vaquita, *Phocoena sinus*). Acceleration has been proposed as a proxy for energy expenditure in both marine and terrestrial animals (Halsey et al., 2009a; Pagano and Williams, 2019; Qasem et al., 2012; Wilson et al., 2006; Yoda et al., 1999; Yoda et al., 2001), however it requires calibration with direct measurement of energy expenditure first. Additionally, the relationship between acceleration and energy expenditure in terrestrial mammals has shown variation resulting from different behaviors and environmental characteristics (Bidder et al., 2012; Shepard et al., 2013; Wilson et al., 2013a) and has been difficult to define in marine mammals that are also adapted for locomotion on land or through flight (Halsey et al., 2011a; Ladds et al., 2017; Volpov et al., 2015). However, if acceleration can be calibrated in marine mammals it would allow for measurement of energy expenditure in these species in the wild.

Dissertation outline

I used open-flow respirometry and animal-borne accelerometers to measure energy expenditure during rest and locomotion in cold and warm water marine mammal species in order to better understand how the interaction of these two essential variables impact the overall energetic budget. Through measuring these costs, I also sought to provide the foundation for development of energetic models in these species and evaluate metrics for quantifying energy expenditure in marine mammals using tri-axial acceleration.

In **Chapter 1**, I examine the interaction between resting metabolic rate and locomotion in two warm-water marine mammal species: Hawaiian monk seals (*Neomonachus schauinslandi*) and West Indian manatees (*Trichechus manatus latirostris*). These energetic costs were compared to related species from colder habitats to examine the relative impact of condition-dependent maintenance costs on total locomotor costs. I show that these tropical and sub-tropical species exhibit lower RMRs relative to similarly sized polar or temperate marine mammals. However, this low RMR does not confer an energetic advantage in overall locomotor costs.

In **Chapter 2**, I measure energetic expenditure during rest and locomotion in beluga whales (*Delphinapterus leucas*) as the first step towards creating a population consequences of disturbance model to aid conservation of the Cook Inlet beluga whale population. I show that RMR for beluga whales is consistent with predicted values for similarly sized cold-water marine mammals and examine the causes of variation in metabolic measurements for this species. I also define relationships between energy

expenditure and locomotor metrics that can be used in the wild and demonstrate the marked decrease that occurs in aerobic dive limit as a result of high-speed swims that are typically observed in marine mammals following disturbance.

In **Chapter 3**, I evaluate the use of dynamic acceleration and stroke-based locomotor metrics for measuring energy expenditure in beluga whales, Atlantic bottlenose dolphins (*Tursiops truncatus*), and West Indian manatees. I found significant relationships between dynamic acceleration metrics and oxygen consumption in all three species and significant predictive relationships between all locomotor metrics and oxygen consumption in multi-species comparisons of odontocetes (beluga whale and bottlenose dolphins) and the three study species combined. I also examine the impacts of increased drag and surface swimming relative to submerged swimming on energetic expenditure during locomotion and demonstrate the increased costs associated with both comparison variables.

Together, these chapters provide novel information regarding the interaction between maintenance and locomotor costs in marine mammals, determined energetic costs to aid in the conservation of the Cook Inlet beluga whale population, and calibrated techniques that will allow future physiological study of marine mammals in the wild. Finally, in the synthesis I discuss how this dissertation improves our understanding of marine mammal conservation physiology through an examination of two of the primary energetic costs associated with living in the marine environment. Further, I discuss how this and similar physiological research can be an essential tool in the management and conservation of threatened and endangered species.

Chapter 1

Metabolic tradeoffs in tropical and subtropical marine mammals: Unique maintenance and locomotor costs in West Indian manatees and Hawaiian monk seals

---

Abstract

Unlike the majority of marine mammal species, Hawaiian monk seals (*Neomonachus schauinslandi*) and West Indian manatees (*Trichechus manatus latirostris)* reside exclusively in tropical or subtropical waters. Although potentially providing an energetic benefit through reduced maintenance and thermal costs, little is known about the cascading effects that may alter energy expenditure during activity, dive responses, and overall energy budgets for these warm water species. To examine this, we used open-flow respirometry to measure the energy expended during resting and swimming in both species. We found the average resting metabolic rates (RMR) for both the adult monk seal (753.8 ± 26.1 $kJ \cdot hr^{-1}$, mean ± s.e.m) and manatees (887.7 ± 19.5 $kJ \cdot hr^{-1}$) were lower than predicted for cold water marine mammal species of similar body mass. Despite these relatively low RMRs, both total cost per stroke and total cost of transport (COT_{TOT}) during submerged swimming were similar to predictions for comparably sized marine mammals (adult monk seal: Cost per stroke = 5.0 ± 0.2 $J \cdot kg^{-1} \cdot stroke^{-1}$, COT_{TOT} = 1.7 ± 0.1 $J \cdot kg^{-1} \cdot m^{-1}$; manatees: Cost per stroke = 2.0 ± 0.4 $J \cdot kg^{-1} \cdot stroke^{-1}$, COT_{TOT} = 0.87 ± 0.17 $J \cdot kg^{-1} \cdot m^{-1}$). These lower maintenance costs result in less variability in adjustable metabolic costs that occur during

submergence for warm water species. However, these reduced maintenance costs do not appear to confer an advantage in overall energetic costs during activity, potentially limiting the capacity of warm-water species to respond to anthropogenic or environmental threats that require increased energy expenditure.

Introduction

Thermoregulation and locomotion represent two of the most energetically costly physiological demands for marine mammals (Davis, 2014; Gallivan et al., 1983; Noren et al., 1999; Whittow, 1987; Williams et al., 1999). Maintaining homeothermy can be especially challenging due to elevated levels of heat transfer while in water (Whittow, 1987). To maintain thermal balance, many marine mammals exhibit higher maintenance metabolic rates than terrestrial mammals of similar body mass (Williams et al., 2001). This, in turn, leads to elevated food consumption rates which necessitate increased investment in the energy expended for foraging activities (Rosen et al., 2007).

Theoretically, living in warm water should reduce these maintenance costs due to a decrease in the thermal gradient for heat transfer compared to cold-water marine mammal species. In view of this, optimal energetic theory would predict an advantage for warm-water species. However, we find that nearly all marine mammal lineages, including those comprising the largest and smallest marine mammal species, exhibit increased species diversity in polar and temperate regions (Kaschner et al., 2011; Pompa et al., 2011). Of the 129 extant marine mammal species, less than 15% are found exclusively in subtropical or tropical waters (IUCN 2020). These distributions are driven in part by the higher primary productivity, and hence food resource availability,

of colder marine regions. Thus, the majority of marine mammal species appear to maintain energetic balance by taking advantage of this increased prey availability to compensate for the elevated maintenance demands associated with living in cold water. Superior insulation in the form of thick blubber layers, novel fur structures and densities, and modified dermal perfusion provide an additional thermal advantage, and have allowed marine mammals to radiate into some of the most thermally challenging habitats on earth (Castellini, 2009; Whittow, 1987).

For the few marine mammal species that live in tropical regions, lower productivity and increased competition from ectotherms (Tittensor et al., 2010) as well as elevated anthropogenic impacts (Merchant et al., 2014; New et al., 2013; Nowacek et al., 2004) represent unique challenges to maintaining daily energy balance. Species in warmer habitats must also contend with overheating during physical exertion as a result of decreased perfusion of blood to the extremities and lower gradients for heat loss through the blubber layer, especially when diving (Noren et al., 1999; Pabst et al., 2002; Scholander et al., 1950). Previous studies have hypothesized that the avoidance of excess heat retention and consequent thermal imbalance occurring in warm water habitats has necessitated the maintenance and in some cases a reduction in heat production for tropical marine mammals relative to polar or temperate congeners (Davis, 2019). This is evident in the lower basal metabolic rates (BMR) and resting metabolic rates (RMR) reported for some warm-water species (Davis, 2019). Such environmentally-dependent adaptability (Lovegrove, 2005; Speakman, 1997) has obvious benefits for sustaining lower maintenance costs in resource-limited habitats.

What is unclear, are the potential impacts of this low metabolic rate on the energetics of activity, diving, and, consequently, overall energetic costs of the animals.

As noted above, locomotion represents a significant component of the overall energy demands for animals, and defines an individual's ability to acquire food, avoid predation, as well as locate and move to suitable habitats (Maresh et al., 2015; Shepard et al., 2013; Williams et al., 2015; Williams et al., 2017a). In general, aquatic locomotion results in comparatively high transport costs in mammals, requiring significant morphological and physiological adaptations for oxygen conservation during swimming and diving (Feldkamp, 1987; Fish, 1994; Fish, 1998; Fish et al., 2008). Maintaining energy balance is further complicated in marine mammals by breath-holding and the dive response which can alter the relationship between maintenance costs and locomotor costs as the animals surface and submerge (Brown et al., 2004; Wikelski and Cooke, 2006; Williams et al., 2006).

In this study, we determined how the interaction between the energetic costs for maintenance and locomotor functions are altered with tropical or subtropical living by marine mammals, by measuring the metabolic responses of two warm-water species from distinct evolutionary lineages; Hawaiian monk seals (*Neomonachus schauinslandi*) and West Indian manatees (*Trichechus manatus latirostris)*. Extant monk seal species are considered basal evolutionary forms of the phocid lineage (Scheel et al., 2014). They are found exclusively in the warm waters around Hawaii and the Mediterranean Sea, despite being closely related to both temperate and polar species such as Northern elephant seals (*Mirounga angustirostris*) and Weddell seals

(*Leptonychotes weddellii*), respectively. Extant sirenians are similarly found in warm waters and include some of the oldest marine mammal lineages; they are the only remaining herbivorous group. The energetic costs for maintenance and locomotor activities of these species were determined by measuring surface and submerged resting metabolic rates (RMR), submerged swimming metabolic rate, the total cost per stroke, and total cost of transport (COT_{TOT}). We also evaluated the effect of the dive response on energy expenditure, by comparing the energetics of continuous surface swimming to submerged swimming in West Indian manatees. These data were then used to examine the metabolic flexibility that occurs at the interface between maintenance and locomotion costs in these warm water species when diving.

Methods

Animals

We conducted resting and swimming trials with two adult male West Indian manatees (manatee 1: 34 years old, 545 kg; manatee 2: 31 years old, 819 kg) at the Mote Marine Laboratory and Aquarium (Sarasota, FL) and one adult male and one juvenile male Hawaiian monk seal (12 years old, 198 kg; 3 years old, 97 kg) at the Long Marine Laboratory (Santa Cruz, CA). Trials took place in saltwater pools with depths ranging from 1.5 to 3 m for the manatees and 3 m for the monk seals. Water temperature was maintained between 25.0- 27.8°C for both species. Manatees were fed multiple times daily with an herbivorous diet of romaine lettuce, kale, carrots, beets, and apples. Hawaiian monk seals were fed a mixed fish diet. Both diets were supplemented with multivitamins. Training for specific behaviors occurred for 6-12

months before data collection, using positive reinforcement and operant conditioning techniques. Because free-ranging manatees graze for up to 8 hours each day (Bengston, 1983), the manatees in this study were fed throughout data collection to best approximate wild conditions and facilitate training and data collection. Manatees are also hind-gut fermenters, resulting in distribution of digestive costs over ≥ 5 days (Gallivan and Best, 1986). As a result, manatees do not exhibit an increased metabolic rate after feeding which would influence measurements in other marine mammals (Costa and Kooyman, 1984; Gallivan and Best, 1986). Monk seals remained fasted throughout all data collection trials. All procedures were approved by the Mote Marine Laboratory and University of California Santa Cruz Institutional Care and Use Committees following National Institutes of Health guidelines, and conducted under Marine Mammal Permits through the US National Marine Fisheries Service Office of Protected Species and US Fish and Wildlife Service (#MA770191-5).

Experimental Design

We used open-flow respirometry to measure oxygen consumption ($\dot{V}_{O_2}$) and evaluate energy expenditure. Oxygen consumption was measured using a plexiglass metabolic dome (manatee: 102 × 102 × 36 cm, monk seal: 160 × 100 × 60 cm) mounted on the water surface (Fig. 1). Stroke frequency was measured simultaneously during swims using acceleration recorded by animal-borne tags. Three experimental states were measured in both species: surface resting, submerged resting, and submerged swimming. Surface swimming was also measured in manatees to evaluate the cost of transit swims commonly performed by this species in the wild (Fig. 2).

Resting Metabolic Rate (RMR)

For both species, RMR was determined while the animals stationed under a metabolic dome for 10-20 min while resting dorsal side up on the water surface with minimal movement. Monk seals were fasted throughout the measurement of RMR, and manatees were fed every 20-30 s during the measurements to simulate free-ranging conditions and maintain positioning. Animals were moved into position beside the metabolic dome 1-3 min prior to data collection to prevent movement costs from influencing resting measurements.

Submerged Resting Metabolic Rate

Resting metabolic rate during submergence (RMR_{sub}) was determined following dives to 3 m for durations of 2 to 8 min. Animals held position dorsal side up on the bottom of the pool with minimal movement. Manatees were fed once every 30 s during submergence. Trials ended at the trainer's signal to surface inside the metabolic dome for measurement of oxygen consumption. All submergence trials were within the calculated aerobic dive limit (cADL) based on an oxygen store of 20.0 ml $O_2 \cdot kg^{-1}$ for West Indian manatees (Davis, 2014) and 44.7 ml $O_2 \cdot kg^{-1}$ for Hawaiian monk seals (Thometz et al., 2015). After surfacing, the post-submergence metabolic rate was measured using the same behavioral protocols as for RMR.

Energetic cost of submerged swimming

To measure the energetic cost of submerged swimming, the animals were trained to submerge to a depth of 1-2 m and remain submerged while swimming an 18 m circuit with continuous stroking until recalled to the dome by the trainer. Swim

speeds represented the preferred speeds for both manatees and monk seals and were performed for 1-2 min and 4-6 min, respectively, to simulate typical dive durations (Reynolds, 1981; Wilson et al., 2017). Following each swim, the animals were signaled to return and surface inside a metabolic dome for measurement of recovery oxygen consumption as described above.

Energetic cost of surface swimming

The energetic cost of surface swimming was measured in manatees using a continuous current generator (Endless Pools, Aston, PA). The generator maintained current speeds of 0.3 to 0.5 $m \cdot s^{-1}$ during data collection. Manatees were trained to station 15-30 cm in front of the current generator and maintain steady-state horizontal swimming for 5-15 min while surfacing inside a metabolic dome for breaths (Fig. 2). Food reinforcement was provided every 20-30 s. The metabolic dome was mounted on the water surface 10 cm in front of the current generator throughout data collection. Oxygen consumption was measured for 10-15 min prior to the start and after cessation of swimming to establish baseline oxygen consumption for each trial.

Data collection and analysis

Oxygen Consumption

Oxygen consumption was measured with open-flow respirometry using protocols from Williams et al. (2004). Throughout surface rest and swimming and immediately following submerged trials, animals were trained to restrict their breathing to a plexiglass dome mounted on a PVC frame and resting on the water surface. Air was pulled through the dome at a rate of 250-400 $L \cdot min^{-1}$ with a calibrated vacuum

pump (FlowKit Mass Flow Generator, Sable Systems International Inc., North Las Vegas, NV, USA). Water temperature during data collection ranged from 25.0 to 27.8°C, and air temperature ranged from 15°C to 36°C. The air flow rate was regulated and subsampled for oxygen content using a mass flow controller and oxygen analyzer (FoxBox Respirometry System, Sable Systems International Inc., North Las Vegas, NV, USA). Prior to oxygen analysis, subsamples were passed through a series of six tubes filled with desiccant (Drierite, W. A. Hammond Drierite, Xenia, OH, USA) and CO_2 absorbent (Sodasorb, W. R. Grace & Co, Chicago, IL, USA). Subsample oxygen content was continuously monitored and recorded at 1 Hz using Expedata Analysis software (Sable Systems International Inc., North Las Vegas, NV, USA). These values were corrected for standard temperature and pressure and converted to $\dot{V}_{O_2}$ assuming a respiratory quotient of 0.76 for manatees (Ortiz et al., 1999) and 0.77 for monk seals (Davis et al., 1985) and using equations from Withers (1977) and Fedak et al. (1981). The system was calibrated before each data collection period using dry ambient air (20.95% O_2) and weekly with N_2 gas according to the protocols of Fedak et al. (1981) and Davis et al. (1985).

For measurement of RMR, the animals stationed in the dome for 15-20 min with minimal movement. The lowest oxygen consumption measured for a minimum of 5 min for monk seals and 10 min for manatees was recorded for each trial. A baseline RMR was measured for submergence trials to calculate the metabolic rate during submergence and determine when the animal had fully recovered. The baseline RMR was measured prior to submergence for manatees and immediately following complete

recovery from submergence trials for monk seals. Submerged resting and submerged swimming metabolic rates were measured by calculating the oxygen consumption during recovery that was in excess of RMR. When assessing the cost associated with stroking during a dive in manatees, extended stationary periods that occurred between the end of the swim and the first post-dive breath were subtracted from total dive costs. Stationary periods with no movement for longer than 5 s at the end of the dive were removed, assuming an oxygen consumption rate equal to submerged resting. Surface swimming metabolic rate in manatees was calculated as the average oxygen consumption measured throughout the swimming behavior after reaching a steady state swim speed.

Swim Mechanics

Swim mechanics were measured using submersible tri-axial accelerometers (manatee: CATS-Diary, Customized Animal Tracking Solutions, Oberstdorf, Germany; monk seal: HOBO Pendant G Data Logger, Onset Computer Corporation, Bourne, MA). Acceleration was measured in $m \cdot s^{-2}$ at 10Hz for manatees and 20Hz for monk seals and converted to g ($1g = 9.81\ m \cdot s^{-2}$). For manatees, the accelerometer was attached on the dorsal center line at the peduncle using an aluminum mounting bracket attached to a nylon and neoprene strap. The frontal area of the CATS-Diary accelerometer and mounting bracket was 30 cm^2 (< 1% manatees frontal surface area). For monk seals the accelerometer was attached around the left rear flipper using a neoprene strap. The frontal area of the HOBO accelerometer was 10 cm^2 (<1% monk seal frontal surface area). Desensitization training started 6 months before data

collection to prevent the attachment from influencing swimming mechanics. Total number of strokes per dive (S_{dive}) were determined using X-axis acceleration (longitudinal axis) and counting a full stroke cycle as one individual stroke. S_{dive} was then divided by the total dive time in minutes to determine stroke frequency (f_S, strokes·min^{-1}). Because the animals were trained to swim continuously during diving, total cost per stroke (J·kg^{-1}·stroke^{-1}) was analyzed, as determined by dividing the total energy expended during each dive (J·kg^{-1}) by S_{dive}. Note that this differs from the net cost per stroke, often referred to as locomotor cost (Williams et al., 2004), in which maintenance costs are removed from the total oxygen consumption. Total cost of transport (COT_{TOT}, J·kg^{-1}· m^{-1}) was determined by dividing the total energy expended during the dive by the total distance the animal swam during the trial.

Analyses

Two-sample T-tests were used to compare oxygen consumption rates at rest and during submerged swimming as well as to compare oxygen consumption between individual animals. All analyses were conducted in R (R Core Team, 2019) and JMP Pro (Version 14.3.0, SAS Institute Inc., Cary, NC, 1989-2019). All results are presented as mean ± s.e.m unless otherwise noted.

Results

Resting Metabolic Rates

The average RMR for the adult monk seal was 753.8 ± 26.1 kJ·hr^{-1} (n = 31). For comparison, the previously published average RMR for the juvenile monk seal (Williams et al., 2011) was 594.3 ± 8.2 kJ·hr^{-1}. The average RMR for both manatees

combined was 887.7 ± 19.5 $kJ \cdot hr^{-1}$ (n = 68). RMR for manatee 1 was 945.6 ± 27.8 $kJ \cdot hr^{-1}$ (n = 35). RMR for manatee 2 was 826.4 ± 23.4 $kJ \cdot hr^{-1}$ (n = 33). Although the monk seal values were higher than predicted for terrestrial mammals (Davis, 2019), the RMR of the adult monk seal was 41% lower than predicted for a similarly sized marine mammal (Williams et al., 2001). In comparison, the previously published value for the juvenile monk seal was 27% lower than predicted for marine mammals. RMR for both manatees combined was 68% lower than predicted for marine mammals in addition to being lower than predicted for terrestrial mammals (Fig. 3).

Submerged Resting Metabolic Rates

We found significant differences between submerged and surface RMR for both species. The adult monk seal exhibited a RMR_{sub} of 41.3 ± 4.2 $J \cdot kg^{-1} \cdot min^{-1}$ (n = 10); a 35% decrease from mass specific RMR (63.1 $J \cdot kg^{-1} \cdot min^{-1}$ ± 2.4, t = 4.48, $p < 0.0001$) while resting on the surface. The juvenile monk seal showed a non-significant decrease of 8% from 101.9 $J \cdot kg^{-1} \cdot min^{-1}$ (RMR) to 93.0 ± 15.1 $J \cdot kg^{-1} \cdot min^{-1}$ (RMR_{sub}, n = 7). Average manatee RMR_{sub} was 11.8 ± 1.3 $J \cdot kg^{-1} \cdot min^{-1}$ (n = 20); a 48% decrease from mass specific RMR (22.6 ± 0.6 $J \cdot kg^{-1} \cdot min^{-1}$, t = 8.22, $p < 0.0001$) while resting on the water surface. Manatee 1 exhibited an RMR_{sub} of 7.6 ± 1.4 $J \cdot kg^{-1} \cdot min^{-1}$ (n = 10); a 61% decrease from mass specific RMR (19.3 ± 0.6 $J \cdot kg^{-1} \cdot min^{-1}$, t = 9.02, $p < 0.0001$). Manatee 2 exhibited an RMR_{sub} of 16.0 ± 1.2 $J \cdot kg^{-1} \cdot min^{-1}$ (n = 10); a 39% decrease from mass specific RMR (26.2 ± 0.7 $J \cdot kg^{-1} \cdot min^{-1}$, t = 7.55, $p < 0.0001$) (Fig. 4).

Energetic cost of submerged swimming

At an average preferred swimming speed of 1.4 $m \cdot s^{-1}$ (range: 0.9 to 2.0 $m \cdot s^{-1}$)

measured in this study, the energetic cost of submerged swimming for the adult monk seal was 151.7 ± 7.6 $J \cdot kg^{-1} \cdot min^{-1}$ (n = 13 dives), and for the juvenile monk seal was 229.5 ± 23.5 $J \cdot kg^{-1} \cdot min^{-1}$ (n = 11 dives). The average total cost per stroke for the adult monk seal was 5.0 ± 0.2 $J \cdot kg^{-1} \cdot stroke^{-1}$ (n = 13 dives), and 7.8 ± 0.5 $J \cdot kg^{-1} \cdot stroke^{-1}$ (n = 9 dives) for the juvenile monk seal. These values are comparable to those reported by Williams et al. (2004) for Weddell seals (mean: 4.78 $J \cdot kg^{-1} \cdot stroke^{-1}$) and by Davis et al. (1985) for harbor seals (mean: 5.74 $J \cdot kg^{-1} \cdot stroke^{-1}$) and as predicted for stroke costs for other phocid seals (Fig. 5).

At the average preferred swimming speed of 0.34 $m \cdot s^{-1}$ (n = 14 dives, range: 0.26 - 0.41 $m \cdot s^{-1}$), the energetic cost of submerged swimming for both manatees combined was 18.8 ± 4.1 $J \cdot kg^{-1} \cdot min^{-1}$ (Fig. 7). The average total cost per stroke was 2.0 ± 0.4 $J \cdot kg^{-1} \cdot stroke^{-1}$ (n = 14 dives) (Fig.5), which more closely compares to the stroke costs of cetaceans such as harbor porpoises (2.20 $J \cdot kg^{-1} \cdot stroke^{-1}$, Otani et al., 2001) and bottlenose dolphins (3.31 $J \cdot kg^{-1} \cdot stroke^{-1}$, Williams et al., 2017b).

Total Cost of Transport

Despite measured adult RMRs that were 46% and 71% lower than predicted for the monk seal and manatee, respectively, COT_{TOT} for adults of both species were within 26% of the predicted values for marine mammals as described by the equation $COT_{TOT} = 7.79 \cdot mass^{-0.29}$ (Williams, 1999, Fig. 6). Average COT_{TOT} for the adult monk seal was 1.7 ± 0.1 $J \cdot kg^{-1} \cdot m^{-1}$ (n = 12, 4% higher than predicted), and average COT_{TOT} for the juvenile monk seal was 2.8± 0.4 $J \cdot kg^{-1} \cdot m^{-1}$ (n = 10, 37% higher than predicted). Average COT_{TOT} for both manatees combined was 0.87 ± 0.17 $J \cdot kg^{-1} \cdot m^{-1}$ (n = 14,

26% lower than predicted).

Energetic cost of surface swimming in manatees

At an average sustained speed of 0.38 $m \cdot s^{-1}$ (n = 16 swims, range: 0.28 - 0.44 $m \cdot s^{-1}$), the average energetic cost of surface swimming for the manatees was 25.7 ± 1.7 $J \cdot kg^{-1} \cdot min^{-1}$. This was a non-significant increase of 6.9 $J \cdot kg^{-1} \cdot min^{-1}$ or 27% over the submerged swim cost (n = 30, t = 1.62, p = 0.1162). COT_{TOT} and total cost per stroke also showed non-significant increases over submerged swim costs. COT_{TOT} increased by 27% to 1.18 ± 0.1 $J \cdot kg^{-1} \cdot m^{-1}$ (n = 30, t = 1.64, p = 0.1119) during surface swimming. The total cost per stroke increased 24% to 2.62 $J \cdot kg^{-1} \cdot stroke^{-1}$ (n = 30, t = 1.59, p = 0.1233).

Discussion

The effects of tropical or subtropical living on energetic costs

In this study we found that two independent lineages of marine mammals living in warm waters showed similar patterns in metabolic responses. That is, lower RMRs relative to similarly sized marine mammal species residing in colder habitats (Fig. 3). This might be expected, as the thermal gradient for tropical or subtropical species in warm water is lower than for temperate or polar relatives in cold water. For example, the mass-specific RMR of Hawaiian monk seals is 8% and 42% lower than those measured for closely related Antarctic Weddell seals (Castellini et al., 1992) and Northern elephant seals (Costa et al., 1986), respectively, despite the Hawaiian monk seal's smaller body size. Note that the larger difference in metabolic rates for the monk seal and elephant seal may also be attributed in part to differences in methodologies as

well as the reproductive state of the animals.

In the case of extant sirenians, the warmer environment has also allowed for the maintenance of an herbivorous diet that is absent in all other marine mammal species. The low caloric value herbivorous diet, consumed in a continuous grazing mode of feeding, is sufficient to support metabolic demands in the manatee that are comparatively low, even relative to the carnivorous monk seal. Although the increased bone density found in sirenian species (Domning and de Buffrenil, 1991; Ingle and Porter, 2020) possibly accounts for part of the relative decrease in RMR compared to other marine mammals (Rea and Costa, 1992), this input is likely minimal compared to the effects of diet and environmental temperature (Costa and Maresh, 2017). Interestingly, although the extinct Steller's sea cow maintained an herbivorous diet while residing in the Bering Sea, its estimated mass was 10 metric tons (Scheffer, 1972), or over 12 times the mass of the largest manatee in this study. The result would have been a thermally favorable relationship between surface area and volume for heat transfer for the sea cow compared to the species' extant relatives. Likely, this resulted in a decreased need for an elevated metabolic rate for heat production compared to other cold-water marine mammals.

These findings provide insight into how metabolic rates may have changed in marine mammals across evolutionary time. The origins of sirenians (Domning, 1982) and *Monachus* seals (de Muizon, 1982; Fyler et al., 2005) from the warm waters (23.5-36°C) of the Tethys Sea (Alsenz et al., 2013) would have resulted in these mammals making a comparatively direct thermal transition from terrestrial to marine

living. Alternatively, if Hawaiian monk seals originated in the North Pacific as with many other pinniped species (Fyler et al., 2005; Hafed et al., 2020), the return to a lower metabolic rate might have acted as an adaptation to the reduced prey availability found in the warmer environments (Villegas-Amtmann et al., 2017). Ultimately, the West Indian manatee has evolved one of the lowest relative resting metabolic rates for a mammal, even compared to the phylogenetically-related terrestrial artiodactyls representing their original ancestry (Davis, 2019). The Hawaiian monk seal, on the other hand, exhibits maintenance costs that are lower than cold-adapted marine mammals (Fig. 3) and similar to what would be predicted for terrestrial mammals (Kleiber, 1975), that are representative of original ancestral physiological state. This would suggest that a comparatively low RMR, as the basal condition for mammals, might have conferred an evolutionary advantage and been retained in those lineages that have continued to live in tropical waters (Berta et al., 2006). In comparison, species such as the Weddell seal and Northern elephant seal that radiated to colder waters in pursuit of increased prey resources, incurred higher total maintenance costs, and thus a higher RMR, as a result of the increased thermoregulatory load.

In the present study, these low maintenance costs for warm water marine mammals did not translate into an overall lower total cost of transport, however. Because the downregulation of maintenance costs during a dive (Fig. 4) combined with stroke costs that were similar to predicted for other marine mammals (Fig. 5), we expected that an overall lower total amount of energy would have been expended during submerged swimming. For example, the Hawaiian monk seal's RMR is

approximately 41% lower than predicted for similarly sized marine mammals (Fig. 3). Yet, the COT_{TOT} of the monk seal was as predicted for similarly sized marine mammals, indicating that the low RMR does not confer a selective advantage in terms of the total energy expended during submerged locomotion. In comparison, the phylogenetically related Weddell seal has an RMR that is similar to predicted for a similarly sized marine mammal and exhibits a cost per stroke that is similar to the Hawaiian monk seal. This unexpected similarity in locomotor costs may be explained by differences in metabolic suppression that occur during submergence for the Weddell seal and the monk seal. The submerged swimming metabolic rate of the Hawaiian monk seal is approximately 2.4 times higher than its RMR. In contrast, the Weddell seal's submerged swimming metabolic rate (90.45 $J \cdot kg^{-1} \cdot min^{-1}$, Castellini et al., 1992) is only 1.1 times its RMR (Fig. 7). Such a marked difference may indicate a limit in metabolic variability during underwater activity for warm-adapted and cold-adapted species as detailed below.

Surface swimming vs submerged swimming

To fully understand why the low RMR of the tropical species does not translate into an energetic advantage during submerged locomotion, it is necessary first to examine the effects of surface versus submerged swimming on energetic costs. Surface swimming represents the behavioral transition between resting metabolic states at the water surface and submerged active states when diving. As such, it is an essential variable when examining the energy budget for marine mammals. In manatees for example, two common modes of locomotion are submerged feeding dives and cruising

swims at the surface (Reynolds, 1981). To examine the difference between these behavioral modes, we measured the cost of swimming both at the surface and while submerged. Both behaviors were performed within 1-2 meters (< 2.5 times body diameter) of the water surface, maintaining similar resistance from surface drag in both swimming modes (Williams, 1989). Accounting for similar activity levels for each mode, we found a distinct (although statistically non-significant) difference in the costs associated with these different locomotor modes (Fig. 8). Total swimming costs, total cost per stroke, and COT_{TOT} were lower during submergence for the manatees, consistent with the downregulation of overall maintenance costs in association with the dive response. These results are important when the field behaviors of manatees are considered. For example, during migration the locomotor costs would be elevated relative to foraging periods due to the increased cost of surface swimming in addition to the increased duration of swimming each day. In contrast, during submerged grazing or submerged rest periods, the daily energy demands would be lower due to both the lower total maintenance costs during the dive and a lower activity level during the dive.

Filling the energetic gap between maintenance and locomotor costs

As stated above, the low RMR measured in tropical and subtropical species does not appear to confer an energetic advantage during diving when compared to phylogenetically related species found in colder waters. Breaking down each species energy budgets into three categories, essential maintenance costs, movement costs, and condition-dependent maintenance costs, demonstrates how species-specific variability in each component contributes to the energy budget of these animals. Essential

maintenance costs describe the energy required for functions that continuously operate to ensure survival. These include maintaining blood flow to the heart and brain, basic cellular respiration, and postural muscle function, as well as growth and maturation in juveniles or fetal development during pregnancy. These costs are a product of basic biological necessity and thus determined primarily by evolutionary lineage and size (Schmidt-Nielsen, 1984). Movement costs include the energy expended for locomotor movements such as muscle contraction. As shown above, movement costs are also consistent across evolutionary lineages and determined primarily by muscle function, hydrodynamics, and biomechanics (Williams, 1999; Williams et al., 2004).

In comparison, condition-dependent maintenance costs refer to variable functions such as heat production and digestion that take place as needed throughout the body. Unlike essential maintenance costs or kinetic costs, condition-dependent maintenance is reactive to both the environment and the activities the animal undertakes such as diving. These costs can increase to compensate for physiological needs such as restoration of oxygen stores, exercise recovery, acute thermoregulatory responses, and tissue repair, or even responses to chronic disturbance (Holt et al., 2015; Williams et al., 2017a). Importantly, condition-dependent maintenance costs can also be downregulated when necessary to ensure metabolic fuel is sustained for essential maintenance costs (Hill et al., 1987; Ponganis, 2015). This downregulation can occur on several scales, from long-term responses associated with low food resource availability or quality (Rea and Costa, 1992; Rosen and Trites, 1999) or short term responses as occurs during prolonged diving (Davis, 2019; Davis and Williams, 2012).

As shown for the manatee during submerged versus surface swimming, the dive response serves to instigate a downregulation which eliminates the condition-dependent costs as a by-product of oxygen conservation associated with the dive response (Davis, 2019; Ponganis, 2015). Vasoconstriction, which restricts blood flow to the core and essential tissues, and the deferment of digestion until after the dive represent types of non-essential physiological processes that may be downregulated or delayed (Davis, 2014; Hindle et al., 2019; Noren et al., 1999; Zapol et al., 1979). The combination of this downregulation of non-essential processes and increased heat production due to muscle activity theoretically reduces the need for energy investment in condition-dependent maintenance costs while diving.

Species like the Hawaiian monk seal, residing in warmer environments, incur lower overall maintenance costs while resting due to a reduction in condition-dependent maintenance costs such as thermoregulation. Although beneficial during rest, these already low costs have a limited range for downregulation during a dive, and so confer little advantage to reducing overall swimming costs. Conversely, for a polar species such as Weddell seals, the increased condition-dependent maintenance costs normally associated with thermoregulation at the surface can be significantly decreased during a dive. As a result, total swimming costs for these closely related phocid species appear to be independent of environmental temperature per se. This reduces the cost of swimming relative to RMR in cold water species and explains the lack of energetic advantage conferred by the low RMR in tropical or subtropical species. In manatees this is demonstrated by the cost of swimming at the surface compared to both resting

and submerged swimming. Since oxygen is not a limited resource while swimming at the surface, condition-dependent costs remain elevated and surface swimming incurs a higher total cost than either resting or swimming while submerged.

Further evidence for the balance between metabolic downregulation and swimming costs is provided by the juvenile Hawaiian monk seal measured in this study. Along with an elevated RMR compared to the adult conspecific, the juvenile monk seal also exhibited a high cost per stroke and COT_{TOT} relative to similarly sized adult marine mammals (Figs. 5 and 6). In view of the increased essential maintenance costs associated with growth and maturation in the immature seal, costs that cannot be deferred during a dive, the measured increase in total locomotor costs relative to both the adult monk seal and other marine mammal species would be expected.

Conclusion

This study has focused on marine mammal species from two unique lineages that inhabit tropical and subtropical waters. Clearly the metabolic physiology of these animals differs from cold-water species. The latter appear to exhibit increased metabolic variability during a dive due to increased reliance on condition-dependent maintenance costs that can be downregulated when submerged. The tropical and subtropical species studied exhibit a lower RMR overall as a result of decreased condition-dependent maintenance costs. While this reduced metabolic variability, and thus did not translate to an energetic advantage during diving, the low RMR might still prove beneficial during recovery at the water surface. Conversely, the lower RMR could also manifest in a lower maximum aerobic scope, although this has yet to be

investigated for warm water marine mammals. This, combined with the elevated locomotor costs, could potentially limit the energetic capacity of these species to respond to anthropogenic or environmental threats requiring increased energy expenditure. Further examination of these species' post-dive recovery energetics would help to clarify this metabolic interaction and warrants additional study.

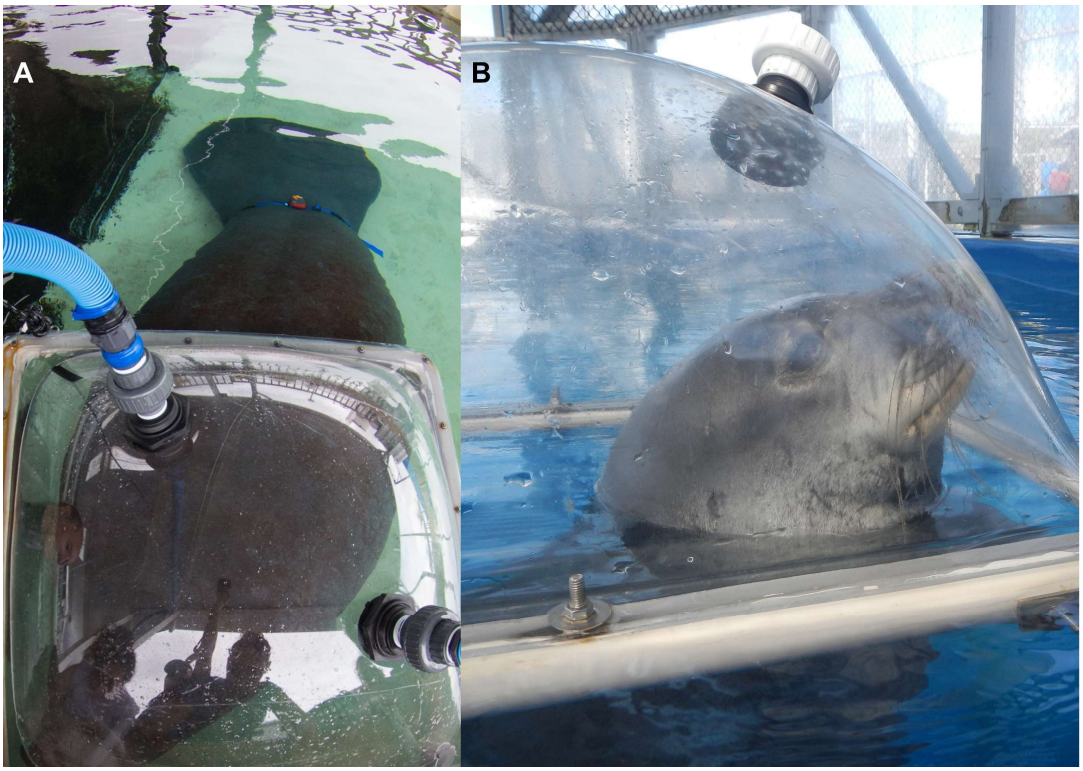

Figure 1.1: Metabolic chambers for measuring oxygen consumption in (A) West Indian manatees and (B) Hawaiian monk seals. Resting and recovery behaviors were trained for 6-12 months prior to data collection to ensure quiescent behavior throughout trials.

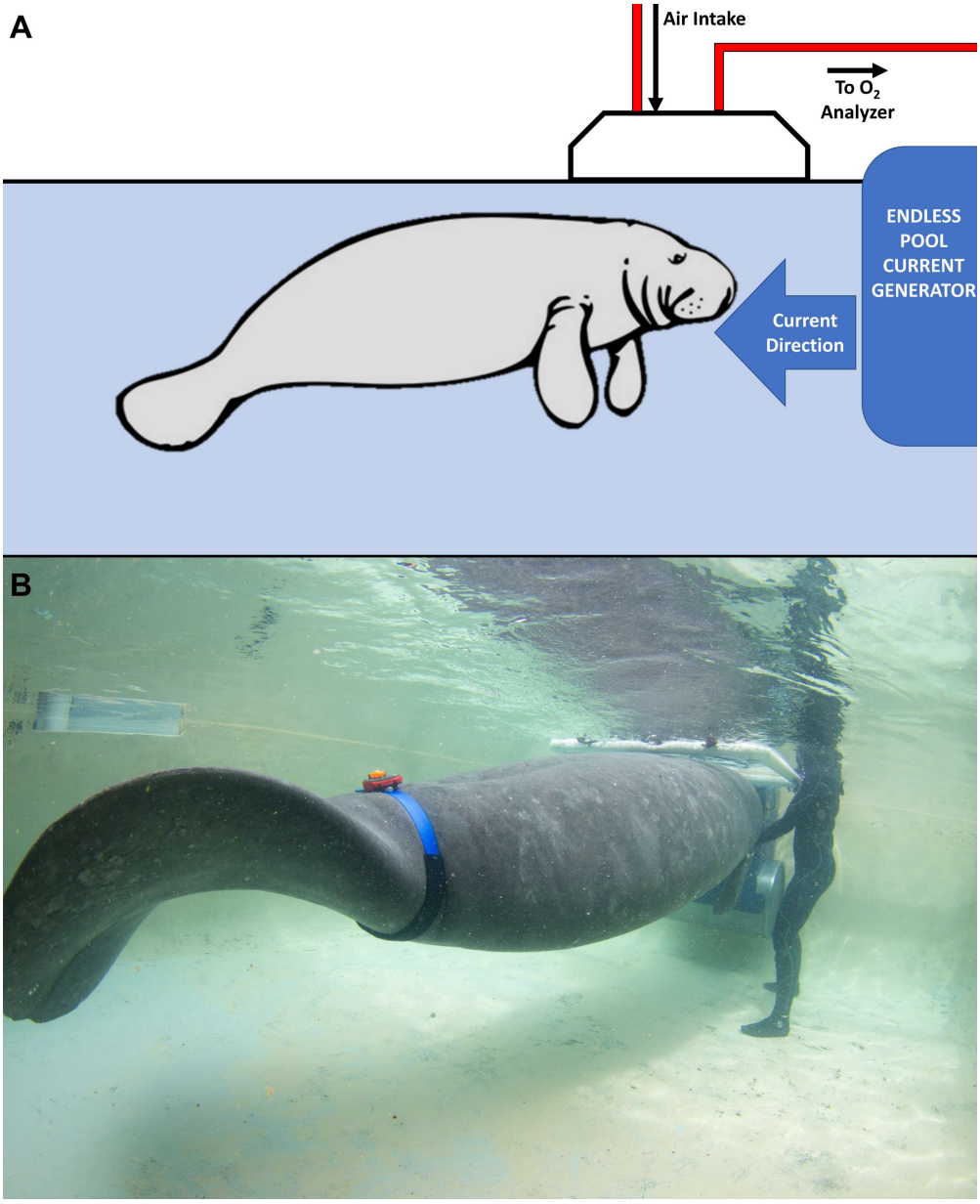

Figure 1.2: (A) Swim flume and respirometry dome used for measuring the energetic cost of surface swimming in West Indian manatees. (B) Manatee 1 participating in swim measurement with accelerometer attached to a peduncle belt. Concurrent measurement of oxygen consumption and 3-axis acceleration was performed for determination of both overall swim and individual stroke cost.

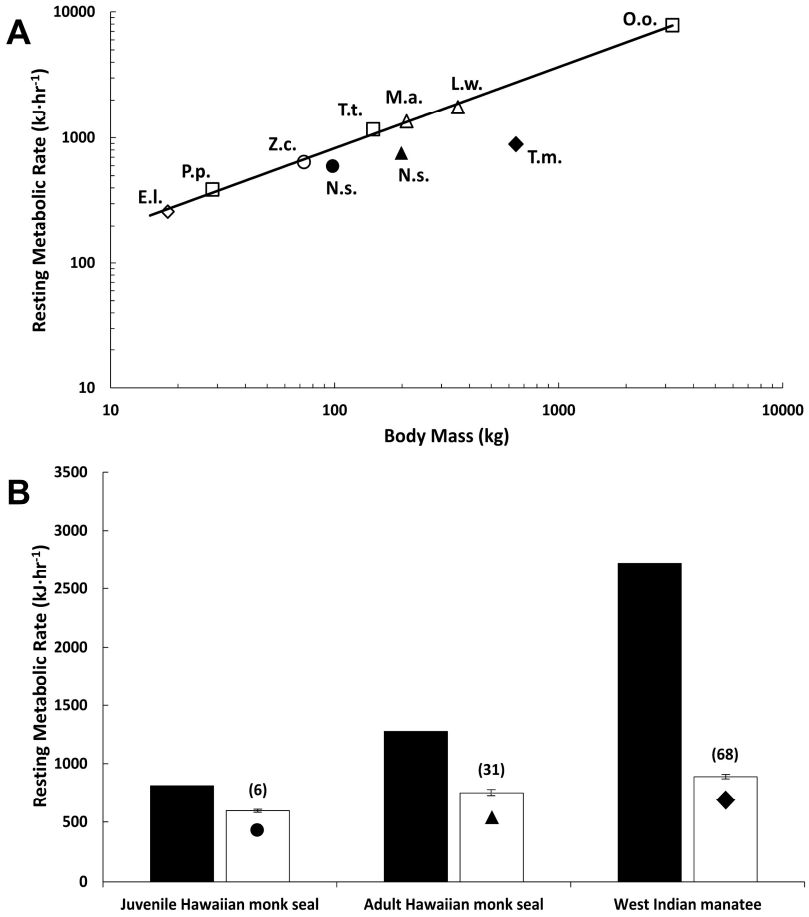

Figure 1.3: (A) Resting metabolic rate (RMR, $kJ \cdot hr^{-1}$) versus body mass (kg) for marine mammals. Solid line is the allometric regression for marine mammals stationing on the water surface adapted from Williams et al. (2001) ($RMR = 41.5 \cdot M^{0.65}$). Closed symbols represent mean RMR for the juvenile Hawaiian monk seal (N.s. closed circle), adult Hawaiian monk seal (N.s. closed triangle), and West Indian manatees (T.m. closed diamond). Open symbols represent mean RMR for sea otters (E.l. diamond; Williams, 1989), harbor porpoise (P.p. square, Kanwisher and Sundnes, 1965), California sea lions (Z.c. circle, Liao, 1990), bottlenose dolphins (T.t. square, Williams et al., 2001), northern elephant seals (M.a. triangle, Costa et al., 1986), Weddell seals (L.w. triangle, Castellini et al., 1992), and killer whales (O.o. square, Kriete, 1995). (B) Predicted (black bar, Williams et al., 2001) and measured (white bar) resting metabolic rate (RMR, $kJ \cdot hr^{-1}$) for Hawaiian monk seals and West Indian manatees. Height of bar and lines represent mean RMR ± 1 s.e.m. Mean RMR for West Indian manatees was 68% lower than predicted for similarly sized marine mammals while RMR for the adult Hawaiian monk seal was 41% lower than predicted. RMR for the juvenile Hawaiian monk seal (Williams et al., 2011a) was 27% lower than predicted.

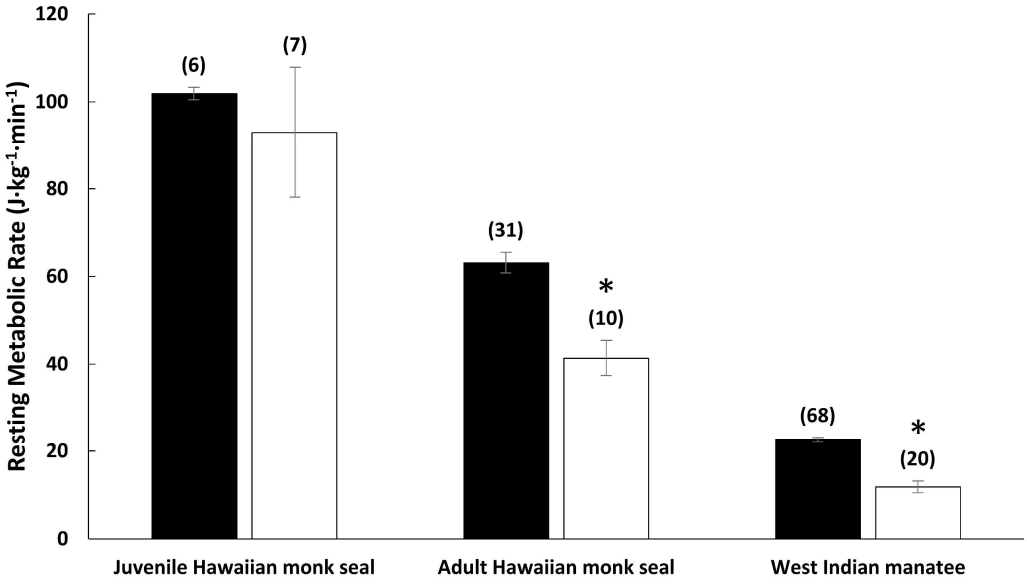

Figure 1.4: Mass-specific resting metabolic rate for tropical and subtropical marine mammals floating on the water surface (black bars) and submerged to 3 m (white bars). Height of bar and lines represent mean RMR ± 1 s.e.m. * indicates significant decreases in submerged values that were found in both the adult Hawaiian monk seal (35% decrease, $p < 0.0001$, $n = 10$ dives) and West Indian manatees (48% decrease, $p < 0.0001$, $n = 20$ dives). The juvenile Hawaiian monk seal exhibited a small but non-significant decrease from surface to submerged RMR (8% decrease, $n = 7$ dives).

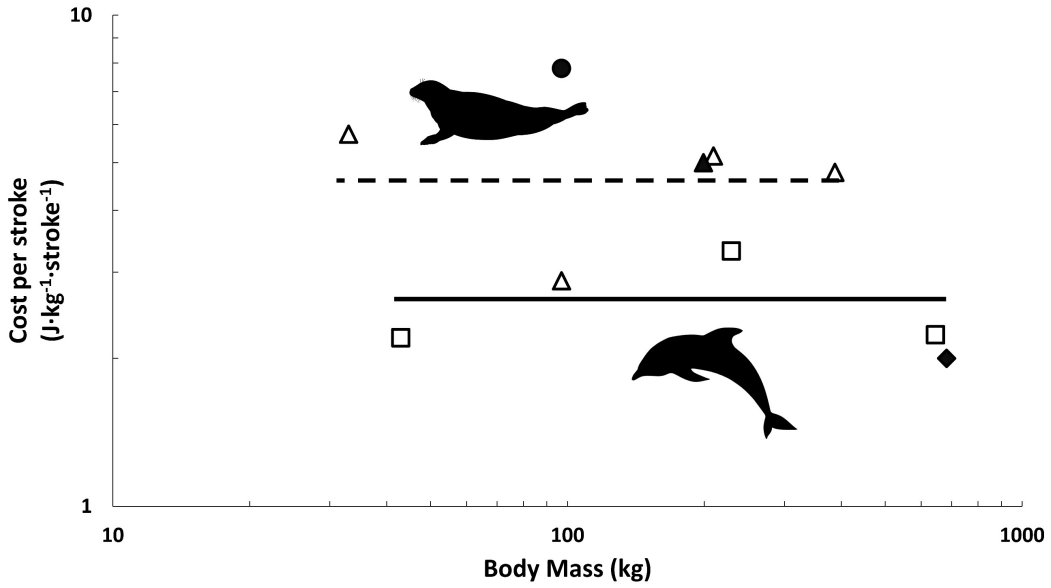

Figure 1.5: Cost per stroke ($J \cdot kg \cdot stroke^{-1}$) versus body mass (kg) for swimming juvenile Hawaiian monk seal (closed circle), adult Hawaiian monk seal (closed triangle), and West Indian manatees (closed diamond) from present study, in relation to swimming phocid seals (open triangles) and cetaceans (open squares). Phocid and cetacean points represent mean stroke costs of harbor seals (Davis et al., 1985), harp seals (Fish et al., 1988; Innes, 1984), elephant seals (Maresh et al., 2014), Weddell seals (Williams et al., 2004b), harbor porpoises (Otani et al., 2001), bottlenose dolphins, and beluga whales (Williams et al., 2017b). Cost per stroke is reported as the average cost per one full stroke cycle and calculated as described in methods. Lines represent the mean cost per stroke for phocid seals (dashed) and cetaceans (solid). Despite lower RMRs relative to other marine mammals, the adult study animals exhibited stroke costs similar to species with comparable stroking mechanics. The juvenile Hawaiian monk seal exhibited an elevated stroke cost as is expected for an individual with increased essential maintenance costs associated with growth and maturation.

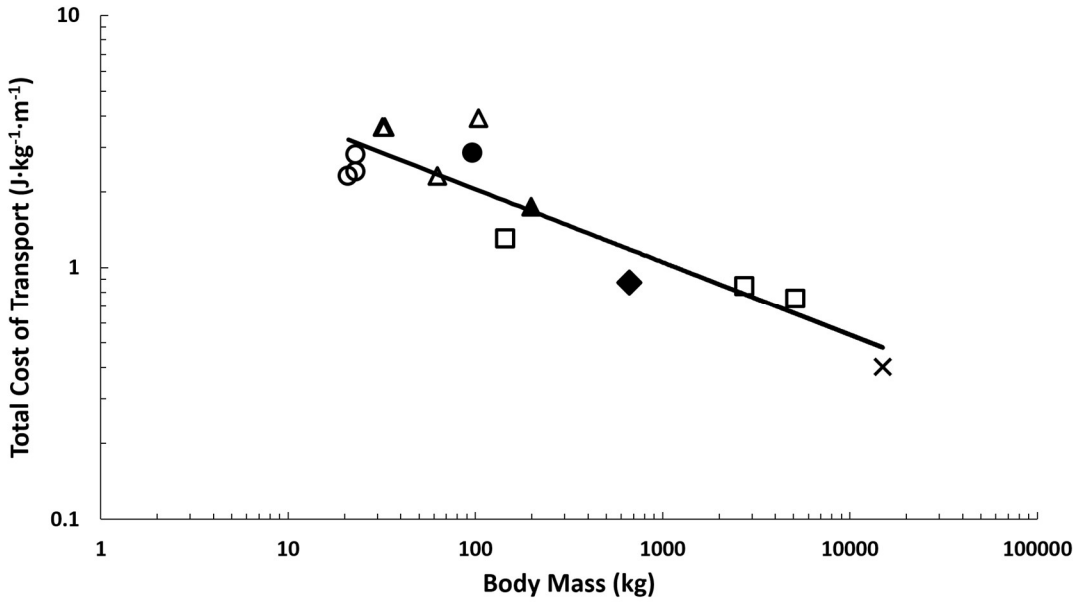

Figure 1.6: Total cost of transport in relation to body mass for Hawaiian monk seals and West Indian manatees in relation to other swimming marine mammals. Data for phocid seals (open triangles), California sea lions (open circles), bottlenose dolphins and killer whales (open squares), and grey whales (X) adapted from (Williams, 1999). The adult Hawaiian monk seal (closed triangle, 4% above predicted), juvenile Hawaiian monk seal (closed circle, 37% above predicted) and West Indian manatees (closed diamond, 26% below predicted) measured in this study exhibited an average COT_{TOT} similar to other swimming marine mammals despite significantly lower resting metabolic rates.

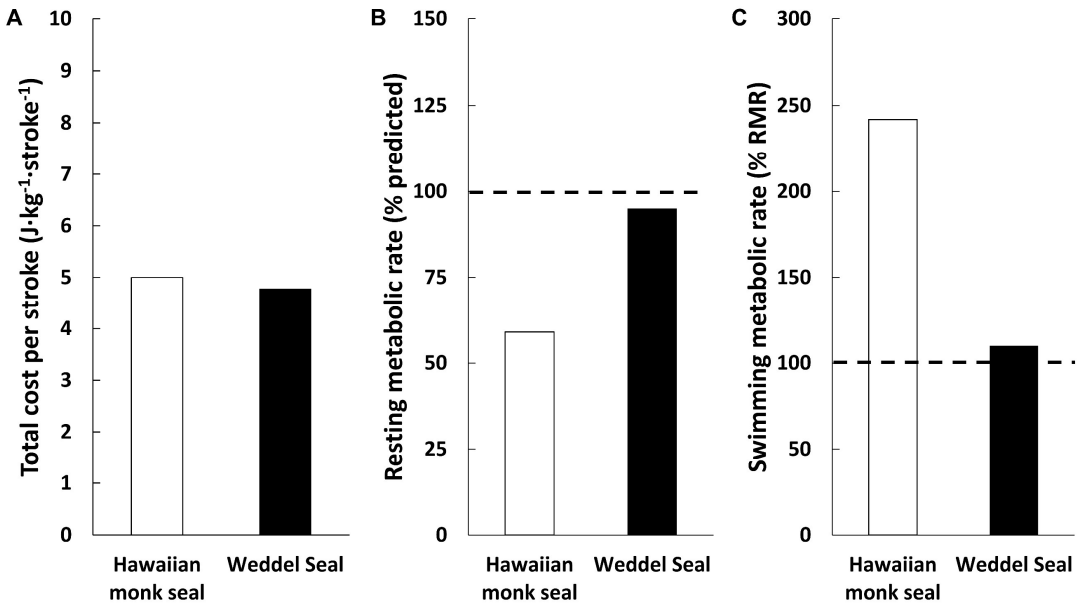

Figure 1.7: (A) Cost per stroke ($J \cdot kg \cdot stroke^{-1}$), (B) resting metabolic rate relative to predicted value for a similarly sized marine mammal, and (C) swimming metabolic rate relative to RMR for Hawaiian monk seal (white bar) and Weddell seals (black bar, Castellini et al., 1992; Williams et al., 2004). Dashed line in B and C represent 100% predicted RMR and 100% actual RMR, respectively. Both species exhibit similar costs per stroke despite markedly different relative RMRs. Increased relative swimming metabolic rate in the Hawaiian monk seal over Weddell seals is a result of lower condition dependent metabolic costs in Hawaiian monk seals. These decreased costs result in a lower RMR, but also decreased metabolic flexibility during a dive as there are fewer non-essential metabolic costs that can be downregulated by the dive response. This results in a higher relative and actual swimming metabolic rate when compared to Weddell seals.

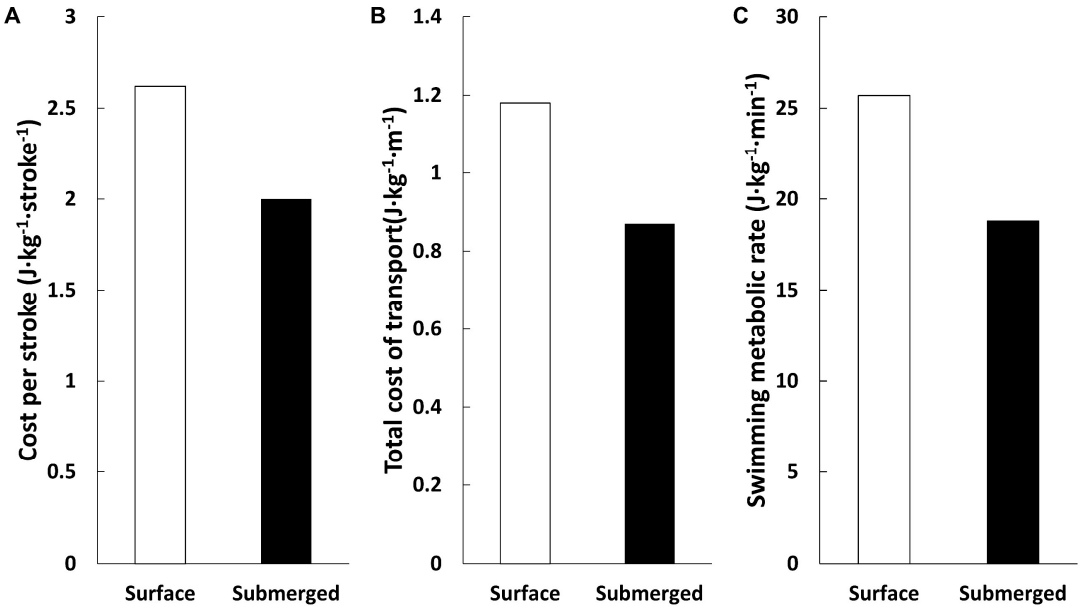

Figure 1.8: Manatee (A) cost per stroke ($J \cdot kg \cdot stroke^{-1}$), (B) total cost of transport ($J \cdot kg \cdot m^{-1}$), and (C) swimming metabolic rate ($J \cdot kg \cdot min^{-1}$) at the surface (white bars) and while submerged (black bars). Manatees exhibited similar relative decreases in metabolic rate in all 3 submerged metrics.

Chapter 2

Conservation Energetics of beluga whales (*Delphinapterus leucas*): Measuring resting and diving metabolism to understand threats to an endangered population

---

Abstract

Energy use and acquisition represent a critical balance that is essential for survival in wild animals. In marine mammals such as beluga whales (*Delphinapterus leucas*) understanding this balance can provide insight into how these species interact with the environment around them and respond to disturbance. Measuring the energetics of rest and locomotion is the first step in developing bioenergetic models to examine these interactions. We used open-flow respirometry to measure oxygen consumption during rest and submerged swimming in beluga whales and compared these measurements with a commonly studied odontocete, Atlantic bottlenose dolphins (*Tursiops truncatus*). Both resting metabolic rate (RMR, 3012 ± 126.0 $kJ \cdot hr^{-1}$) and total cost of transport (COT_{TOT}, 1.4 ± 0.1 $J \cdot kg^{-1} \cdot m^{-1}$) in beluga whales were consistent with predicted values for similarly sized marine mammals in cold environments, including the bottlenose dolphins measured in this study. Using the measured RMR and submerged locomotor costs, we also calculated field metabolic rate and surface swimming costs for beluga whales. The rate of oxygen consumption ($\dot{V}_{O_2,\text{dive}}$) during submerged swimming was then coupled with concurrently measured locomotor metrics to define predictive relationships for the energetic costs associated with submerged

swimming in beluga whales. We found significant relationships between $\dot{V}_{O_2,\text{dive}}$ and swim speed, stroke rate (f_S), and partial dynamic acceleration in the X and Y axes combined. We also calculated the aerobic dive limit in beluga whales (8.8 min) and demonstrate the effect of high-speed disturbance responses on the species' diving capacity. Finally, we use these data to calculate prey requirements for the endangered Cook Inlet beluga whale population. This study provides conservation managers with the data needed to quantify energy expenditure in beluga whales as well as predict the impact of disturbance on overall energy budget.

Introduction

As the primary currency of survival, energy use and acquisition represent a critical equilibrium that must be maintained by all living organisms (Brown et al., 2004). This balance defines an individual's ability to move through the environment, acquire food, thermoregulate, and reproduce among other essential functions that determine fitness (Costa, 1991; Costa and Maresh, 2017; Lockyer, 2007; Nagy, 2001; Nagy et al., 1999; Williams, 1999). Measuring energy expenditure or predicting necessary energy intake in free-ranging, wild animals is often difficult. Marine mammals in particular present a significant challenge as a result of their isolated habitat and cryptic behaviors. Yet, understanding the energetic budget for these species is of increased importance for conservation and management (Cooke et al., 2014; Wikelski and Cooke, 2006), due to both the important ecological role of many marine mammals (Estes, 1996; Roman et al., 2014; Williams et al., 2004a; Williams et al., 2011a) as well as the increased levels of anthropogenic disturbance they may be exposed to (Costa,

2012; Kendall et al., 2013; Lotze et al., 2017; McHuron et al., 2017; Pirotta et al., 2019; Williams et al., 2017a).

Although bioenergetic models can help define these ecological roles and responses to disturbance, these models require accurate assessment of energetic parameters, including resting metabolic rate (RMR) and locomotor costs (Costa, 2012; Pirotta et al., 2018a; Pirotta et al., 2018b). Accurate RMR measurements provide a baseline for evaluating energetic balance in individuals as well as populations (Costa, 2012). When added to active metabolic rates, these energetic demands determine prey biomass requirements for populations (Bejarano et al., 2017; Benoit-Bird, 2004; Rosen and Trites, 2013), provide a foundation for estimating field metabolic rate (FMR) (Noren, 2010; Williams et al., 2004a) and, ultimately, help inform management decisions (Hays et al., 2019; Noren, 2010; Rechsteiner et al., 2013). Locomotor behavior and energetic costs in free-ranging species can also offer insight into the energetic impact of disturbance responses in the wild (Bejarano et al., 2017; Costa and Maresh, 2017; Costa et al., 2016; Gallagher et al., 2017; Maresh et al., 2014; McHuron et al., 2017; McHuron et al., 2018; New et al., 2013; Otani et al., 2001; Pirotta et al., 2018a; Pirotta et al., 2018b; Villegas-Amtmann et al., 2015; Williams et al., 2017b; Williams et al., 2017a).

Despite the importance of accurate energetic metrics, previous work studying the physiology of beluga whales, and large cetaceans in general, has been limited. To date, most metabolic and energetic research on cetaceans has focused on smaller species including harbor porpoises (approx. 50 kg, *Phocoena phocoena*, McDonald et

al., 2017; Otani et al., 2001; Rojano-Doñate et al., 2018; Worthy et al., 1987) and bottlenose dolphins (approx. 200 kg, *Tursiops truncatus*, Miedler et al., 2015; Peddemors, 1990; Williams et al., 1999; Williams et al., 2017b; Yazdi et al., 1999) and comparatively few measurements performed with killer whales (3500 kg, *Orcinus orca*, Williams et al., 2017; Worthy et al., 2014). The RMR of captive beluga whales (*Delphinapterus leucas*) has previously only been measured in one adult male (Rosen and Trites, 2013), one pregnant adult female, and juveniles of both sexes (Kasting et al., 1989). However, the studies differed in the level of RMR beyond what can be explained by sex or reproductive status. In other studies, the respiratory rate in captive beluga whales was used as a proxy for metabolic demand (George and Noonan, 2014). The accuracy of this method is unknown, particularly when variation in breathing volume and duration is taken into account (Roos et al., 2016). Similar studies with beluga whales found a paradoxical decrease in respiration with increasing swim speed, demonstrating a need for higher resolution measurements over extended durations (Shaffer et al., 1997).

In view of the inconclusive metabolic data for beluga whales, the goal of this study was to evaluate the energetics of resting and active beluga whales. These data were compared to a smaller, routinely studied odontocete, the Atlantic bottlenose dolphin. These, in turn, were compared to the energetics of other marine mammals, including sea otters, otariids, and phocid seals, using different forms of swimming locomotion. We measured the RMR of the animals stationing calmly at the water surface as well as submerged swimming metabolic rate and cost of transport. Oxygen

consumption data from the beluga whales were then matched with locomotor metrics collected with animal-borne instruments and visual observation to determine locomotor costs and develop predictive metrics for assessing energy expenditure in wild beluga whales. Ultimately, the study was designed to provide wildlife managers with the physiological data required to create predictive energetic models to determine the impacts of anthropogenic disturbance on beluga whales.

Methods

Animals

We conducted resting and active trials on two adult female and one adult male beluga whales at Georgia Aquarium (Atlanta, GA), and two adult male Atlantic bottlenose dolphins, at the Long Marine Laboratory (LML, Santa Cruz, CA) (Table 2.1). Trials were conducted in saltwater pools with a maximum depth of 7.3 m for beluga whales and 9.1 m for dolphins and with average water temperatures of 15°C for beluga whales and 20°C for dolphins. Both species were fed a mixed fish diet. Training for both active and resting behaviors began 6 months before data collection using positive reinforcement and operant conditioning techniques. Active measurements were conducted during fasted conditions for dolphins (> 8 hr since the last feeding) and during both fasting and fed conditions for beluga whales to determine the effect of both states on swimming metabolic costs. All procedures were approved by the Georgia Aquarium Institutional Research Committee and University of California Santa Cruz Institutional Care and Use Committee following the National Institutes of Health guidelines and conducted under Marine Mammal Permits through the US National

Marine Fisheries Service Office of Protected Species and National Oceanic and Atmospheric Administration Office of Protected Resources.

Experimental Design

We measured energy expenditure during resting and active behaviors using open-flow respirometry to measure oxygen consumption. Measurements were taken using a plexiglass metabolic dome (beluga whale: 127 × 81 × 36 cm, dolphin: 85 × 58 × 36 cm) mounted on the water surface (Fig. 2.1). Stroke mechanics and acceleration were measured simultaneously during swims with 3-axis accelerometers (CATS-Diary, Customized Animal Tracking Solutions, Oberstdorf, Germany) in belugas 2 and 3, and strokes were counted manually through both live and visual recording of beluga 1. Surface resting metabolic rate was measured in all animals and submerged swimming was measured in all beluga whales and dolphin 1.

Resting Metabolic Rate

Resting metabolic rate (RMR) was determined during steady-state resting behavior while floating freely at the water surface. Animals stationed dorsal side up under the metabolic dome for 10-15 minutes with minimal movement (Fig. 2.1). All resting measurements were performed under fasted conditions (> 8 hours since last feed) and animals were moved into position beside the metabolic dome 1-3 minutes before data collection to prevent movement costs from influencing resting measurements.

Energetic cost of submerged swimming

Animals were trained to remain submerged 1-2 meters below the water surface and swim a measured circuit (beluga whale: 34 m lap length; dolphin: 59 m lap length) with continuous stroking until recalled to the metabolic dome by the trainer. Swim speeds represented the preferred speed for each animal and duration ranged from 1.5-3 min for dolphins and 2-4 min for beluga whales to approximate typical diving behaviors (Goetz et al., 2012). Following the swim, the animals were recalled and signaled to surface inside the metabolic dome for measurement of recovery oxygen consumption.

Data collection and analysis

Oxygen Consumption

Oxygen consumption was measured with open-flow respirometry using protocols from Williams et al., (2004). Throughout surface rest and swimming and immediately following submerged trials, the animals were trained to only breathe under a plexiglass metabolic dome mounted on a PVC frame and resting on the water surface (Fig. 2.1). Air was pulled through the dome at a rate of 500 $L \cdot min^{-1}$ for beluga whales and 300 $L \cdot min^{-1}$ for dolphins with a calibrated vacuum pump (FlowKit Mass Flow Generator, Sable Systems International Inc., North Las Vegas, NV, USA). Environmental air temperature ranged from 20°C to 27°C. Air flowrate was regulated and subsampled for oxygen content using a mass flow controller and oxygen analyzer (FoxBox Respirometry System, Sable Systems International Inc., North Las Vegas, NV, USA). Prior to oxygen analysis, subsamples were passed through a series of 6

tubes filled with desiccant (Drierite, W. A. Hammond Drierite, Xenia, OH, USA) and CO_2 absorbent (Sodasorb, W. R. Grace & Co, Chicago, IL, USA). Subsampled oxygen content was continuously monitored and recorded at 1Hz on a laptop computer using Expedata Analysis software (Sable Systems International Inc., North Las Vegas, NV, USA). These values were corrected for standard temperature and pressure and converted to $\dot{V}_{O_2}$ assuming a respiratory quotient of 0.77 (Davis et al., 1985) and using equations from Withers (1977) and Fedak et al. (1981). The system was calibrated before each data collection period using dry ambient air (20.95% O_2) and weekly with N_2 gas according to the protocols of Fedak et al. (1981) and Davis et al. (1985).

For RMR measurement, the lowest mean oxygen consumption for a minimum of 5 min was recorded for each trial. Additionally, RMR was measured immediately following complete recovery from submergence trials as determined by a return to resting oxygen consumption levels. Submerged swimming metabolic rates ($\dot{V}_{O_2,\text{dive}}$, $J \cdot kg^{-1} \cdot min^{-1}$) were measured by calculating the oxygen consumption during recovery that was in excess of RMR.

Acceleration

Acceleration was measured in beluga whales using submersible tri-axial accelerometers recording in $m \cdot s^{-2}$ at 20 Hz and converted to *g* (1 g = 9.81 $m \cdot s^{-2}$). The three axes measured were defined as longitudinal or caudal-rostral acceleration (X-axis), dorso-ventral acceleration (Y-axis), and lateral acceleration (Z-axis). The accelerometer was attached on the dorsal center line immediately forward of the dorsal ridge using a suction cup mount, representing the typical site used for tag deployment

on cetaceans. The frontal area of the CATS-Diary accelerometer and mount was approximately 60 cm^2 (< 2% belugas frontal surface area). Desensitization training started 6 months before data collection to prevent the attachment from influencing swimming mechanics.

Stroke mechanics and Cost of Transport

Total strokes per dive (S_{dive}) were determined using X-axis acceleration (longitudinal axis) and counting a full stroke cycle as one individual stroke. S_{dive} was then divided by the total dive time in minutes to determine stroke frequency (f_S, strokes·min^{-1}). Cost per stroke ($J \cdot kg^{-1} \cdot stroke^{-1}$) was determined by dividing the total energy expended during the dive ($J \cdot kg^{-1}$) by S_{dive}. The total cost of transport (COT_{TOT}, $J \cdot kg^{-1} \cdot m^{-1}$) was determined in both species by dividing the total energy expended during the dive by the total distance the animal swam during the trial. Distance was determined through visual and video recorded observation filmed on overhead surveillance camera and analyzed using Tracker Video Analysis and Modeling Tool (Tracker 5.0.7, Open Source Physics). Swim speed ($m \cdot s^{-1}$) was determined by dividing the total distance swum by the total dive duration.

For dynamic acceleration metrics, static (i.e., gravitational) acceleration was calculated using a 2 s running mean of the raw acceleration. This was subtracted from the raw acceleration and the absolute value was calculated as the dynamic acceleration (Wilson et al., 2006). Partial dynamic body acceleration (PDBA, *g*) of the individual axes was calculated as the mean dynamic acceleration of the axis during the dive period. PDBA of combined axes was calculated as the mean acceleration during the

dive period calculated from the sum of the dynamic acceleration from two individual axes. Overall dynamic body acceleration (ODBA, *g*) represents the mean acceleration during the dive period calculated from the sum of the dynamic acceleration from the 3 individual axes (Halsey et al., 2009b; Wilson et al., 2006).

Analyses

Two-sample T-tests were used to compare fed and fasted dives. Linear mixed models were used to examine the relationship between $\dot{V}_{O_2,\text{dive}}$ and dive duration, f_S, swim speed and acceleration in beluga whales. To account for repeated samples from the animals in the study, individual animals were treated as repeated measures using date as the time variable with single auto-regression in all models. Single-axis, two-axis, and three-axis accelerometer metrics were analyzed, with the most robust relationship between $\dot{V}_{O_2}$ and acceleration reported below as determined by AICc and BIC scores. Analyses were conducted in R (R Core Team, 2019) and JMP Pro (Version 14.3.0, SAS Institute Inc., Cary, NC, 1989-2019). All results are presented as mean ± s.e.m unless otherwise noted.

Results

Resting Metabolic Rates

Average RMR for all three beluga whales was 3012 ± 126.0 $kJ \cdot hr^{-1}$ (n = 39, Table 2.2, Fig. 2.2). Mass-specific RMR across the three whales averaged 65.8 ± 2.73 $J \cdot kg^{-1} \cdot min^{-1}$ (n = 39, Table 2.1). As would be expected based on body mass (Kleiber, 1975), the average RMR for the two bottlenose dolphins measured in this study was

lower than for the beluga whales at 1140 ± 15.9 kJ·hr^{-1} (n=37) (Fig. 2.2). Mass specific RMR across both dolphins was 111 ± 1.7 J·kg^{-1}·min^{-1} (n = 37) (Table 2.2, Fig. 2.2).

Swimming Metabolic Costs

We found no significant difference in the cost of diving during fasted or fed states for beluga whales (n = 30 dives, t = -0.57, P = 0.5713). Preferred swimming speed for the beluga whales in this study averaged 1.3 m·s^{-1} (range: 0.9 to 1.9 m·s^{-1}). At this speed, the energetic cost of submerged swimming averaged 117 ± 8.4 J·kg^{-1}·min^{-1} across all 3 whales (n = 30 dives). Average cost per stroke was 3.4 ± 0.2 J·kg^{-1}·stroke^{-1} (n = 30 dives). COT_{TOT} averaged 1.4 ± 0.1 J·kg^{-1}·m^{-1} (n = 30 dives), approximately 27% higher than predicted for a similarly sized marine mammal (Williams, 1999, Table 2.2, Fig. 2.3). The mean preferred swimming speed for the bottlenose dolphin measured in this study was 1.4 m·s^{-1} (range: 1.2 to 2.1 m·s^{-1}). At this speed, the energetic cost of submerged swimming for Dolphin 1 was 159 ± 15.9 J·kg^{-1}·min^{-1} (n = 11 dives). COT_{TOT} for the dolphin was 1.9 ± 0.2 J·kg^{-1}·m^{-1} (n = 11 dives), approximately 6% higher than predicted (Table 2.2, Fig. 2.3).

Predicting Energetic output

To determine the relationship between $\dot{V}_{O_2,\text{dive}}$ and locomotion, we examined the correlation between $\dot{V}_{O_2,\text{dive}}$ and dive duration, f_S, swim speed, and acceleration. There was no significant relationship between dive duration (mean 177 ± 6.9 s; range: 119-233 s) and $\dot{V}_{O_2,\text{dive}}$ (n = 26 dives, r^2 = 0.03, P = 0.36). There were, however, highly

significant linear relationships between $\dot{V}_{O_2,\text{dive}}$ and both f_S (Eqn. 1, strokes·min^{-1}) and swim speed (Eqn. 2, m·s^{-1}) (Fig. 2.4).

$$\dot{V}_{O_2,\text{dive}} = -51.62 + 5.01 \cdot f_S \quad (1)$$

(n = 30 dives, df = 1,28, F = 25.53, P < 0.0001, AICc = 304.28, BIC = 308.29)

$$\dot{V}_{O_2,\text{dive}} = -86.90 + 152.09 \cdot \text{Swim Speed} \quad (2)$$

(n = 30 dives, df = 1,28, F=54.93, P < 0.0001, AICc = 288.48, BIC = 291.76)

Additionally, we found significant linear relationships between $\dot{V}_{O_2,\text{dive}}$ and multiple dynamic acceleration metrics (see chapter 3), with the most robust relationship found between $\dot{V}_{O_2,\text{dive}}$ and PDBA(x,y) (Eqn. 3, *g*) (Fig. 2.5).

$$\dot{V}_{O_2,\text{dive}} = -102.52 + 1670.39 \cdot \text{PDBA(x,y)} \quad (3)$$

(n = 20 dives, df = 1,18, F = 18.19, P = 0.0005, AICc = 184.77, BIC = 186.26)

Discussion

Resting metabolic rate variability in beluga whales

In this study we found that beluga whales exhibit an RMR that is within 1% of the predicted RMR for similarly sized marine mammals residing in cold temperate or polar environments (Williams et al., 2001). As such, the RMR of beluga whales followed the pattern of many cold-water marine mammals in which resting metabolism is markedly elevated above predictions for similarly sized terrestrial mammals (Kleiber, 1975) (Fig. 2.2). Likewise, the RMR measured in the Atlantic bottlenose

dolphins in this study were within 2% of the predicted values for marine mammals and elevated above values for terrestrial mammals (Fig. 2.2).

The RMR for the three whales measured is similar to values reported by Kasting et al. (1989) but higher than those reported by Rosen and Trites (2013) for a 17 year-old male beluga whale despite similar measurement methodology. As suggested by the authors, however, the whale measured in that study was markedly larger than the average beluga whale at 1,341 kg. The mass of that whale has since declined under veterinary supervision to 1,073 kg, supporting Rosen and Trites' hypothesis that its low metabolic rate was due to a lower metabolically active mass relative to total mass as a result of elevated adipose tissue levels. This has also been seen in northern elephant seal pups, where $\dot{V}_{O_2}$ correlates more strongly to lean body mass than total body mass (Rea and Costa, 1992).

This variability suggests that care is needed when measuring and reporting the metabolic rate in this species. Given the marked seasonal changes in body condition seen in beluga whales (Breton-Honeyman et al., 2016), metabolic rates need to be viewed relative to changes in blubber deposition and lean body mass that can modify the metabolic rate and food requirements. This is especially important when trying to model the energetic and physiological impacts of anthropogenic disturbances on beluga whales, including those that are currently affecting the CIBW population (NMFS, 2016).

Calculating the cost of surface swimming

Cook Inlet beluga whales typically inhabit shallow coastal waters, and, as such, spend over 78% of their time swimming at or near the surface compared to 21.6% of their time diving (Goetz et al., 2012). This makes the cost of surface swimming a potentially significant part of maintaining energy balance for this species. Unfortunately, measuring the energetic cost of surface swimming is problematic due to the animal's size and swimming speed. As with resting metabolic rate however, we found that locomotor costs were consistent with predicted values for similarly sized marine mammals, including a COT_{TOT} within 27% of the expected value (Fig. 2.3). This enabled us to use the measured RMR and submerged swimming cost to model the average cost of surface swimming.

FMR was calculated as 3 times RMR (Noren, 2010; Williams et al., 2004a), resulting in an FMR of 51,800 $kcal \cdot day^{-1}$ or 217,000 $kJ \cdot day^{-1}$ for a 763kg beluga whale. Using a submerged swimming metabolic rate of 116.7 $J \cdot kg^{-1} \cdot min^{-1}$ and an average time spent diving each day of 21.6%, we calculated a surface swimming cost of 172.1 $J \cdot kg^{-1} \cdot min^{-1}$. This value is 47% greater than the submerged swimming costs, likely due to both increased surface drag (Williams, 1989) and decreased dive response when swimming at the surface (see Ch. 1). Given the proportion of each day that beluga whales spend at or near the surface as opposed to diving, it is essential to consider the difference in these costs when calculating changes to FMR as a result of behavioral changes or disturbance responses. The cost of diving to avoid a perceived predator, for

example, could be lower than the cost of swimming at the surface to escape (Williams et al., 2017a).

Predicting energetic costs

Using animal-borne accelerometers in this study, we found a strong correlation between $\dot{V}_{O_2,\text{dive}}$ and f_S, swim speed, and acceleration during a dive. It is important to note that though f_S, swim speed, and combined X and Y-axis (dorso-ventral) dynamic acceleration provided significant relationships, stroke rate and swim speed included 50% more samples as one whale was not measured using the accelerometer tag. When swim speed and f_S are considered only from the animals with concurrent accelerometer measurement, the predictive strength of both variables decreases. Swim speed remains a significant predictor for $\dot{V}_{O_2,\text{dive}}$ (n = 20 dives, df = 1,18, F = 9.48, P = 0.0065, AICc = 190.28, BIC = 194.94), however f_S no longer yields a significant relationship (n = 20 dives, df = 1,18, F = 3.76, P = 0.0682, AICc = 191.76, BIC = 196.43). Although this indicates a stronger correlation between acceleration and energetic cost, it also demonstrates that both stroke rate and speed are robust predictors of energetic cost during a dive when measured properly.

Locomotor metrics provide a unique opportunity to measure metabolic rate continuously in the field with wild animals once calibrated. As described above, it is essential to account for the difference in energetic costs between surface and submerged swimming. Specifically, surface swimming incurs an additional energetic expense as a result of a decreased dive response and, as such, requires a correction

factor. Using the above-calculated 47% increase in surface swimming costs we can define a correction factor of 1.47. Combined with equations 1-3 for calculating $\dot{V}_{O_2,\text{dive}}$ from f_S, swim speed, and PDBA(x,y) respectively, we can then calculate the cost of surface swimming ($\dot{V}_{O_2,\text{swim}}$, $J \cdot kg^{-1} \cdot min^{-1}$) using equations 4-6:

$$\dot{V}_{O_2,\text{swim}} = (-51.62 + 5.01 \cdot f_S) \cdot 1.47 \quad (4)$$

$$\dot{V}_{O_2,\text{swim}} = (-86.90 + 152.09 \cdot \text{Swim Speed}) \cdot 1.47 \quad (5)$$

$$\dot{V}_{O_2,\text{swim}} = (-102.52 + 1670.39 \cdot \text{PDBA(x,y)}) \cdot 1.47 \quad (6)$$

The correction factor accounts for the differences in maintenance costs exhibited at the surface and while submerged as a result of the dive response. This provides higher resolution into the costs expended by this species during different locomotive modes and enables more accurate modeling of changes in costs resulting from different disturbance responses.

Aerobic Dive Limit

In addition to the costs associated with swimming and diving, defining a marine mammal's aerobic dive limit (ADL) is essential for understanding their capacity to remain submerged during a dive (Davis et al., 2013; Kooyman et al., 1980). For arctic species such as the beluga whale, that must contend with changing sea ice cover, the ADL also determines how much of the environment is available to them as a result of sea ice extent (Williams et al., 2011b; Williams et al., 2017a). Using the average cost of submerged swimming measured in this study and assuming a mass-specific oxygen

store of 51 ml $O_2 \cdot kg^{-1}$ (Shaffer et al., 1997), we calculated the aerobic dive limit (cADL) for beluga whales to be 8.8 min. This is comparable to the 9 min cADL found by Shaffer et al. (1997) through measurement of post-dive blood lactate levels in beluga whales. Using the average swimming speed in this study of 1.4 $m \cdot s^{-1}$, this would translate to a linear swimming distance of 737 m.

Importantly, the rate of oxygen consumption exhibited by beluga whales during a dive is positively correlated with swim speed (Figure 4). Increased swimming speed, as a typical response to disturbance in odontocetes (Williams et al., 2017a; Williams et al., 2017b), would then result in faster depletion of onboard oxygen stores. For example, the highest speed measured in this study was 1.9 $m \cdot s^{-1}$. Using Eqn. 2, the calculated $\dot{V}_{O_2,\text{dive}}$ at 1.9 $m \cdot s^{-1}$ is 202.1 $J \cdot kg^{-1} \cdot min^{-1}$ or 10.1 ml $O_2 \cdot kg^{-1} \cdot min^{-1}$. At that speed, cADL would decrease from 8.8 min to 5.1 min and the linear swim distance covered in a single dive would decrease from 737 m to 578 m. Performing the same calculations for the maximum speed measured in beluga whales, 7.6 $m \cdot s^{-1}$ (Richard et al., 1998), yields a cADL of just 1.0 min and a linear swim distance of 437 m. Relative to preferred swimming speeds, this is a decrease in cADL and linear swim distance of 89% and 41% respectively.

While these calculations describe a marked increase in oxygen consumption during high speed swims, they do not account for the non-linear increase in oxygen consumption seen with some marine mammal species at higher speeds (Williams et al., 2017b). Thus, it might underestimate the rate at which beluga whales consume their

onboard oxygen stores and overestimate the dive durations available to them during an extreme flight behavior.

Cook Inlet Beluga Whales

The Cook Inlet beluga whale (CIBW) is a population of particular concern for conservation due to small numbers and proximity to substantial anthropogenic activity (NMFS, 2016). Designated as a distinct population segment due to its geographic isolation from other beluga whale populations, the CIBW was listed as endangered under the Endangered Species Act in 2008 after significant depletion resulting from unregulated subsistence hunting. Despite increased regulation, this population has failed to recover and is currently estimated to include fewer than 400 individuals (NMFS, 2016). Anthropogenic disturbances including noise pollution, catastrophic spills, and the cumulative effects of multiple simultaneous disturbances were all classified as threats of high concern for CIBW (NMFS, 2016). Yet, our understanding of their physiology has been limited and thus our capacity to measure the effect of those threats on individual beluga whales or the population. The resting metabolic rate (RMR) and locomotor costs measured above, represent the foundation for further development of bioenergetic models that can inform both policy and management decisions (Costa, 2012; Pirotta et al., 2018a; Pirotta et al., 2018b; Wikelski and Cooke, 2006).

In addition to modeling the population's ability to respond to disturbance, energetic measurements allow wildlife managers to determine prey requirements and examine the interaction between trophically-linked species in an ecosystem. For

example, multiple salmonid species are important prey for the Cook Inlet beluga whale (Goetz et al., 2012b; Quakenbush et al., 2015). Using the above FMR and assuming a digestive efficiency similar to killer whales (85%, *Orcinus orca*, Williams et al., 2011b), we calculated that an average individual beluga whale would need to consume approximately four Chinook salmon (*Oncorhynchus tshawytscha*, Noren, 2010), 16 Chum salmon (*Oncorhynchus keta*, Noren, 2010), nine Sockeye salmon (*Oncorhynchus nerka*, Davis et al., 1998), seven Coho salmon (*Oncorhynchus kisutch*, Davis et al., 1998), or 19 Pink salmon (*Oncorhynchus gorbuscha*, Davis et al., 1998) per day. As this region includes threatened or endangered populations of Chinook, Chum, Sockeye, and Coho salmon, understanding these prey requirements is important for management of both beluga whales and salmon species in the Cook Inlet.

Relevance to wild populations

As declining sea ice cover exposes the arctic environment to increased anthropogenic disturbances, it has led to novel and increasing impacts on the species that are found there. Cook Inlet beluga whales are exposed to multiple stressors as a result of their proximity to populated areas (NMFS, 2016), including threats from catastrophic events such as oil spills, noise pollution due to construction and shipping, and the cumulative effects of multiple stressors impacting individuals concurrently. Narwhals (*Monodon monoceros*), a close evolutionary relative to beluga whales, also face acoustic disturbance as a result of seismic exploration, among other inputs, and are now listed as near threatened. The results of this study may provide insights that

can be applied to other large wild odontocetes, most notably as a model for closely related species such as the narwhal.

This study has provided the baseline and locomotor metabolic data required to model the impacts of these threats and disturbances on the CIBW population. The integration of these data into population consequences of disturbance (PCoD) models will further enable scientists to predict the impacts of anthropogenic disturbances on both individuals and larger populations such as the CIBW distinct population segment.

Table 2.1: Demographic and morphometric data for beluga whales and Atlantic bottlenose dolphins in this study.

Animal	**Name**	**Sex**	**Age** y	**Mass** kg
Beluga 1	Maple	Female	13	764
Beluga 2	Qinu	Female	10	693
Beluga 3	Nunavik	Male	9	817
Dolphin 1	Rain	Male	7	165
Dolphin 2	Donley	Male	10	180

Table 2.2: Mean metabolic and locomotor values (mean ± s.e.m) for animals in this study. Numbers in parentheses represent the sample size per individual.

Animal	**RMR** $J \cdot kg^{-1} \cdot min^{-1}$	**RMR** $kJ \cdot hr^{-1}$	**Swimming Metabolic Rate** $J \cdot kg^{-1} \cdot min^{-1}$	**Cost per Stroke** $J \cdot kg^{-1} \cdot stroke^{-1}$	**Total Cost of Transport** $J \cdot kg^{-1} \cdot m^{-1}$	**Average Speed** $m \cdot s^{-1}$
Beluga 1	83.3 ± 2.56 (14)	3808 ± 106.0 (14)	160 ± 13.7 (10)	4.0 ± 0.3 (10)	1.7 ± 0.1 (10)	1.6 ± 0.9 (10)
Beluga 2	59.0± 1.33 (11)	2479 ± 68.2 (11)	96.4 ± 6.9 (10)	3.43 ± 0.2 (10)	1.3 ± 0.1 (10)	1.2 ± 0.2 (10)
Beluga 3	53.7± 3.91 (14)	2636 ± 196.4 (14)	93.5 ± 11.6 (10)	2.9 ± 0.3 (10)	1.3 ± 0.1 (10)	1.2 ± 0.3 (10)
Beluga Mean	**65.8 ± 2.73 (39)**	**3012± 126.0 (39)**	**118 ± 8.4 (30)**	**3.4 ± 0.17 (30)**	**1.4 ± 0.1 (30)**	**1.3 ± 0.5 (30)**
Dolphin 1	115 ± 2.4 (20)	1143 ± 24.4 (20)	159 ± 15.9 (11)		1.9 ± 0.2 (11)	1.4 ± 0.4 (11)
Dolphin 2	105 ± 1.9 (17)	1136 ± 20.2 (17)				
Dolphin Mean	**111 ± 1.7 (37)**	**1140 ± 15.9 (37)**	**159 ± 15.9 (11)**		**1.9 ± 0.2 (11)**	**1.4 ± 0.4 (11)**

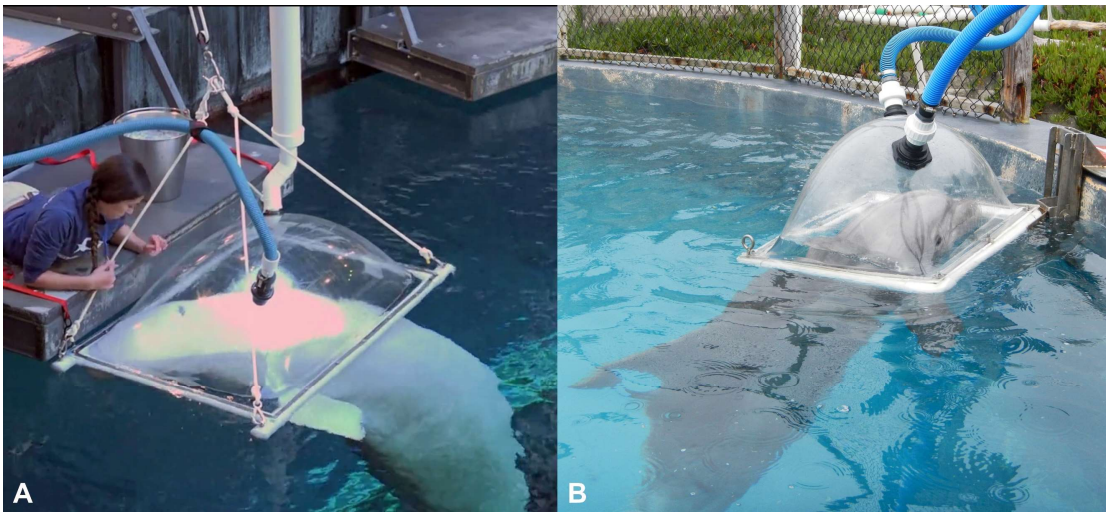

Figure 2.1: Metabolic chambers for measuring oxygen consumption in (A) beluga whales at Georgia Aquarium and (B) Atlantic bottlenose dolphins at Long Marine Laboratory. Both resting and post-dive recovery behaviors were trained for 6 months prior to data collection to minimize extraneous behaviors during experimental trials.

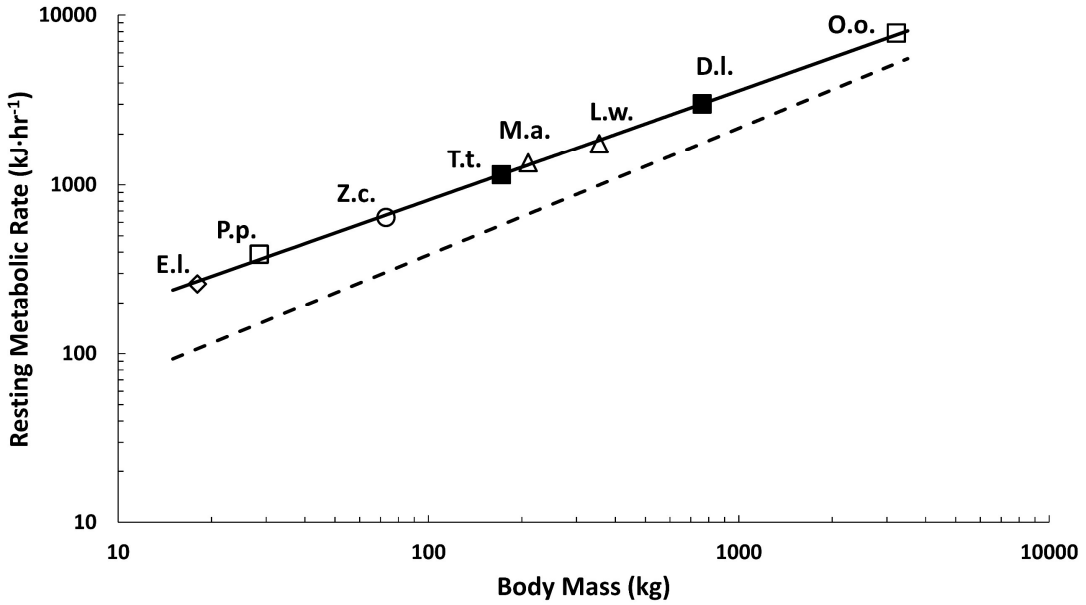

Figure 2.2: Resting metabolic rate (RMR, $kJ \cdot hr^{-1}$) versus body mass (kg) for diving marine mammals. Solid line is the allometric regression for marine mammals stationing on the water surface adapted from Williams et al. (2001) ($RMR = 41.5 \cdot M^{0.65}$). Dashed line is the predicted regression for domestic terrestrial mammals as described by Kleiber (1975). The closed squares represent mean RMR for beluga whales (D.l. current study) and Atlantic bottlenose dolphins (T.t. current study) and are both with 2% of the predicted RMR. Open symbols represent mean RMR for sea otters (E.l. diamond; Williams, 1989), harbor porpoise (P.p. square, Kanwisher and Sundnes, 1965), California sea lions (Z.c. circle, Liao, 1990), northern elephant seals (M.a. triangle, Costa et al., 1986), Weddell seals (L.w. triangle, Castellini, et al.,1992), and killer whales (O.o. square, Kriete, 1995).

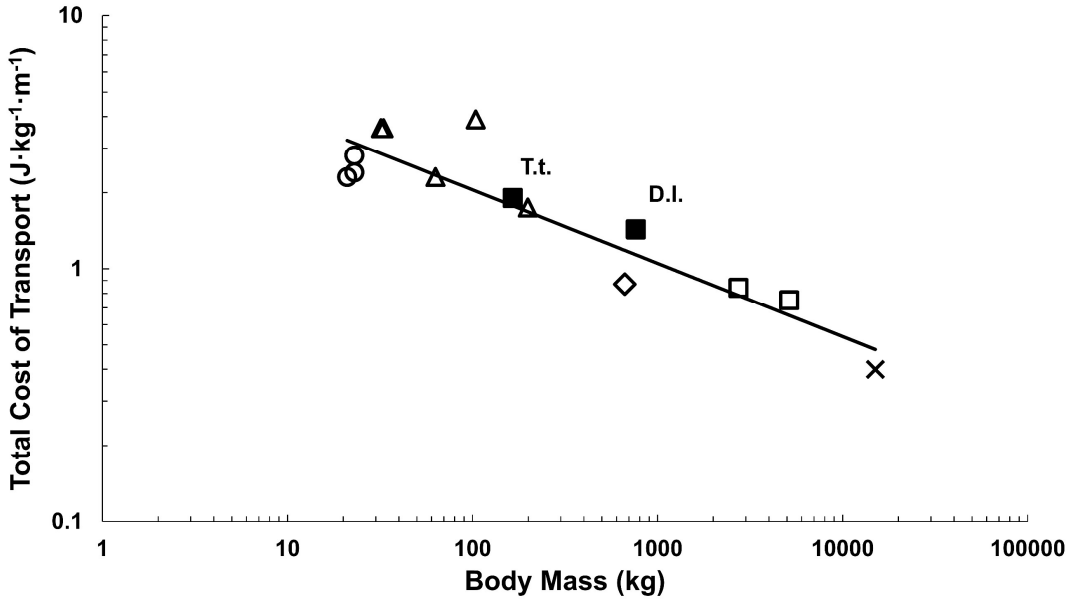

Figure 2.3: Total cost of transport in relation to body mass for beluga whales in relation to other swimming marine mammals. Data for phocid seals (open triangles), California sea lions (open circles), West Indian manatees (open diamond), killer whales (open squares), and grey whales (X) adapted from Williams (1999) and chapter 1. The mean COT_{TOT} for the beluga whales (D.l. closed square) in this study was approximately 27% higher than predicted for a similarly sized marine mammal and the COT_{TOT} for the Atlantic bottlenose dolphin (T.t. closed square) was approximately 6% higher than predicted.

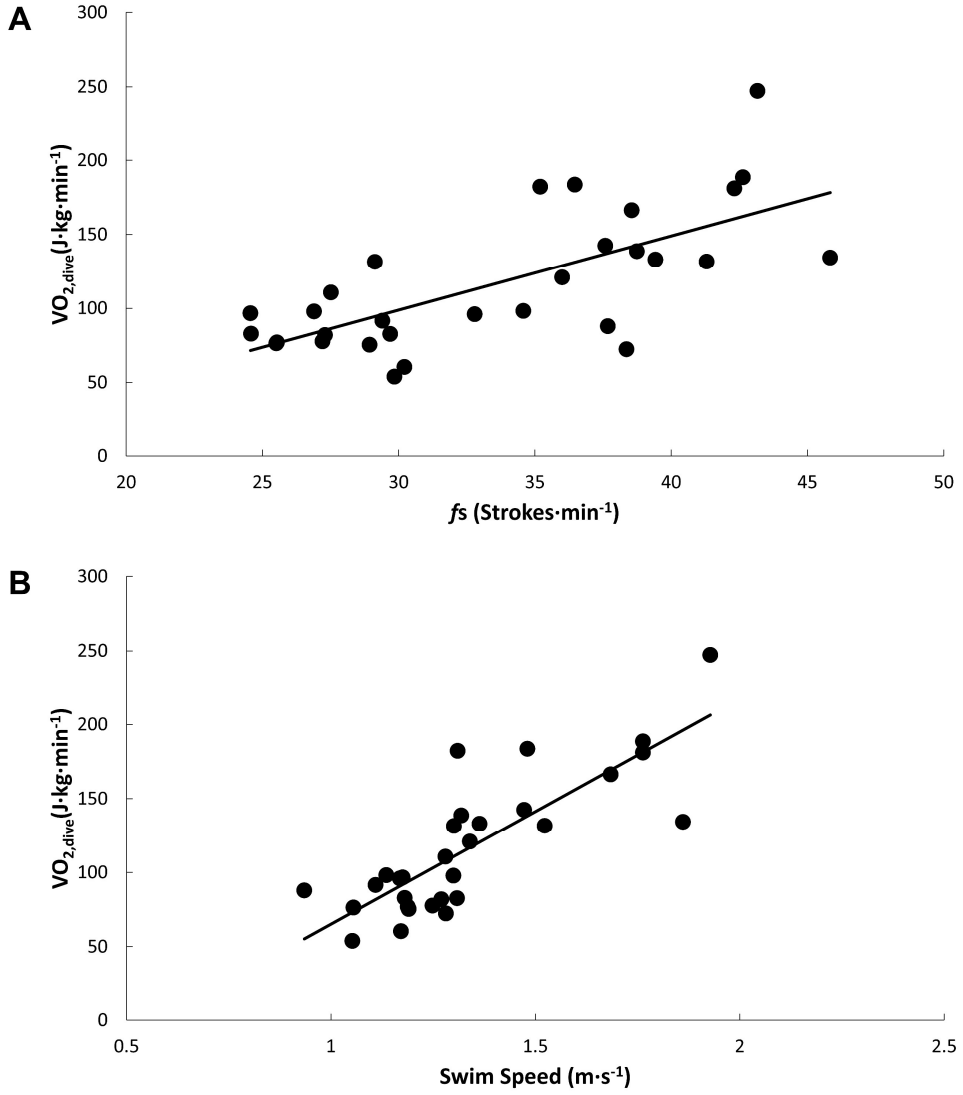

Figure 2.4: The rate of oxygen consumption during a dive plotted against (A) f_S and (B) swim speed for all 3 beluga whales combined. Each point represents the average value and rate of oxygen consumption for a single dive by an individual animal. Solid lines are the linear regressions as described by equations 1 and 2.

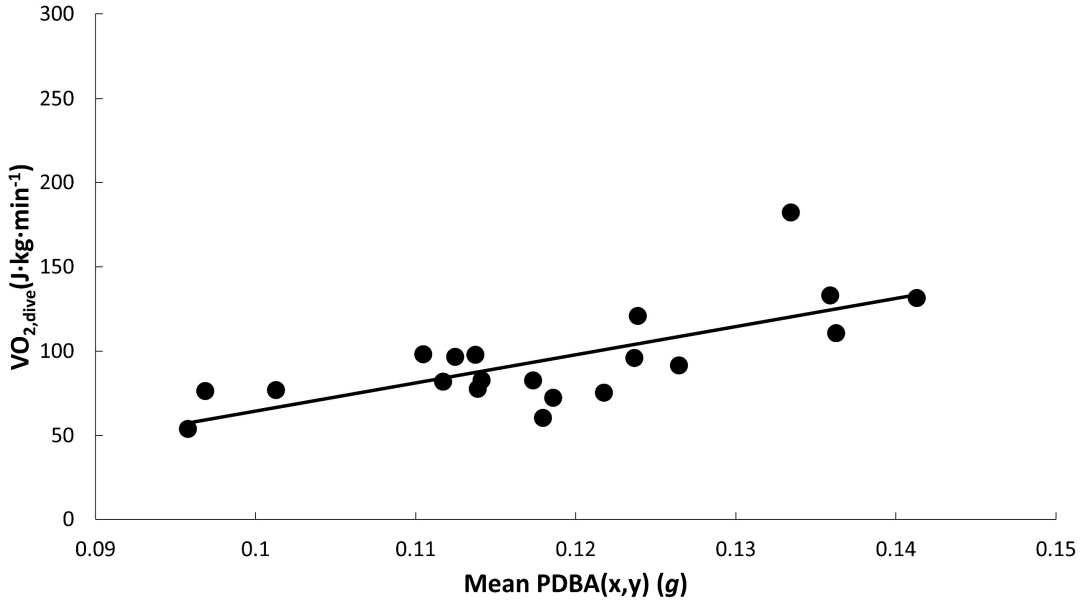

Figure 2.5: The rate of oxygen consumption during a dive plotted against mean PDBA(x,y) for beluga whales 2 and 3 combined. Each point represents the mean acceleration and rate of oxygen consumption for a single dive by an individual animal. Solid line is the linear regression as described by equation 3.

Chapter 3

Energetic costs of swimming and diving: Acceleration as a metric for predicting energy expenditure in cetaceans and sirenians

---

Abstract

Understanding the relationship between energy use and the overall energy budget can provide insight into the health and survival of wild animals. Due to the cryptic lifestyle of groups such as cetaceans and sirenians however, measuring energy expenditure in the wild is often difficult. Advances in acceleration measurement and analysis have provided new opportunities for examining the energetic costs associated with locomotion, which is a critical aspect of energy use. To define these costs, we measured acceleration, stroke frequency (f_S), and oxygen consumption during submerged swimming in three marine mammal species: beluga whales (*Delphinapterus leucas*), Atlantic bottlenose dolphins (*Tursiops truncatus*), and West Indian manatees (*Trichechus manatus latirostris*). The rate of oxygen consumption during a dive ($\dot{V}_{O_2,\text{dive}}$) was then compared to partial, overall, and vectorial dynamic acceleration as well as f_S. We found significant predictive relationships between $\dot{V}_{O_2,\text{dive}}$ and locomotor metrics in all three species, as well as in multi-species comparisons of the odontocetes (beluga whales and bottlenose dolphins) and all three species combined. In all groups, the strongest predictive relationship was found between $\dot{V}_{O_2,\text{dive}}$ and mean dynamic acceleration measured in the propulsive axes (X and Y-axis) combined. Mean overall

and vectorial dynamic acceleration as well as mean partial dynamic acceleration measured in the different propulsive axes also exhibited predictive relationships with $\dot{V}_{O_2,\text{dive}}$. Additionally, we measured significant differences in the rate of oxygen consumption due to both increased drag and surface swimming relative to submerged swimming. These findings offer insight into the relationship between acceleration and oxygen consumption in cetaceans and sirenians, define predictive relationships between $\dot{V}_{O_2,\text{dive}}$ and locomotor metrics for the species in this study, and provide additional steps towards using acceleration as a proxy for energy expenditure in the wild.

Introduction

Measuring energy expenditure in free-ranging, wild animals provides insight into critical processes that affect the health and survival of both individuals and larger populations (Brown et al., 2004). This is due to the critical balance between energetic costs and the caloric intake from food, which in turn dictates resource requirements and the ability to support important life-history events such as reproduction (Costa, 1991; Costa and Maresh, 2017; Lockyer, 2007; Nagy, 2001; Nagy et al., 1999; Williams, 1999). The daily balance of energy also determines species-specific resilience, that is, the capacity of a species to respond to disturbances in their environment through high intensity (Williams et al., 2017a) or prolonged activity (Costa, 2012; Tyack, 2008; Villegas-Amtmann et al., 2015; Wright et al., 2011). Despite the central importance of this energy management, measuring these costs in wild animals is often difficult, due in part to cryptic behaviors and isolated habitats. For animals that never venture onto

land, such as cetaceans and sirenians, our ability to quantify energetic costs is especially challenging. Not surprisingly, this has made determining the effects of anthropogenic disturbance difficult and led to a lack of information needed for developing effective conservation strategies and long-term protection (Hunt et al., 2013; NMFS, 2016; Williams et al., 2014). Recent advances in miniaturized accelerometer technology have helped to solve this problem by providing new research tools for predicting energetic costs in free-ranging cryptic species.

Dynamic acceleration has been proposed as a unique method for measuring energy expenditure in both marine (Pagano and Williams, 2019; Yoda et al., 1999; Yoda et al., 2001) and terrestrial animals (Halsey et al., 2009b; Qasem et al., 2012; Wilson et al., 2006), and has allowed the determination of energetic cost of specific movements and behaviors. By calculating partial dynamic body acceleration (PDBA) and combining tri-axial acceleration into whole body metrics such as overall dynamic body acceleration (ODBA) (Halsey et al., 2009b; Wilson et al., 2006) and vectorial dynamic body acceleration (VeDBA) (Qasem et al., 2012), it is possible to subtract the constant effects of gravity or extended effects of momentum from the acceleration produced by an animal's movements. The resulting data can then be used to analyze the acceleration produced specifically for locomotive purposes by an animal.

Numerous studies have demonstrated the potential of this method for examining the energetics of cryptic species (Halsey et al., 2009b; Jeanniard-du-Dot et al., 2016; Pagano and Williams, 2019; Wilson et al., 2006; Wilson et al., 2019). They have also indicated some of the challenges and limitations that can occur with different animal

behaviors or environmental characteristics (Shepard et al., 2013; Wilson et al., 2013a). For example, in terrestrial animals, locomotion on inclined surfaces can cause discrepancies between acceleration and energetic cost (Bidder et al., 2012; Bidder et al., 2017). In the marine environment, researchers have measured variation in the relationship between acceleration and the energetic cost of diving in species that also have adaptions for flight or terrestrial locomotion such as with cormorants (Halsey et al., 2011b) and otariids (Ladds et al., 2017; Volpov et al., 2015), respectively. Energetic analyses from acceleration are also complicated by increases in metabolism that are not related to locomotion (i.e., thermoregulation), and can result in variations in energetic cost that obscure the contribution of locomotion to overall energy expenditure (Halsey et al., 2011b; Wilson et al., 2019).

Cetaceans and sirenians provide an opportunity to examine the relationship between energy output and acceleration during locomotion in species adapted for obligate swimming. Both of these groups utilize caudal oscillation as the primary form of propulsion in thunniform and subcarangiform modes respectively (Fish, 1996; Kojeszewski and Fish, 2007). We hypothesize that in these species the relationship between energy expenditure during a dive and the acceleration produced will be statistically stronger than previously measured for amphibious pinnipeds or diving birds. If true, this would allow for the use of animal-borne accelerometers to serve as a metric for predicting energetic costs in these orders.

Here, we worked with seven individual animals representing three different species: beluga whales (*Delphinapterus leucas*), Atlantic bottlenose dolphins (*Tursiops*

truncatus), and West Indian manatees (*Trichechus manatus latirostris*). Using animal-borne submersible tri-axial accelerometers, we measured acceleration produced by the swimming movements of the animals during a dive and calculated the dynamic acceleration in each axis, each pair of axes, and all three axes combined in ODBA and VeDBA. Dynamic acceleration metrics were then compared to oxygen consumption measured using open-flow respirometry to evaluate the accuracy of dynamic acceleration to predict energetic cost in each species, as well as other odontocetes and swimmers employing caudal oscillation for propulsion.

Methods

Animals

We conducted diving trials with two adult male Florida manatees at the Mote Marine Laboratory and Aquarium (Sarasota, FL), two adult female beluga whales and 1 adult male beluga whale at Georgia Aquarium (Atlanta, GA), and two adult male Atlantic bottlenose dolphins, at the Long Marine Laboratory (Santa Cruz, CA) (Table 3.1). Trials were conducted in saltwater pools with average water temperatures and maximum depths of 28°C and 3m (manatees), 15°C and 7.3m (beluga whales), and 20°C and 9.1m (dolphins). Manatees were fed an herbivorous diet of romaine lettuce, kale, carrots, beets, and apples. Beluga whales and dolphins were fed a mixed fish diet. All diets were supplemented with multivitamins. Training for specific behaviors occurred for 6-12 months before data collection, using positive reinforcement and operant conditioning techniques. Manatees were fed throughout data collection to best approximate free-ranging conditions and facilitate training and data collection. Because

manatees are hind-gut fermenters, which results in the distribution of digestive costs across ≥ five days, discrete feeding events did not influence individual metabolic measurements (Gallivan and Best, 1986). Active measurements in beluga whales were conducted during both fasting and fed conditions to determine the effect of both states on swimming metabolic costs. Active measurements in dolphins were conducted under fasted conditions (> 8 hr since the last feeding). All procedures were approved by the Georgia Aquarium Institutional Research Committee and Mote Marine Laboratory and Aquarium and University of California Santa Cruz Institutional Care and Use Committees following National Institutes of Health guidelines and conducted under Marine Mammal Permits through the US National Marine Fisheries Service Office of Protected Species, US National Oceanic and Atmospheric Administration Office of Protected Resources, and US Fish and Wildlife Service.

Experimental Design

Oxygen consumption was measured using open-flow respirometry to evaluate energy expenditure during swimming. Measurements were performed using a plexiglass metabolic dome (manatee: 102 × 102 × 36 cm, beluga whale: 127 × 81 × 36 cm, dolphin: 85 × 58 × 36 cm) mounted on the water surface (Fig. 3.1). Acceleration and stroke mechanics were measured simultaneously during swims with 3-axis accelerometers in all animals except for beluga 1. For beluga 1, strokes were counted manually via both live and visual recordings. Resting and submerged swimming was measured in all animals. Additionally, surface swimming was measured in manatees to compare the costs of swimming at the surface and while submerged.

Energetic cost of submerged swimming

The energetic cost of submerged swimming was measured in animals trained to submerge to a depth of 1-2 m and remain submerged while swimming a measured circuit (manatees: 18m; belugas: 34m; dolphins: 59m) with continuous stroking until recalled to the dome by the trainer. Swim speeds represented the preferred, voluntary speeds for all animals and were performed for 1-4 min. Following the swim, the animals were signaled to return and surface inside the metabolic dome for measurement of recovery oxygen consumption as described above.

Energetic cost of surface swimming

The energetic cost of surface swimming was measured in manatees using a continuous current generator (Endless Pools, Aston, PA). The current generator maintained water current speeds of 0.3 to 0.5 $m \cdot s^{-1}$ during data collection. Manatees were trained to station 15-30 cm in front of the current generator and maintain steady-state horizontal swimming for 5-15 min while surfacing inside the metabolic dome for breaths. Food reinforcement was provided every 20-30 s. The metabolic dome was mounted on the water surface 10 cm in front of the current generator throughout data collection. Oxygen consumption was measured for 10-15 min before and after swimming to establish baseline oxygen consumption for each trial.

Data collection and analysis

Oxygen Consumption

Oxygen consumption was measured with open-flow respirometry using protocols from Williams et al. (2004) as described in chapters 1 and 2. Briefly,

throughout surface rest and swimming and immediately following submerged trials, the animals were trained to only breathe under a plexiglass metabolic dome mounted on a PVC frame that floated on the water surface (see Ch. 1 and 2). Using a calibrated vacuum pump (FlowKit Mass Flow Generator, Sable Systems International Inc., North Las Vegas, NV, USA), air was pulled through the dome at a rate of 300-400 $L \cdot min^{-1}$ for manatees, 500 $L \cdot min^{-1}$ for beluga whales, and 300 $L \cdot min^{-1}$ for dolphins. Air temperature during data collection ranged from 15°C to 36°C. Air-flow rate was regulated and subsampled for oxygen content using a mass flow controller and oxygen analyzer (FoxBox Respirometry System, Sable Systems International Inc., North Las Vegas, NV, USA). Prior to oxygen analysis, subsamples were passed through a series of 6 tubes filled with desiccant (Drierite, W. A. Hammond Drierite, Xenia, OH, USA) and CO_2 absorbent (Sodasorb, W. R. Grace & Co, Chicago, IL, USA). Subsample oxygen content was continuously monitored and recorded at 1 Hz using Expedata Analysis software (Sable Systems International Inc., North Las Vegas, NV, USA). These values were corrected for standard temperature and pressure and converted to $\dot{V}_{O_2}$ using equations from Withers (1977) and Fedak et al. (1981). We assumed a respiratory quotient of 0.76 for manatees based on their herbivorous diet (Ortiz et al., 1999) and a respiratory quotient of 0.77 for beluga whales and dolphins based on other marine mammals measured on a mixed fish diet (Davis et al., 1985; Williams et al., 2004b). The system was calibrated before each data collection period using dry ambient air (20.95% O_2) and weekly with N_2 gas according to the protocols of Fedak et al. (1981) and Davis et al. (1985).

For RMR measurement, animals stationed in the dome for 10-20 min with minimal movement and the lowest oxygen consumption for a minimum of 5 min for beluga whale and dolphins and 10 min for manatees was recorded for each trial. For submergence trials, baseline RMR was used for calculating the metabolic rate during submergence and confirming the animal had fully recovered. Baseline RMR was measured immediately prior to submersion for manatees and immediately following recovery for beluga whales and dolphins. The rate of oxygen consumption during submerged swimming ($\dot{V}_{O_2,\text{dive}}$, $J \cdot kg^{-1} \cdot min^{-1}$) was measured by calculating the oxygen consumption during recovery that was in excess of RMR. When assessing the cost associated with stroking during a dive in manatees, periods with no movement for longer than 5 s that occurred between the end of locomotion and the first post-dive breath were subtracted from total dive costs. The energetic cost of these extended stationary periods was calculated assuming an oxygen consumption rate equal to submerged resting (see Ch. 1). Surface swimming metabolic rate ($\dot{V}_{O_2,\text{swim}}$, $J \cdot kg^{-1} \cdot min^{-1}$) in manatees was calculated as the average oxygen consumption measured throughout the swimming behavior after reaching a steady-state swim speed.

Acceleration and Stroke Mechanics

Acceleration was measured using submersible tri-axial accelerometers (CATS-Diary, Customized Animal Tracking Solutions, Oberstdorf, Germany) recording in $m \cdot s^{-2}$ at 10Hz for manatees and 20Hz for beluga whales and dolphins and converted to g ($1\ g = 9.81\ m \cdot s^{-2}$). The three axes measured were defined as longitudinal or caudal-rostral acceleration (X-axis), dorso-ventral acceleration (Y-axis), and lateral

acceleration (Z-axis) (Fig. 3.1). For manatees, the accelerometer was attached along the dorsal center line at the peduncle using an aluminum mounting bracket attached to a nylon and neoprene strap (Fig. 3.1). The frontal area of the CATS-Diary accelerometer and mounting bracket was 30 cm^2 (< 1% manatees frontal surface area). For beluga whales and dolphin 1, the accelerometer was attached along the dorsal center line immediately forward of the dorsal ridge using a suction cup mount (Fig. 3.1). The frontal area of the CATS-Diary accelerometer and mount was approximately 60 cm^2 (< 2% belugas frontal surface area, < 4% dolphin frontal surface area). For dolphin 2, the accelerometer was attached along the dorsal center line immediately forward of the dorsal ridge using a custom-made neoprene vest. Desensitization training started 6 months before data collection to prevent the attachment from influencing swimming mechanics.

Total strokes per dive (S_{dive}) were determined using X-axis acceleration (longitudinal axis) and counting a full stroke cycle as one individual stroke. S_{dive} was then divided by the total dive time in minutes to determine stroke frequency (f_S, strokes·min^{-1}). For dynamic acceleration metrics, static or gravitational acceleration was calculated using a 2 s running mean of the raw acceleration. This was subtracted from the raw acceleration and the absolute value was calculated as the dynamic acceleration per Wilson et al. (2006). Partial dynamic body acceleration (*g*) of either the individual x, y, or z axes (PDBA(x), PDBA(y), PDBA(z)) or the sum of two axes (PDBA(x,y), PDBA(x,z), PDBA(y,z)) was calculated as the mean dynamic acceleration of the axis or combined axes during the diving period. Overall dynamic

body acceleration (ODBA, g) represents the mean acceleration during the diving period calculated from the sum of the dynamic acceleration from all three individual axes (Halsey et al., 2009b; Wilson et al., 2006). VeDBA represents the mean acceleration during the diving period calculated from the vectorial sum of the dynamic acceleration from the three individual axes (g) (Qasem et al., 2012).

Analyses

Linear mixed models were used to examine the relationship between $\dot{V}_{O_2,\text{dive}}$, and locomotor metrics in individual species. Due to the same individuals being sampled multiple times in all three species, individual was treated as the subject in a repeated measure approach using date as a time variable with single auto-regression in all models in this study.

Analysis of covariance procedures (ANCOVA) were used to compare the relationships between $\dot{V}_{O_2}$ and acceleration for manatees swimming at the surface and submerged as well as for dolphins measured with the suction cup and neoprene vest instrument attachments. In both models $\dot{V}_{O_2}$ was the dependent variable and the locomotor metric (continuous) and comparison variables (categorical- manatees: surface versus submerged; categorical- dolphins: suction cup versus vest) were fixed. The interaction between the comparison variable and locomotor metric was initially included to assess the homogeneity of slopes assumption for ANCOVA, that is to determine if the slope of the relationship between the locomotor metric and $\dot{V}_{O_2}$ differed as a function of the comparison variable (full model). If the interaction was not significant (an indication that the slopes were similar) a reduced model was then

performed without the interaction to determine if there was a significant relationship between the locomotor metric and $\dot{V}_{O_2}$ and if there was a difference in $\dot{V}_{O_2}$ as a result of the comparison variable (i.e. the elevations of the lines differed).

When examining multi-species datasets, the log of all variables was used in comparing $\dot{V}_{O_2,\text{dive}}$ with f_S and acceleration to account for progressively increasing variation with increased swim speeds and acceleration. Three models were performed to test the relationships between $\dot{V}_{O_2,\text{dive}}$ and each locomotor metric in the combined species dataset. In all three models $\dot{V}_{O_2,\text{dive}}$ was the dependent variable and the locomotor metric was a fixed variable. First (Model 1), an ANCOVA was performed with species [treated as a fixed variable] and the interaction between species and individual locomotor metric as the model terms to assess the homogeneity of slopes assumption and determine if the slope of the relationship between $\dot{V}_{O_2,\text{dive}}$ and each locomotor metric differed as a function of species. If the interaction was not significant, indicating the slopes were similar, a second ANCOVA was performed as a reduced model. This second model (Model 2) included species[fixed] without the interaction term to determine if there was a significant relationship between $\dot{V}_{O_2,\text{dive}}$ and the locomotor metric and if there was a difference in $\dot{V}_{O_2,\text{dive}}$ due to species. Finally, to determine the predictive relationships between $\dot{V}_{O_2,\text{dive}}$ and locomotor metrics, model 3 was performed using linear regressions with $\dot{V}_{O_2,\text{dive}}$ as the dependent variable, individual locomotor metrics as the fixed variable, and individual as a repeated measure as described above. To determine the relationship between $\dot{V}_{O_2,\text{dive}}$ and locomotion

across species in the multi-species comparisons, species was not included as a factor in the final model. Relative strengths of individual locomotor metrics within model three were determined using AICc and BIC. Analyses were conducted in R (R Core Team, 2019) and JMP Pro (Version 14.3.0, SAS Institute Inc., Cary, NC, 1989-2019).

Results

Beluga whales

No significant difference was found between submerged swimming costs during fasted or fed states (n = 30 dives, t = -0.57, $P = 0.5713$). We found significant positive linear relationships between $\dot{V}_{O_2,\text{dive}}$ and six of the nine calculated metrics (Table 3.2, Fig. 3.2) based on measurements of $\dot{V}_{O_2,\text{dive}}$ and f_S in all three beluga whales (n = 30 dives) as well as acceleration in belugas 2 and 3 (n = 20 dives). f_S measured from all three whales showed the highest statistical significance of the nine metrics measured. As AICc and BIC scores assess the relative strength of similar models with equivalent sample sizes, they could not be used to compare f_S and acceleration metrics as a result of the increased sample size for f_S. From acceleration measured with beluga whales 2 and 3, PDBA(x,y), PDBA(y), and VeDBA exhibited the most robust relationships between $\dot{V}_{O_2,\text{dive}}$ and acceleration according to AICc and BIC scores (Table 3.2, Fig. 3.2).

Atlantic bottlenose dolphins

There was no significant difference between the RMR measured for both dolphins ($F = 0.2624$, $P = 0.6115$) (Table 3.1). In comparing the relationship between

$\dot{V}_{O_2,\text{dive}}$ and all locomotor metrics, there was also no significant difference in the slope of the relationship for all locomotor metrics for the dolphin measured with the suction cup instrument attachment versus the neoprene instrument attachment (Table 3.3). However, there was a significant difference in $\dot{V}_{O_2,\text{dive}}$ as a result of the attachment method (Table 3.3), with the neoprene instrument attachment resulting in elevated levels of oxygen consumption (Fig. 3.3). As a result, locomotor metrics were separated based on the attachment method.

Comparisons of $\dot{V}_{O_2,\text{dive}}$ and locomotor metrics measured using a suction cup attachment yielded significant positive linear relationships from eight of the nine locomotor metrics examined. PDBA(x,y), PDBA(x), and ODBA yielded the strongest relationships (n = 10, Table 3.4, Fig. 3.4). The only metric measured in this study that did not produce a significant relationship was f_S (Table 3.4).

Comparing $\dot{V}_{O_2,\text{dive}}$ and locomotor metrics measured using the neoprene instrument attachment yielded significant positive linear relationships from five of the nine locomotor metrics examined (Table 3.5, Fig. 3.5). PDBA(y,z) generated the most robust relationship followed by ODBA and PDBA(z). As the same instrument, location, and orientation were used for data collection, there are two likely causes for the variation from measurements performed using the suction cup attachment. The first is variation resulting from increased flexibility allowed by the neoprene mount, causing extraneous instrument movement and introducing greater variation into the data collection. The second possibility is the increased drag produced by the neoprene

resulted in modified swim kinematics as the animal attempted to compensate. Either change could have caused the modified acceleration signatures seen in the results.

West Indian Manatee

In comparing the relationship between $\dot{V}_{O_2,\text{dive}}$ or $\dot{V}_{O_2,\text{swim}}$ and all locomotor metrics for manatees, there was no significant difference in the slope of the relationship between submerged and surface swimming for eight of the nine metrics (Fig. 3.6). For the eight metrics that met the homogeneity of slopes assumption, there was a significant difference between $\dot{V}_{O_2,\text{dive}}$ and $\dot{V}_{O_2,\text{swim}}$ as a result of swimming at the surface or submerged (Table 3.6). As such, surface and submerged swimming were examined separately.

For submerged swimming, f_S is the only metric that did not exhibit a significant relationship with $\dot{V}_{O_2,\text{dive}}$ (Table 3.7). All other metrics yielded significant linear relationships. The strongest relationships were found between $\dot{V}_{O_2,\text{dive}}$ and PDBA(x,y), ODBA, and PDBA(y) (Table 3.7, Fig. 3.7). In comparison, surface swimming (n = 26 swims) yielded significant linear relationships from all locomotor metrics measured in this study (Table 3.8). The strongest relationships were found between $\dot{V}_{O_2,\text{swim}}$ and PDBA(z), PDBA(x,z), and VeDBA (Fig. 3.8).

Multi-species comparisons

Despite the different sizes and ranges of both acceleration and $\dot{V}_{O_2,\text{dive}}$ in the different species examined in this study, we found no significant difference in the slopes of the relationships between $\dot{V}_{O_2,\text{dive}}$ and the locomotor metrics for either the

combined odontocete dataset (Table 3.9) or dataset containing all three species (Table 3.10). Examining the magnitude of the relationship between locomotion and $\dot{V}_{O_2,\text{dive}}$ showed significant differences in the mean values between species for eight of the nine metrics in odontocetes (Table 3.9) and all metrics when examining all three species combined (Table 3.10). This is as expected due to the different sizes and swim speeds represented by the species in this study.

Therefore, to determine the general relationship between locomotor metrics and $\dot{V}_{O_2,\text{dive}}$ across species, model three was used as described above to define the linear regressions for the odontocete dataset and all three species combined. For odontocetes, all locomotor metrics measured in this study were significant, with PDBA(x,y), PDBA(x), and ODBA yielding the strongest relationships (Table 3.11, Fig. 3.9). Including manatee submerged swimming in the second combined dataset increased the explanatory capacity of all measured metrics for $\dot{V}_{O_2,\text{dive}}$. The strongest relationships measured from all three species combined were found from PDBA(x,y), PDBA(y), and ODBA (Table 3.12, Fig. 3.10).

Discussion

Predicting $\dot{V}_{O_2,dive}$ from locomotion

This study found significant relationships between $\dot{V}_{O_2,\text{dive}}$ and multiple locomotor metrics for all three species of marine mammals tested under various conditions. Although there is variation in the strength of the different relationships across species, we observed trends when examining the predictive capacity of both stroke rate and acceleration metrics within and across species. By examining the

variation measured in the context of these trends, we can define the key factors to consider when using locomotion to measure energy expenditure in free-swimming animals. To this end, we compared the results for three different species swimming submerged while wearing a streamlined instrument attachment system: beluga whales and dolphins wearing the accelerometer attached with suction cups and manatee submerged swimming wearing an instrument strap on the peduncle.

Stroke Rate (f_S)

A significant correlation was measured between f_S and $\dot{V}_{O_2,\text{dive}}$ in beluga whales as well as in both multi-species analyses. This relationship demonstrates that f_S can predict energy expenditure when time is accounted for. However, the only instance where f_S provided a stronger predictive relationship than acceleration metrics was in beluga whales. This is due in part to the 50% increase in sample size for f_S compared to acceleration. When f_S is considered only from the beluga whales with whom we measured concurrent acceleration, we observe a weaker, and no longer significant, relationship between f_S and $\dot{V}_{O_2,\text{dive}}$ (Table 3.2).

This indicates that f_S is not as good a predictor as dynamic acceleration as a proxy for energy expenditure. While f_S does account for variation in stroke effort resulting in modified stroke speeds, it does not account for changes in stroke amplitude. In comparison, both increased stroke frequency and increased stroke amplitude would translate to increased acceleration. This accounts for the stronger relationship between $\dot{V}_{O_2,\text{dive}}$ and acceleration metrics relative to f_S. However, in addition to the significant relationships between f_S and $\dot{V}_{O_2,\text{dive}}$ measured in this study, Williams et al. (2017b)

measured a significant relationship between f_S and $\dot{V}_{O_2,\text{dive}}$ in Atlantic bottlenose dolphins resulting from an increased sample size and broader f_S range than measured in this study. This demonstrates that f_S can be used to predict $\dot{V}_{O_2,\text{dive}}$ when necessary in similar species to those measured in this study. Such examples can include the use of f_S from the re-examination of previously collected stroke datasets or visual collection of stroke data when direct instrumentation or measurement of acceleration is not feasible. When possible however, it is recommended that acceleration should be preferentially used over f_S.

Partial or Whole-Body Dynamic Acceleration

Comparing single axis acceleration for the three species, we find that the propulsive axes provide the highest predictive strength. Beluga whales and manatees exhibited the most robust single-axis relationship between $\dot{V}_{O_2,\text{dive}}$ and Y-axis dynamic acceleration, measuring dorso-ventral displacement of the instrument as the animal performs a stroke. Dolphins showed the strongest single-axis relationship between $\dot{V}_{O_2,\text{dive}}$ and X-axis dynamic acceleration, which measures the forward and backward surge as the animal is propelled forward with each stroke. The reason for this variation between the Y and X-axis could not be definitively determined in this study. Still, given the similar measurement protocols for all three species, this may be a result of different swimming kinematics. Both dolphins and beluga whales utilize a thunniform swimming motion (Fish, 1996) that minimizes rostral and fore-body movement during swimming. However, the increased flexibility found in beluga whales could allow for increased dorso-ventral movement that is translated to the acceleration signature. In

comparison, manatees were measured using a strap around the peduncle to approximate current tagging protocols for the species in the wild. This placement might register increased acceleration relative to the more rostral placement in the other two species. Importantly, we found that the combination of the X and Y-axis dynamic acceleration provided stronger or nearly equivalent predictive capacity in all three species. This indicates that by integrating both propulsive axes, PDBA(x,y) provides a more accurate representation of the locomotive cost incurred by these species.

In comparison, the whole body metrics examined in this study did not provide stronger predictive capacity than PDBA(x,y). They exhibited a weaker or similar predictive ability to the single-axis metrics of PDBA(x) or PDBA(y) when examined in individual species. There are two possible explanations for this result. First, it could be due to the limited lateral movement exhibited by the animals in this study. As the animals were trained to swim a simple circuit and minimize extraneous activity to maintain behavioral focus, there were fewer 3-dimensional maneuvers than might be typically observed in activities such as foraging dives.

The second potential cause for the relative strength of 2-axis acceleration metrics is that forward propulsion is the primary cost incurred by these species during locomotion. As such, including lateral movement in whole-body metrics such as ODBA and VeDBA would introduce a variable into the acceleration signature that is unnecessary for energetic calculations. Turning movements have been shown to result in an increased energetic cost for terrestrial mammals (Wilson et al., 2013a; Wilson et al., 2013b). However, the relative cost of maneuvers by marine mammals is unknown.

Given the different physical forces that must be overcome for aquatic locomotion compared to terrestrial locomotion (Gillis and Blob, 2001), forward propulsion may result in significantly higher costs relative to lateral movements such as turning.

Despite the lower predictive strength relative to PDBA(x,y), both ODBA and VeDBA do exhibit significant relationships with $\dot{V}_{O_2,\text{dive}}$. In the case of VeDBA, this might be beneficial when accelerometer orientation cannot be reliably fixed to the primary axes of movement measured in this study (Fig. 3.1, Qasem et al., 2012; Wilson et al., 2019). Furthermore, periodic instrument movement is common in extended duration deployments utilizing suction cup attachments due to the tendency of suction cups to slide on cetacean skin during high-intensity activities (Cade et al., 2018). In these cases, the calculation of VeDBA minimizes the impact of the variable instrument orientation.

Within the scope of this study, we have determined three factors that should be considered when deciding which metric is best to use for determining $\dot{V}_{O_2,\text{dive}}$ in cetaceans or sirenians. (1) If only one axis of acceleration can be measured, it should be oriented in either the rostral-caudal plane (X-axis) or the dorso-ventral plane (Y-axis) to measure propulsive acceleration preferentially over f_S. (2) If tri-axial acceleration is possible and accelerometer orientation will be reliably fixed to the three orientation planes measured here, combining X and Y-axis dynamic acceleration is recommended to integrate both propulsive axes into a single acceleration metric. However, (3) if it is likely that the instrument will move during data collection, then VeDBA is recommended to account for instrument position variability (Qasem et al.,

2012; Wilson et al., 2019).

Application to Other Species

One important potential application of accelerometry to determine energetic cost, is its application to species that are accessible only in the wild. This limitation to research can be a result of size, as with sperm whales (*Physeter macrocephalus*), or a cryptic, deep-diving lifestyle, typical of beaked whale species (*Ziphiidae* family) and narwhals (*Monodon monoceros*). The current study examined seven individuals representing three species from two different orders, covering a size range greater than 650kg. Interestingly, despite the wide range of body sizes and swim speeds, we observed a similar trend for multi-species comparisons and individual species. Both maintained the most robust predictive relationship between $\dot{V}_{O_2,\text{dive}}$ and PDBA(x,y) compared to the other metrics tested (Tables 2,3,5,7, & 8). In odontocetes, the strength of the relationships declined for PDBA(x) and then ODBA. Conversely, the strongest single-axis metric for all three species combined was PDBA(y) followed by ODBA. Although slightly weaker than ODBA, in both multi-species comparisons VeDBA also exhibited a strong relationship with $\dot{V}_{O_2,\text{dive}}$.

Additional factors should be considered when applying these relationships to other species. Most importantly, these relationships are approximations based on limited data sets. Ideally, the regressions would include greater overlap in acceleration signatures for the three species. A second caveat is the three species examined here are from two distinct marine mammal lineages. However, while manatees have a significantly lower resting metabolic rate than other marine mammal species, they also

exhibit a cost of transport and stroke cost that is consistent with the predicted values for similarly sized marine mammals (see Ch. 1). This is due to the energetics of movement being determined by external physical forces and not resting metabolism. Thus, the relationship between acceleration and locomotor costs should be consistent across species with similar swimming kinematics. This is confirmed with the manatees in this study by the cross-species comparison of the slope of the relationships between locomotor metrics and oxygen consumption (Table 3.10). Though further diversification of the study species is needed, this suggests the possibility of future application of these techniques to measuring energetics in large species, such as baleen whales, that cannot be measured directly.

Refining the Relationship: variation in the relationship between $\dot{V}_{O_2,dive}$ and acceleration

Submerged vs Surface Swimming

A common problem found in using acceleration to predict energetic cost, is a breakdown in the relationship between acceleration and $\dot{V}_{O_2}$ when used over extended periods that include both surface and submerged swimming. Two possible causes for the observed variability that can ensue are increased drag or increased maintenance costs when swimming at the surface. Increased surface drag results from increases in turbulence from wave drag experienced by an animal swimming within 2-3 body diameters of the surface (Hertel, 1966; Williams, 1989). This necessitates increased stroking effort, resulting in an elevated total cost of transport (Williams, 1999). Acceleration metrics can take this into account because they represent a high-resolution

measurement of stroking effort. Thus, as stroke effort increases to account for increased turbulence, acceleration and predicted oxygen consumption should also increase.

Unlike the response to surface drag, increases in energy expended resulting from a change in maintenance costs would not translate to increased acceleration. The dive response is one likely cause of variability in maintenance costs, particularly as it changes between swimming at the surface and swimming submerged. As a result of the dive response, many marine mammals exhibit decreased total maintenance costs during submergence through reduced energy investment in thermoregulation, digestion, and blood flow to non-essential tissues (Davis, 2019; Ponganis, 2015). Research with multiple marine mammal species have shown a significant difference between surface and submerged RMR (see Ch. 1, Hurley and Costa, 2001) and heart rate (Davis and Williams, 2012; Kaczmarek et al., 2018; McDonald et al., 2017; Williams et al., 2017a). Based on this, we might expect that the cost of swimming submerged and swimming at the surface should be significantly different due to these changes in underlying maintenance costs (Halsey et al., 2011b; Wilson et al., 2019). Likely, this results in variability in the relationship between acceleration and $\dot{V}_{O_2}$ as marine mammals move between the surface and submerged swimming.

When we tested the manatees swimming at the surface in this study, we found that Z-axis dynamic acceleration presented the most robust relationship with $\dot{V}_{O_2,\text{swim}}$, followed by PDBA(x,z). Surface swimming resulted in similar levels of total acceleration relative to submerged swimming (Fig. 3.7), indicating this could be a result of increased lateral maneuvering to maintain a position in the generated water flow.

When the surface and submerged swimming relationships for acceleration and $\dot{V}_{O_2}$ were compared, we found no significant difference in the slopes for eight of the nine locomotor metrics and significant differences in $\dot{V}_{O_2}$ as a result of swimming at the surface or submerged for all eight of those metrics (Table 3.6). Thus, a significant difference in the energetic cost occurred between locomotion at the surface and while submerged (Fig. 3.7). Failure to account for these variations between surface and submerged swimming costs would result in a breakdown of the predictive capacity of the acceleration metrics. Instead, the relationship between $\dot{V}_{O_2}$ and locomotion needs to be considered separately for surface and submerged swimming.

Increased Drag

In addition to different modes of swimming, the amount of drag caused by instrument attachment can also affect the energetic cost and change the relationship between acceleration and $\dot{V}_{O_2}$, as we saw with the bottlenose dolphins. Despite both dolphins exhibiting a similar RMR and similar levels of acceleration with both the neoprene and suction cup attachment systems (Fig. 3.3), a significantly higher $\dot{V}_{O_2,\text{dive}}$ was measured from the dolphin wearing the neoprene vest. When the relationships between $\dot{V}_{O_2,\text{dive}}$ and locomotor metrics were compared, we found no significant difference in the slope of the relationships, but a significant difference in $\dot{V}_{O_2,\text{dive}}$ as a result of the attachment method (Table 3.3). This indicates that increased drag increases the rate of oxygen consumption at a given level of acceleration and needs to be accounted for if instrumentation represents a substantial increase in frontal surface area

for the animal (Fig. 3.3).

Conclusion

Through examining three species across a range of sizes and speeds, we have determined that multiple locomotor metrics based on both stroking and acceleration exhibit a predictive capacity for $\dot{V}_{O_2}$. Although there is variation in the strength of the different axes between species, it appears that dynamic acceleration measured in the propulsive axes (X and Y) provide the greatest explanatory power for oxygen consumption during a dive. These data can be used to measure the cost of submerged activity for the species in this study, as well as potentially enabling application to other species that are more difficult or impossible to measure directly.

Table 3.1: Demographic data, mean resting metabolic rate (RMR) and mean total cost of transport (COT_{TOT}) (mean ± s.e.m) for the animals in this study. Numbers in parentheses represent number of individual measurements for each metric.

Animal	**#**	**Name (Sex)**	**Age** y	**Individual Mass** kg	**Mean Mass** kg	**Mean RMR** $kJ \cdot hr^{-1}$	**Mean COT_{TOT}** $J \cdot kg^{-1} \cdot m^{-1}$
Beluga whale	1	Maple (F)	13	764	763 ± 9.2 (39)	3012.4± 126.0 (39)	1.4 ± 0.1 (30)
	2	Qinu (F)	10	693			
	3	Nunavik (M)	9	817			
Atlantic bottlenose dolphin	1	Rain (M)	3	165	172 ± 1.3 (39)	1145.9 ± 16.2 (39)	(suction cup): 1.9 ± 0.2 (10)
	2	Donley (M)	8	180			(neoprene vest): 2.8 ± 0.2 (10)
West Indian manatee	1	Hugh (M)	34	545	676 ± 18.1 (68)	887.7 ± 19.5 (68)	Submerged: 0.87 ± 0.17 (14)
	2	Buffet (M)	31	819			Surface: 1.18 ± 0.1 (16)

Table 3.2: Results of linear mixed effects models examining the relationship between $\dot{V}_{O_2,\text{dive}}$ ($J \cdot kg^{-1} \cdot min^{-1}$) and locomotor metrics in beluga whales. Predictor variables measured include single and double axis dynamic acceleration (*g*), ODBA (*g*), VeDBA (*g*), and f_S ($strokes \cdot min^{-1}$).

Predictor (units)	Equation	df	F Ratio	P	AICc	BIC	# of dives
Mean PDBA(x) (*g*)	$\dot{V}_{O_2,\text{dive}}$ = -19.01 + 1806.47 · Mean PDBA(x)	1,18	5.24	0.0344	193.63	195.11	20
Mean PDBA(y) (*g*)	$\dot{V}_{O_2,\text{dive}}$ = -60.11 + 2808.67 · Mean PDBA(y)	1,18	17.67	0.0005	185.06	186.54	20
Mean PDBA(z) (*g*)	$\dot{V}_{O_2,\text{dive}}$ = 94.66 + 5.43 · Mean PDBA(z) *(Not Significant)*	1,18	0.00	0.9937	198.74	200.22	20
Mean PDBA(x,y) (*g*)	$\dot{V}_{O_2,\text{dive}}$ = -102.74 + 1670.36 · Mean PDBA(x,y)	1,18	18.19	0.0005	184.77	186.26	20
Mean PDBA(x,z) (*g*)	$\dot{V}_{O_2,\text{dive}}$ = 38.11 + 480.40 · Mean PDBA(x,z) *(Not Significant)*	1,18	1.15	0.2983	197.50	198.99	20
Mean PDBA(y,z) (*g*)	$\dot{V}_{O_2,\text{dive}}$ = -11.43 + 963.26 · Mean PDBA(y,z)	1,18	3.67	0.0713	195.02	196.51	20
Mean ODBA (*g*)	$\dot{V}_{O_2,\text{dive}}$ = -47.21 + 819.16 · Mean ODBA	1,18	5.88	0.026	193.08	194.57	20
Mean VeDBA (*g*)	$\dot{V}_{O_2,\text{dive}}$ = -49.24 + 1249.91 · Mean VeDBA	1,18	6.28	0.0221	192.75	194.24	20
f_S whales 2 and 3 ($strokes \cdot min^{-1}$)	$\dot{V}_{O_2,\text{dive}}$ = -12.52 + 2.74 · f_S	1,18	3.76	0.0682	194.94	196.43	20
f_S All 3 whales ($strokes \cdot min^{-1}$)	$\dot{V}_{O_2,\text{dive}}$ = -51.62 + 5.01 · f_S	1,28	25.53	<0.0001	304.28	308.29	30

Table 3.3: Results of ANCOVA examining the relationships between $\dot{V}_{O_2,\text{dive}}$ and locomotor metrics for dolphins measured with the suction cup and neoprene vest instrument attachments. For both the full and reduced model, $\dot{V}_{O_2,\text{dive}}$ was the dependent variable and the locomotor metric was fixed. The comparison variable, suction cup or neoprene instrument attachment, was also included as a fixed variable in both models. The interaction between the comparison variable and locomotor metric showed the slope of the relationship between the locomotor metric and $\dot{V}_{O_2,\text{dive}}$ did not significantly vary as a result of the comparison variable. The reduced model showed both the locomotor metrics and the comparison variable significantly influenced $\dot{V}_{O_2,\text{dive}}$.

Predictor (units)	**Full model**		**Reduced model (no interaction)**							
	Interaction		**Suction cup vs Neoprene**			**Locomotor Metric**			**AICc**	**BIC**
	df	**P value**	**df**	**F Ratio**	**P value**	**df**	**F Ratio**	**P value**		
Mean PDBA(x) (*g*)	1,18	0.7142	1,19	21.70	0.0002	1,19	13.76	0.0015	241.03	243.04
Mean PDBA(y) (*g*)	1,18	0.3369	1,19	16.98	0.0006	1,19	8.54	0.0087	244.85	245.38
Mean PDBA(z) (*g*)	1,18	0.1116	1,19	26.38	<.0001	1,19	10.46	0.0044	243.36	246.86
Mean PDBA(x,y) (*g*)	1,18	0.2558	1,19	21.88	0.0002	1,19	14.31	0.0013	240.66	241.68
Mean PDBA(x,z) (*g*)	1,18	0.2515	1,19	32.66	<.0001	1,19	15.86	0.0008	239.66	242.68
Mean PDBA(y,z) (*g*)	1,18	0.3496	1,19	33.74	<.0001	1,19	16.29	0.0007	239.40	241.41
Mean ODBA (*g*)	1,18	0.631	1,19	18.69	0.0004	1,19	34.93	<.0001	237.95	239.96
Mean VeDBA (*g*)	1,18	0.5601	1,19	33.85	<.0001	1,19	17.46	0.0005	238.68	240.69
f_S (strokes·min^{-1})	1,18	0.2326	1,19	9.84	0.0054	1,19	0.26	0.6191	252.72	254.73

Table 3.4: Results of linear mixed effects models examining the relationship between $\dot{V}_{O_2,\text{dive}}$ ($J \cdot kg^{-1} \cdot min^{-1}$) and locomotor metrics in Atlantic bottlenose dolphins utilizing the suction cup instrument attachment system. Predictor variables measured include single and double axis dynamic acceleration (*g*), ODBA (*g*), VeDBA (*g*), and f_S ($strokes \cdot min^{-1}$).

Predictor (units)	Equation	df	F Ratio	P	AICc	BIC	# of dives
Mean PDBA(x) (*g*)	$\dot{V}_{O_2,\text{dive}}$ = -92.41 + 2948.11 · Mean PDBA(x)	1,9	13.60	0.005	116.97	114.73	11
Mean PDBA(y) (*g*)	$\dot{V}_{O_2,\text{dive}}$ = -304.31 + 4699.99 · Mean PDBA(y)	1,9	6.62	0.0301	126.27	121.20	11
Mean PDBA(z) (*g*)	$\dot{V}_{O_2,\text{dive}}$ = 36.13 + 1058.16 · Mean PDBA(z)	1,9	5.72	0.0405	126.92	121.85	11
Mean PDBA(x,y) (*g*)	$\dot{V}_{O_2,\text{dive}}$ = -276.92 + 2370.53 · Mean PDBA(x,y)	1,9	20.76	0.0014	119.18	114.10	11
Mean PDBA(x,z) (*g*)	$\dot{V}_{O_2,\text{dive}}$ = -19.70 + 887.14 · Mean PDBA(x,z)	1,9	9.25	0.014	124.56	119.48	11
Mean PDBA(y,z) (*g*)	$\dot{V}_{O_2,\text{dive}}$ = -58.93 + 1014.89 · Mean PDBA(y,z)	1,9	7.80	0.021	125.47	120.40	11
Mean ODBA (*g*)	$\dot{V}_{O_2,\text{dive}}$ = -94.37 + 844.41 · Mean ODBA	1,9	11.39	0.0082	123.34	118.26	11
Mean VeDBA (*g*)	$\dot{V}_{O_2,\text{dive}}$ = -79.86 + 1180.58 · Mean VeDBA	1,9	10.23	0.0109	123.98	118.91	11
f_S ($strokes \cdot min^{-1}$)	$\dot{V}_{O_2,\text{dive}} = 1.13 + 5.20 \cdot f_S$ *(Not Significant)*	1,9	0.83	0.3852	131.36	126.29	11

Table 3.5: Results of linear mixed effects models examining the relationship between $\dot{V}_{O_2,\text{dive}}$ ($J \cdot kg^{-1} \cdot min^{-1}$) and locomotor metrics in an Atlantic bottlenose dolphin utilizing the neoprene instrument mount. Predictor variables measured include single and double axis dynamic acceleration (*g*), ODBA (*g*), VeDBA (*g*), and f_S ($strokes \cdot min^{-1}$).

Predictor (units)	Equation	df	F Ratio	P	AIC	BIC	# of dives
Mean PDBA(x) (*g*)	$\dot{V}_{O_2,\text{dive}} = 51.73 + 2399.52 \cdot$ Mean PDBA(x) *(Not Significant)*	1,9	4.37	0.0662	129.30	127.07	11
Mean PDBA(y) (*g*)	$\dot{V}_{O_2,\text{dive}} = 32.66 + 2230.87 \cdot$ Mean PDBA(y) *(Not Significant)*	1,9	3.90	0.0796	126.64	124.40	11
Mean PDBA(z) (*g*)	$\dot{V}_{O_2,\text{dive}} = 20.84 + 2751.10 \cdot$ Mean PDBA(z)	1,9	8.02	0.0196	129.69	127.45	11
Mean PDBA(x,y) (*g*)	$\dot{V}_{O_2,\text{dive}} = 21.73 + 1269.12 \cdot$ Mean PDBA(x,y) *(Not Significant)*	1,9	4.74	0.0575	131.54	126.46	11
Mean PDBA(x,z) (*g*)	$\dot{V}_{O_2,\text{dive}} = -12.50 + 1585.56 \cdot$ Mean PDBA(x,z)	1,9	8.56	0.0169	129.00	126.76	11
Mean PDBA(y,z) (*g*)	$\dot{V}_{O_2,\text{dive}} = -44.07 + 1631.65 \cdot$ Mean PDBA(y,z)	1,9	9.03	0.0148	126.01	123.77	11
Mean ODBA (*g*)	$\dot{V}_{O_2,\text{dive}} = -29.49 + 1064.18 \cdot$ Mean ODBA	1,9	8.03	0.0196	126.64	124.40	11
Mean VeDBA (*g*)	$\dot{V}_{O_2,\text{dive}} = -26.41 + 1576.53 \cdot$ Mean VeDBA	1,9	7.82	0.0208	126.77	124.54	11
f_S ($strokes \cdot min^{-1}$)	$\dot{V}_{O_2,\text{dive}} = 383.75 - 4.64 \cdot f_S$ *(Not Significant)*	1,9	0.93	0.3605	132.57	130.34	11

Table 3.6: Results of ANCOVA examining the relationships between $\dot{V}_{O_2}$ and locomotor metrics for manatees swimming at the surface and while submerged. For both the full and reduced model, $\dot{V}_{O_2}$ was the dependent variable and the locomotor metric was fixed. The comparison variable, surface or submerged swimming, was also included as a fixed variable in both models. The interaction between the comparison variable and locomotor metric showed the slope of the relationship between the locomotor metric and $\dot{V}_{O_2}$ did not significantly vary due to the comparison variable for all locomotor metrics with the exception of PDBA(z). The reduced model showed both the locomotor metrics and the comparison variable significantly influenced $\dot{V}_{O_2}$.

Predictor (units)	**Full model**		**Reduced model (no interaction)**							
	Interaction		**Surface vs Submerged**			**Locomotor Metric**			**AICc**	**BIC**
	df	**P value**	**df**	**F Ratio**	**P value**	**df**	**F Ratio**	**P value**		
Mean PDBA(x) (*g*)	1,22	0.5263	1,23	31.03	<.0001	1,23	41.53	<.0001	166.52	169.82
Mean PDBA(y) (*g*)	1,22	0.3457	1,23	37.24	<.0001	1,23	24.91	<.0001	174.27	177.56
Mean PDBA(z) (*g*)	1,22	0.0076	--	--	--	--	--	--	--	--
Mean PDBA(x,y) (*g*)	1,22	0.6201	1,23	37.95	<.0001	1,23	39.55	<.0001	167.33	170.63
Mean PDBA(x,z) (*g*)	1,22	0.6322	1,23	53.95	<.0001	1,23	44.84	<.0001	165.22	168.51
Mean PDBA(y,z) (*g*)	1,22	0.722	1,23	56.12	<.0001	1,23	32.72	<.0001	170.34	173.63
Mean ODBA (*g*)	1,22	0.8395	1,23	51.33	<.0001	1,23	41.85	<.0001	166.40	169.69
Mean VeDBA (*g*)	1,22	0.9101	1,23	52.85	<.0001	1,23	42.56	<.0001	166.11	169.40
f_S (strokes·min^{-1})	1,22	0.0757	1,23	17.01	0.0004	1,23	0.11	0.7388	193.22	196.51

Table 3.7: Results of linear mixed effects models examining the relationship between $\dot{V}_{O_2,\text{dive}}$ (J·kg^{-1}·min^{-1}) and locomotor metrics in West Indian manatees swimming while submerged. Predictor variables measured include single and double axis dynamic acceleration (*g*), ODBA (*g*), VeDBA (*g*), and f_S (strokes·min^{-1}).

Predictor (units)	**Equation**	**df**	**F Ratio**	**P**	**AICc**	**BIC**	**# of dives**
Mean PDBA(x) (*g*)	$\dot{V}_{O_2,\text{dive}} = 0.05 + 478.91 \cdot$ Mean PDBA(x)	1,10	25.52	0.0005	84.49	80.71	16
Mean PDBA(y) (*g*)	$\dot{V}_{O_2,\text{dive}} = 2.57 + 582.63 \cdot$ Mean PDBA(y)	1,10	24.85	0.0005	80.01	78.46	16
Mean PDBA(z) (*g*)	$\dot{V}_{O_2,\text{dive}} = 0.85 + 671.34 \cdot$ Mean PDBA(z)	1,10	17.64	0.0018	82.79	81.24	16
Mean PDBA(x,y) (*g*)	$\dot{V}_{O_2,\text{dive}} = 0.84 + 269.32 \cdot$ Mean PDBA(x,y)	1,10	27.55	0.0004	79.11	77.57	16
Mean PDBA(x,z) (*g*)	$\dot{V}_{O_2,\text{dive}} = 0.08 + 285.17 \cdot$ Mean PDBA(x,z)	1,10	23.21	0.0007	85.30	81.52	16
Mean PDBA(y,z) (*g*)	$\dot{V}_{O_2,\text{dive}} = 1.45 + 319.43 \cdot$ Mean PDBA(y,z)	1,10	22.74	0.0008	80.75	79.21	16
Mean ODBA (*g*)	$\dot{V}_{O_2,\text{dive}} = 0.66 + 194.77 \cdot$ Mean ODBA	1,10	25.18	0.0005	79.89	78.35	16
Mean VeDBA (*g*)	$\dot{V}_{O_2,\text{dive}} = 0.19 + 292.77 \cdot$ Mean VeDBA	1,10	24.75	0.0006	84.75	80.98	16
f_S (strokes·min^{-1})	$\dot{V}_{O_2,\text{dive}} = 16.53 + 0.05 \cdot f_S$ *(Not Significant)*	1,10	0.00	0.9628	90.92	84.12	14

Table 3.8: Results of linear mixed effects models examining the relationship between $\dot{V}_{O_2,\text{dive}}$ (J·kg^{-1}·min^{-1}) and locomotor metrics in West Indian manatees swimming at the surface. Predictor variables measured include single and double axis dynamic acceleration (*g*), ODBA (*g*), VeDBA (*g*), and f_S (strokes·min^{-1}).

Predictor (units)	Equation	df	F Ratio	P	AICc	BIC	# of dives
Mean PDBA(x) (*g*)	$\dot{V}_{O_2,\text{dive}} = 14.06 + 390.06 \cdot \text{Mean PDBA(x)}$	1,12	15.12	0.0022	94.87	92.98	26
Mean PDBA(y) (*g*)	$\dot{V}_{O_2,\text{dive}} = 20.41 + 386.26 \cdot \text{Mean PDBA(y)}$	1,12	5.24	0.041	101.21	99.32	26
Mean PDBA(z) (*g*)	$\dot{V}_{O_2,\text{dive}} = 2.72 + 1822.95 \cdot \text{Mean PDBA(z)}$	1,12	43.15	< .0001	84.93	83.04	26
Mean PDBA(x,y) (*g*)	$\dot{V}_{O_2,\text{dive}} = 15.30 + 227.74 \cdot \text{Mean PDBA(x,y)}$	1,12	12.23	0.0044	96.45	94.56	26
Mean PDBA(x,z) (*g*)	$\dot{V}_{O_2,\text{dive}} = 11.49 + 332.50 \cdot \text{Mean PDBA(x,z)}$	1,12	19.41	0.0009	92.81	90.92	26
Mean PDBA(y,z) (*g*)	$\dot{V}_{O_2,\text{dive}} = 15.60 + 367.85 \cdot \text{Mean PDBA(y,z)}$	1,12	9.71	0.0089	97.98	96.09	26
Mean ODBA (*g*)	$\dot{V}_{O_2,\text{dive}} = 13.48 + 208.47 \cdot \text{Mean ODBA}$	1,12	14.76	0.0023	95.06	93.17	26
Mean VeDBA (*g*)	$\dot{V}_{O_2,\text{dive}} = 13.58 + 303.90 \cdot \text{Mean VeDBA}$	1,12	15.54	0.002	94.66	92.77	26
f_S (strokes·min^{-1})	$\dot{V}_{O_2,\text{dive}} = 3.15 + 2.86 \cdot f_S$	1,12	5.48	0.0373	101.01	99.13	26

Table 3.9: Results of Models 1 and 2 examining the relationship between $\dot{V}_{O_2,\text{dive}}$ and locomotor metrics for the combined odontocete dataset (beluga whales and dolphins). Model 1 demonstrated no significant effect from the interaction between each locomotor metric and species, showing there was no significant difference in the slope of the relationship between $\dot{V}_{O_2,\text{dive}}$ and the individual locomotor metrics. Model 2 showed that species did have a significant effect on the mean values for two of the locomotor metrics, as is expected given the size difference between the beluga whales and dolphins in this study.

Predictor (units)	Model 1		Model 2							
	Interaction		Species			Locomotor Metric			AICc	BIC
	df	P value	df	F Ratio	P value	df	F Ratio	P value		
Mean PDBA(x) (*g*)	1,27	0.5179	1,28	0.33	0.568	1,28	18.65	0.0002	-42.85	-38.08
Mean PDBA(y) (*g*)	1,27	0.1403	1,28	3.33	0.0786	1,28	18.22	0.0002	-45.43	-41.23
Mean PDBA(z) (*g*)	1,27	0.191	1,28	0.87	0.3593	1,28	2.33	0.1383	-32.37	-28.17
Mean PDBA(x,y) (*g*)	1,27	0.2423	1,28	7.00	0.0132	1,28	37.18	<.0001	-56.09	-51.89
Mean PDBA(x,z) (*g*)	1,27	0.522	1,28	0.00	0.9472	1,28	8.32	0.0075	-37.96	-33.76
Mean PDBA(y,z) (*g*)	1,27	0.7528	1,28	1.22	0.2784	1,28	10.54	0.003	-39.80	-35.60
Mean ODBA (*g*)	1,27	0.8729	1,28	2.14	0.155	1,28	16.78	0.0003	-44.45	-40.25
Mean VeDBA (*g*)	1,27	0.9968	1,28	2.10	0.1587	1,28	16.63	0.0003	-44.35	-40.15
f_S (strokes·min^{-1})	1,37	0.5879	1,38	16.92	0.0002	1,38	21.67	<.0001	-42.95	-36.10

Table 3.10: Results of Models 1 and 2 examining the relationship between $\dot{V}_{O_2,\text{dive}}$ and locomotor metrics for the combined species dataset (beluga whales, dolphins, and manatees). Model 1 demonstrated no significant effect from the interaction between each locomotor metric and species, showing there was no significant difference in the slope of the relationship between $\dot{V}_{O_2,\text{dive}}$ and the individual locomotor metrics. Model 2 showed that species did have a significant effect on the mean values for all locomotor metrics, as is expected given the increased size and speed difference between the three species included in this model.

Predictor (units)	**Model 1**		**Model 2**							
	Interaction		**Species**			**Locomotor Metric**			**AICc**	**BIC**
	df	**P value**	**df**	**F Ratio**	**P value**	**df**	**F Ratio**	**P value**		
Mean PDBA(x) (*g*)	2,38	0.4739	2,40	23.90	<.0001	1,40	26.28	<.0001	-36.55	-29.21
Mean PDBA(y) (*g*)	2,38	0.2007	2,40	14.84	<.0001	1,40	23.60	<.0001	-34.73	-27.39
Mean PDBA(z) (*g*)	2,38	0.3374	2,40	18.62	<.0001	1,40	13.73	0.0006	-27.31	-19.97
Mean PDBA(x,y) (*g*)	2,38	0.0691	2,40	16.53	<.0001	1,40	29.07	<.0001	-38.36	-31.02
Mean PDBA(x,z) (*g*)	2,38	0.8724	2,40	18.68	<.0001	1,40	21.79	<.0001	-33.46	-26.12
Mean PDBA(y,z) (*g*)	2,38	0.7611	2,40	15.26	<.0001	1,40	22.20	<.0001	-33.75	-26.41
Mean ODBA (*g*)	2,38	0.4937	2,40	16.20	<.0001	1,40	25.66	<.0001	-36.13	-28.79
Mean VeDBA (*g*)	2,38	0.5447	2,40	17.88	<.0001	1,40	25.96	<.0001	-36.33	-28.99
f_S (strokes·min^{-1})	2,45	0.1473	2,47	11.56	<.0001	1,47	5.66	0.0215	-9.87	-0.19

3.11: Results of linear mixed effects models examining the relationship between $\dot{V}_{O_2,\text{dive}}$ ($J \cdot kg^{-1} \cdot min^{-1}$) and locomotor metrics in two odontocetes (beluga whales and Atlantic bottlenose dolphins). Predictor variables measured include single and double axis dynamic acceleration (*g*), ODBA (*g*), VeDBA (*g*), and f_S ($strokes \cdot min^{-1}$). Log values were used for predictor and response variables to account for increasing variation with increasing acceleration.

Predictor (units)	Equation	df	F Ratio	P	AICc	BIC	# of dives
Mean PDBA(x) (*g*)	$\log \dot{V}_{O_2,\text{dive}} = 3.87 + 1.58 \cdot \log$ Mean PDBA(x)	1,29	51.10	<.0001	-45.43	-41.24	31
Mean PDBA(y) (*g*)	$\log \dot{V}_{O_2,\text{dive}} = 3.17 + 0.97 \cdot \log$ Mean PDBA(z)	1,29	42.77	<.0001	-44.68	-41.27	31
Mean PDBA(z) (*g*)	$\log \dot{V}_{O_2,\text{dive}} = 2.76 + 0.62 \cdot \log$ Mean PDBA(y)	1,29	22.12	<.0001	-34.16	-30.74	31
Mean PDBA(x,y) (*g*)	$\log \dot{V}_{O_2,\text{dive}} = 3.19 + 1.34 \cdot \log$ Mean PDBA(x,y)	1,29	61.61	<.0001	-51.90	-48.49	31
Mean PDBA(x,z) (*g*)	$\log \dot{V}_{O_2,\text{dive}} = 2.86 + 0.96 \cdot \log$ Mean PDBA(x,z)	1,29	34.10	<.0001	-40.69	-37.27	31
Mean PDBA(y,z) (*g*)	$\log \dot{V}_{O_2,\text{dive}} = 2.75 + 0.83 \cdot \log$ Mean PDBA(y,z)	1,29	35.18	<.0001	-41.21	-37.80	31
Mean ODBA (*g*)	$\log \dot{V}_{O_2,\text{dive}} = 2.74 + 1.03 \cdot \log$ Mean ODBA	1,29	43.31	<.0001	-44.91	-41.50	31
Mean VeDBA (*g*)	$\log \dot{V}_{O_2,\text{dive}} = 2.90 + 1.01 \cdot \log$ Mean VeDBA	1,29	43.16	<.0001	-44.84	-41.43	31
f_S ($strokes \cdot min^{-1}$)	$\log \dot{V}_{O_2,\text{dive}} = 0.51 + 1.04 \cdot \log f_S$	1,39	10.44	0.0025	-30.52	-24.77	41

Table 3.12: Results of linear mixed effects models examining the relationship between $\dot{V}_{O_2,\text{dive}}$ (J·kg^{-1}·min^{-1}) and locomotor metrics in three marine mammals (beluga whales, Atlantic bottlenose dolphins, and West Indian manatees). Predictor variables measured include single and double axis dynamic acceleration (*g*), ODBA (*g*), VeDBA (*g*), and f_S (strokes·min^{-1}). Log values were used for predictor and response variables to account for increasing variation with increasing acceleration.

Predictor (units)	Equation	df	F Ratio	P	AICc	BIC	# of dives
Mean PDBA(x) (*g*)	$\log \dot{V}_{O_2,\text{dive}} = 4.25 + 1.96 \cdot \log$ Mean PDBA(x)	1,42	176.37	<.0001	-4.66	1.45	44
Mean PDBA(y) (*g*)	$\log \dot{V}_{O_2,\text{dive}} = 3.73 + 1.48 \cdot \log$ Mean PDBA(z)	1,42	221.97	<.0001	-13.00	-6.89	44
Mean PDBA(z) (*g*)	$\log \dot{V}_{O_2,\text{dive}} = 3.55 + 1.36 \cdot \log$ Mean PDBA(y)	1,42	159.20	<.0001	-1.056	5.06	44
Mean PDBA(x,y) (*g*)	$\log \dot{V}_{O_2,\text{dive}} = 3.51 + 1.76 \cdot \log$ Mean PDBA(x,y)	1,42	231.49	<.0001	-14.56	-8.45	44
Mean PDBA(x,z) (*g*)	$\log \dot{V}_{O_2,\text{dive}} = 3.40 + 1.66 \cdot \log$ Mean PDBA(x,z)	1,42	189.07	<.0001	-7.14	-1.03	44
Mean PDBA(y,z) (*g*)	$\log \dot{V}_{O_2,\text{dive}} = 3.24 + 1.45 \cdot \log$ Mean PDBA(y,z)	1,42	213.13	<.0001	-11.50	-5.39	44
Mean ODBA (*g*)	$\log \dot{V}_{O_2,\text{dive}} = 3.10 + 1.63 \cdot \log$ Mean ODBA	1,42	220.34	<.0001	-12.73	-6.62	44
Mean VeDBA (*g*)	$\log \dot{V}_{O_2,\text{dive}} = 3.40 + 1.65 \cdot \log$ Mean VeDBA	1,42	209.81	<.0001	-10.93	-4.82	44
f_S (strokes·min^{-1})	$\log \dot{V}_{O_2,\text{dive}} = -0.37 + 1.61 \cdot \log f_S$	1,49	122.49	<.0001	5.37	12.22	52

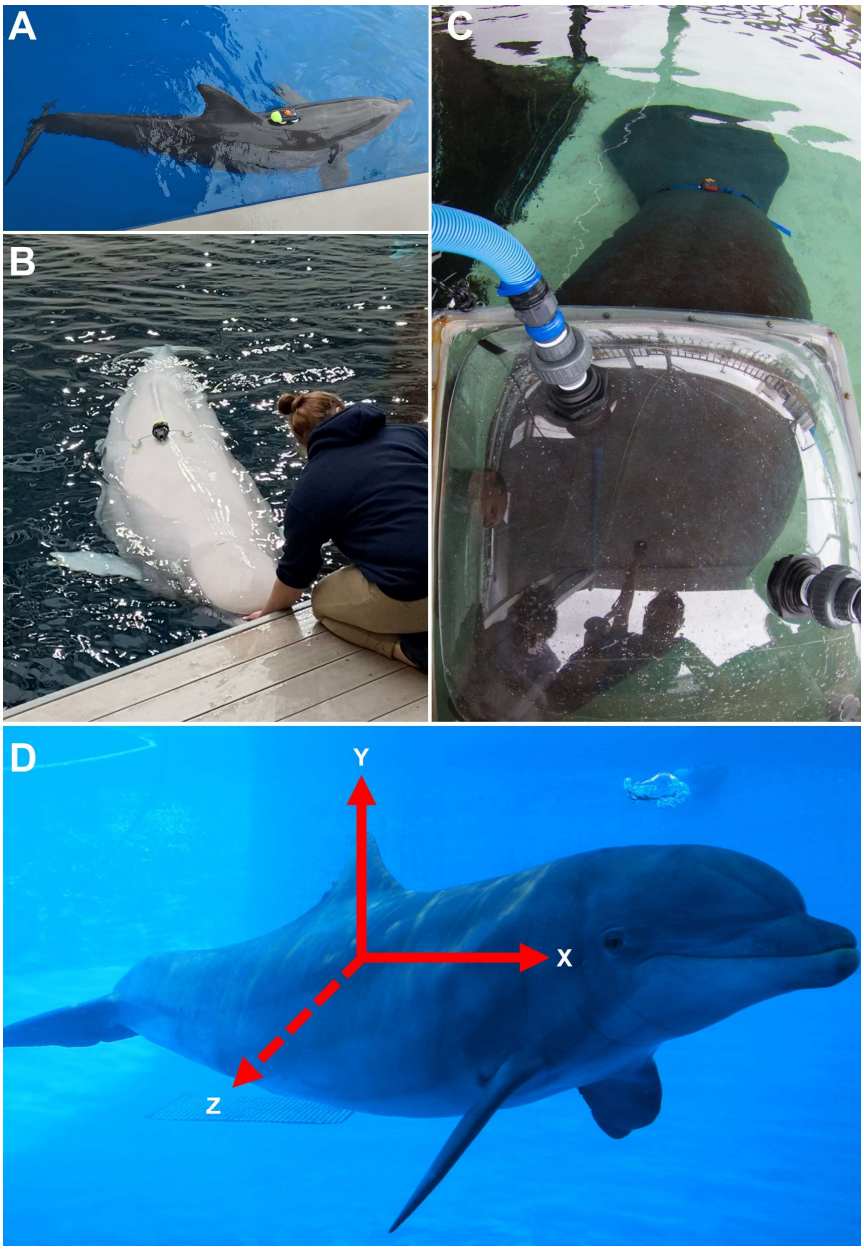

Figure 3.1: Animal borne instrumentation for measuring acceleration in (A) bottlenose dolphins, (B) beluga whales, and (C) manatees. Instrument training began 6-12 months prior to data collection to ensure physiologically relevant status and behaviors throughout trials. (D) Schematic representation of acceleration axes measured using animal-borne accelerometer. X-axis acceleration measured movement in the rostral-caudal plane, Y-axis acceleration measured movement in the dorso-ventral plane, and Z-axis acceleration measured movement in the lateral plane.

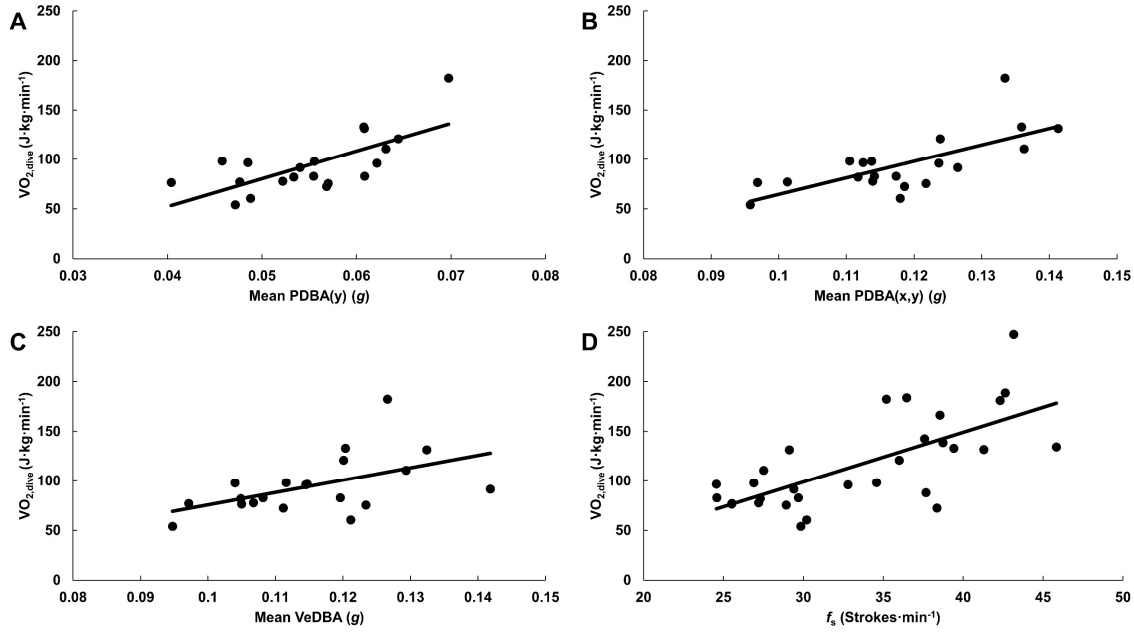

Figure 3.2: The rate of oxygen consumption (J·kg^{-1}·min^{-1}) of beluga whales during a dive plotted against the strongest (A) single, (B) double, and (C) tri-axial dynamic acceleration metrics as well as (D) f_S. For the three categories of acceleration metrics, the whales exhibited the strongest relationships between $\dot{V}_{O_2,\text{dive}}$ and PDBA(y), PDBA(x,y), and VeDBA, respectively. Each point represents the average value and rate of oxygen consumption for a single dive by an individual animal. Solid lines are the least squares linear regressions as described by the corresponding equations in Table 3.2.

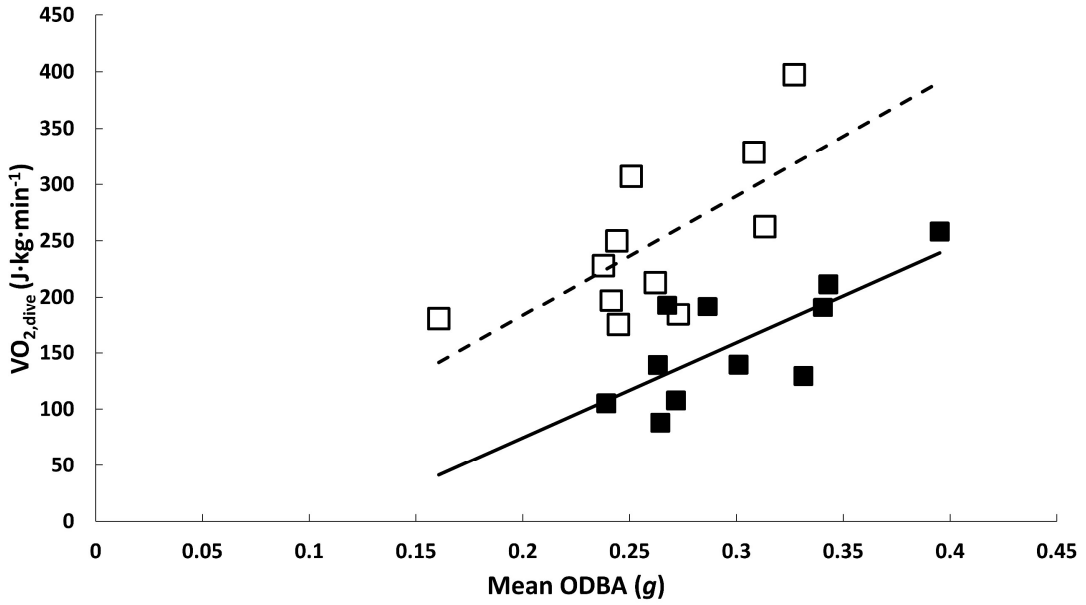

Figure 3.3: The rate of oxygen consumption ($J \cdot kg^{-1} \cdot min^{-1}$) during submerged swimming plotted against mean ODBA for bottlenose dolphins wearing a neoprene instrument mount (Open squares, dashed line) and suction cup instrument mount (closed squares, solid line). ODBA was used as the locomotor metric with the strongest comparative model according to AICc and BIC scores (Table 3.3). Both animals exhibited the same resting metabolic rate and similar levels of acceleration, however the dolphin wearing the wetsuit instrument mount exhibited significantly higher rates of oxygen consumption indicating increased cost compared to the more streamlined suction cup mount.

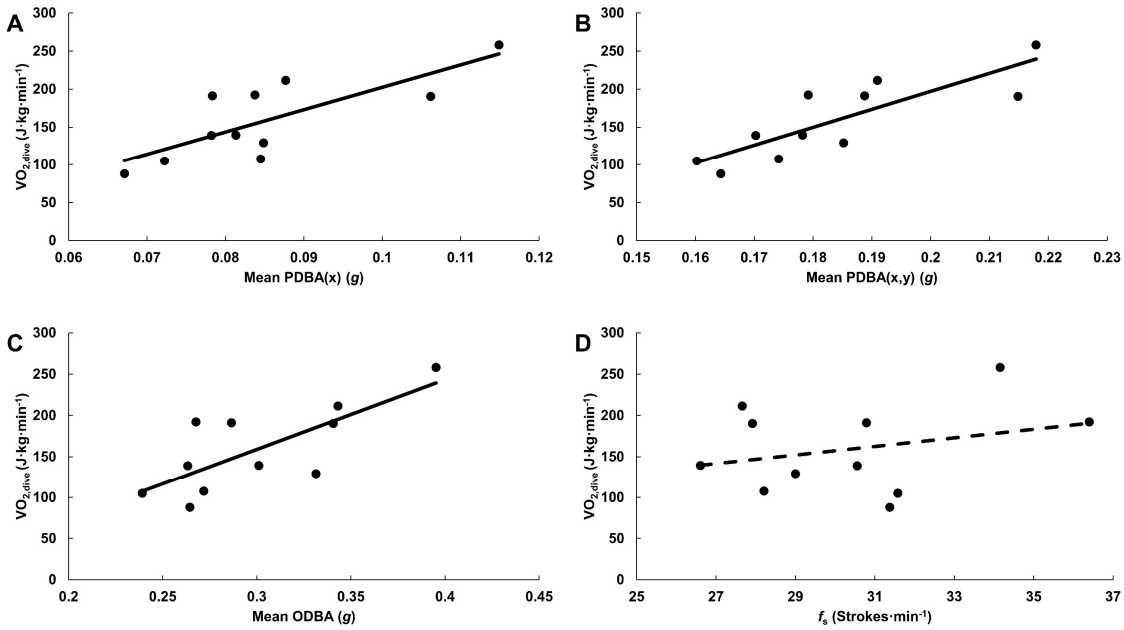

Figure 3.4: The rate of oxygen consumption (J·kg^{-1}·min^{-1}) during a dive in an Atlantic bottlenose dolphin wearing the instrument attached with suction cups plotted against the strongest (A) single, (B) double, and (C) tri-axial dynamic acceleration metrics as well as (D) f_S. For the three categories of acceleration metrics, the dolphin exhibited the strongest relationships between $\dot{V}_{O_2,\text{dive}}$ and PDBA(x), PDBA(x,y), and ODBA, respectively. Each point represents the average value and rate of oxygen consumption for a single dive by an individual animal. Lines are the least squares linear regressions as described by the corresponding equations in table 3.4. Solid lines represent significant relationships. Dashed lines represent non-significant relationships.

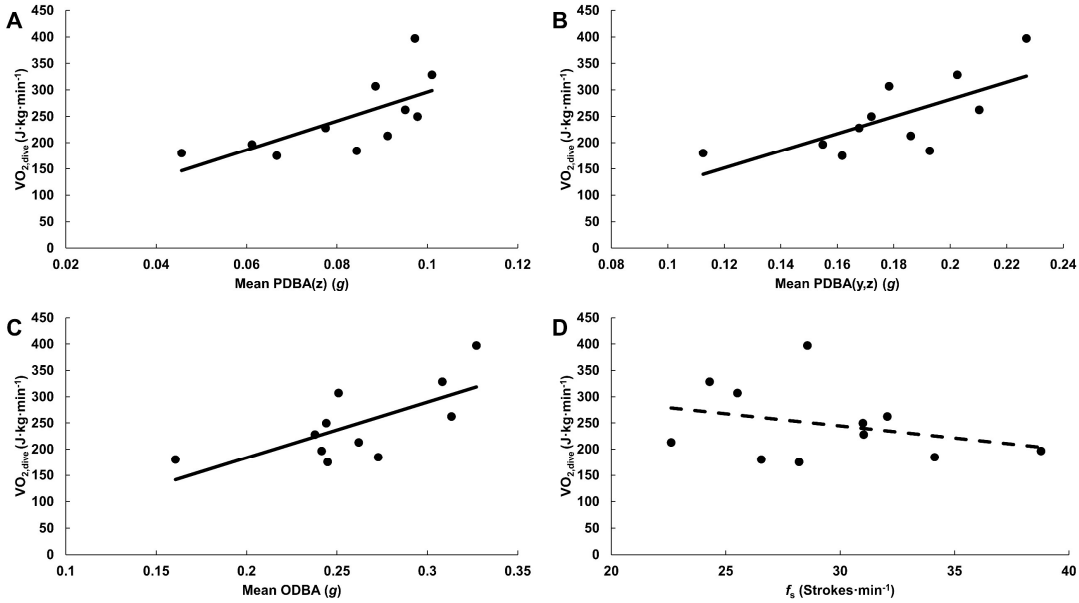

Figure 3.5: The rate of oxygen consumption (J·kg^{-1}·min^{-1}) during a dive in an Atlantic bottlenose dolphin wearing the instrument attached with a neoprene instrument vest plotted against the strongest (A) single, (B) double, and (C) tri-axial dynamic acceleration metrics as well as (D) f_S. For the three categories of acceleration metrics, the dolphin exhibited the strongest relationships between $\dot{V}_{O_2,\text{dive}}$ and PDBA(z), PDBA(y,z), and ODBA, respectively. Each point represents the average value and rate of oxygen consumption for a single dive by an individual animal. Lines are the least squares linear regressions as described by the corresponding equations in Table 3.5. Solid lines represent significant relationships. Dashed lines represent non-significant relationships.

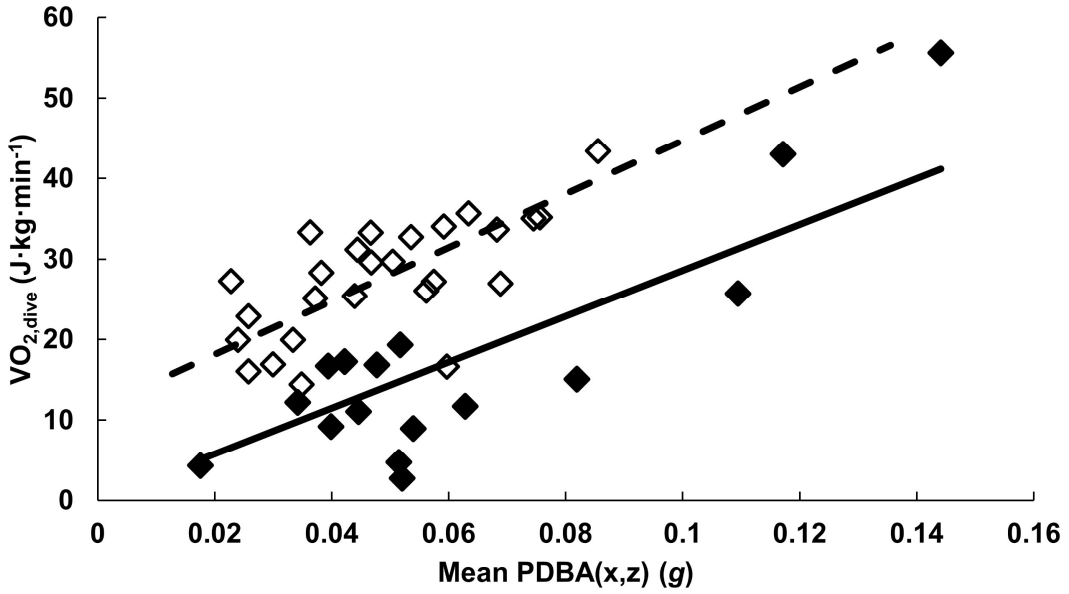

Figure 3.6: The rate of oxygen consumption ($J \cdot kg^{-1} \cdot min^{-1}$) during locomotion plotted against mean PDBA(x,z) for manatees swimming at the surface (open diamonds, dashed line) and submerged (closed diamonds, solid line). PDBA(x,z) was used as the locomotor metric with the strongest comparative model according to AICc and BIC scores (Table 3.6). Despite similar levels of acceleration and no significant difference in the slopes for both modes of locomotion, there was a significant difference in the mean values of the relationships. This indicates an increased cost of locomotion during surface swimming compared to submerged swimming.

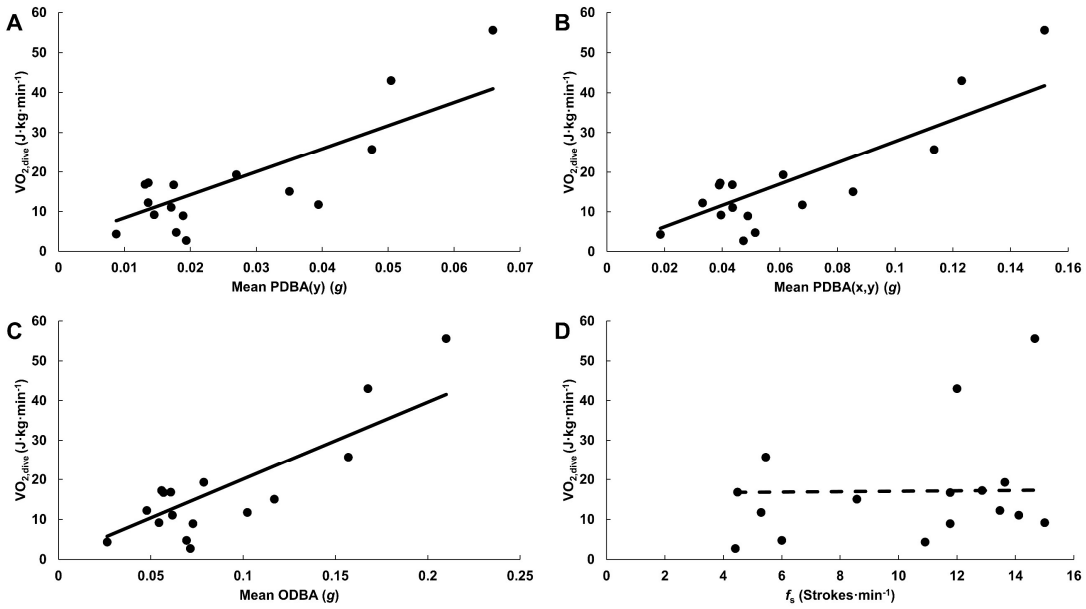

Figure 3.7: The rate of oxygen consumption (J·kg^{-1}·min^{-1}) of manatees swimming submerged plotted against the strongest (A) single, (B) double, and (C) tri-axial dynamic acceleration metrics as well as (D) f_S. For the three categories of acceleration metrics, the manatees exhibited the strongest relationships between $\dot{V}_{O_2,\text{dive}}$ and PDBA(x), PDBA(x,y), and ODBA, respectively. Each point represents the average value and rate of oxygen consumption for a single dive by an individual animal. Lines are the least squares linear regressions as described by the corresponding equations in Table 3.7. Solid lines represent significant relationships. Dashed lines represent non-significant relationships.

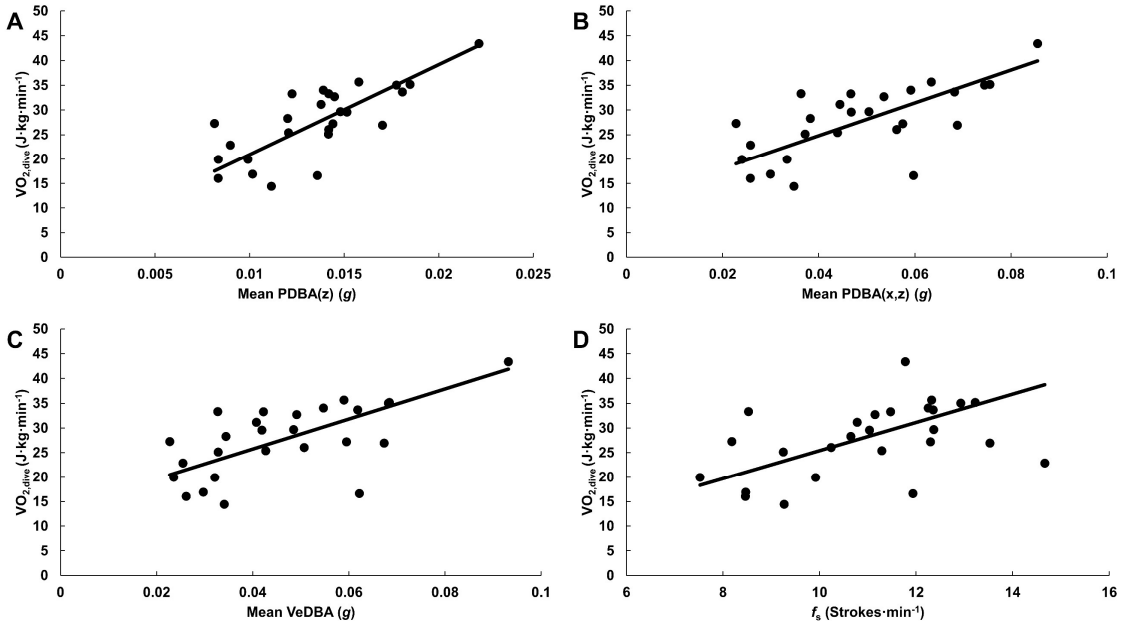

Figure 3.8: The rate of oxygen consumption (J·kg^{-1}·min^{-1}) for manatees swimming at the surface plotted against the strongest (A) single, (B) double, and (C) tri-axial dynamic acceleration metrics as well as (D) f_S. For the three categories of acceleration metrics, manatees exhibited the strongest relationships between $\dot{V}_{O_2,\text{dive}}$ and PDBA(z), PDBA(x,z), and VeDBA, respectively. Each point represents the average value and rate of oxygen consumption for a single dive by an individual animal. Solid lines are the least squares linear regressions as described by the corresponding equations in Table 3.8.

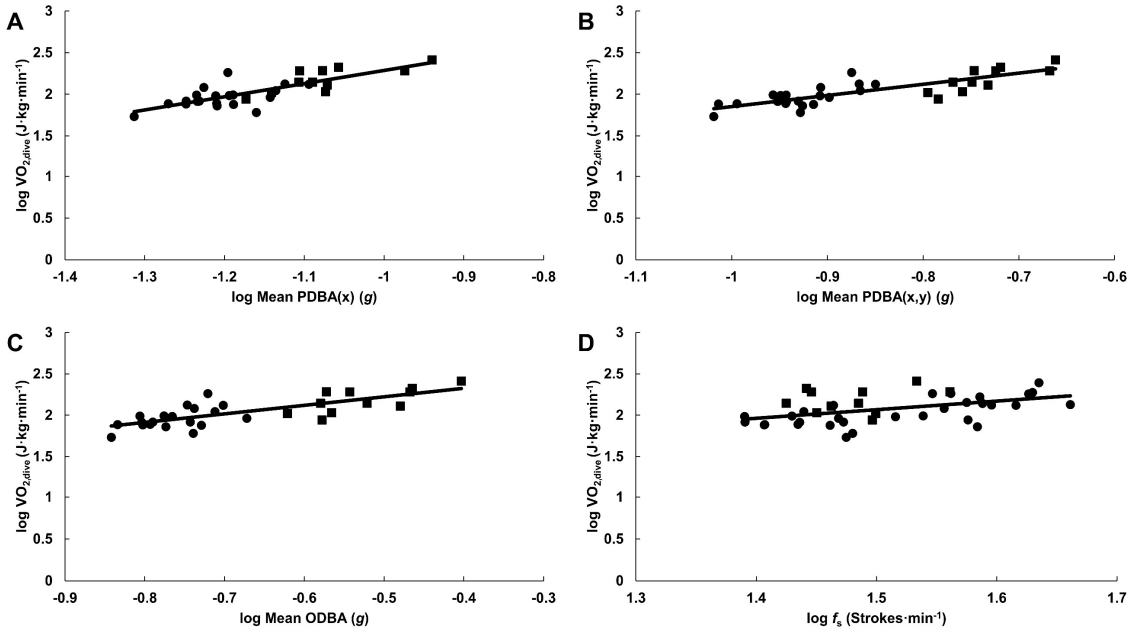

Figure 3.9: The log of the rate of oxygen consumption ($J \cdot kg^{-1} \cdot min^{-1}$) during a dive in two odontocetes, beluga whales (circles) and Atlantic bottlenose dolphins (squares) plotted against the log of the strongest (A) single, (B) double, and (C) tri-axial dynamic acceleration metrics as well as (D) f_S. For the three categories of acceleration metrics, odontocetes exhibited the strongest relationships between log $\dot{V}_{O_2,\text{dive}}$ and log PDBA(x), log PDBA(x,y), and log ODBA, respectively. Each point represents the average value and rate of oxygen consumption for a single dive by an individual animal. Solid lines are the least squares linear regressions as described by the corresponding equations in Table 3.11.

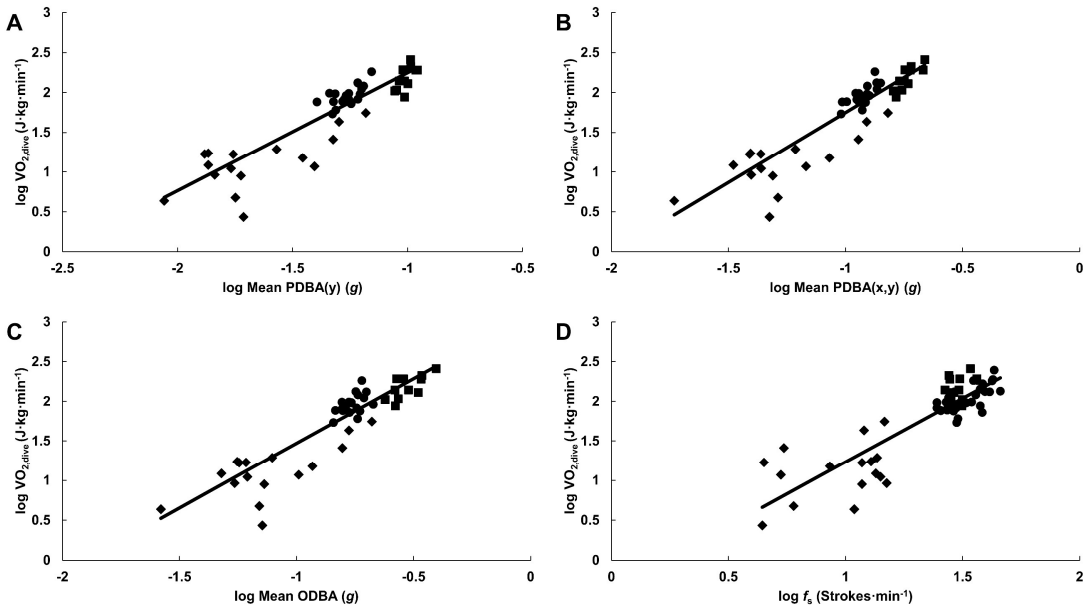

Figure 3.10: The log of the rate of oxygen consumption ($J \cdot kg^{-1} \cdot min^{-1}$) during a dive in beluga whales (circles), Atlantic bottlenose dolphins (squares), and West Indian manatees (diamonds) plotted against the log of the strongest (A) single, (B) double, and (C) tri-axial dynamic acceleration metrics as well as (D) f_S. For the three categories of acceleration metrics, the animals exhibited the strongest relationships between log $\dot{V}_{O_2,\text{dive}}$ and log PDBA(y), log PDBA(x,y), and log ODBA, respectively. Each point represents the average value and rate of oxygen consumption for a single dive by an individual animal. Solid lines are the least squares linear regressions as described by the corresponding equations in Table 3.12.

CONCLUSION

Marine mammals are currently facing unprecedented levels of environmental change and disturbance (Costa, 2012; Kendall et al., 2013; Lotze et al., 2017; McHuron et al., 2017; Pirotta et al., 2019; Williams et al., 2017a). Changes in environmental temperature (Learmonth et al., 2006), prey distribution (Pirotta et al., 2018b), and habitat conditions such as sea-ice extent (Pagano et al., 2018; Williams et al., 2011b) are affecting the availability of previously used resources. Increases in acoustic and environmental pollution (NMFS, 2016; Tyack, 2008; Villegas-Amtmann et al., 2015), commercial shipping (Berman-Kowalewski et al., 2010; Caswell et al., 1999), marine resource exploration (Williams et al., 2017a), and other anthropogenic disturbances are resulting in health impacts and behavioral changes that can affect these species at both the individual and population level (Caswell et al., 1999; Lotze et al., 2017; Martin et al., 2016; Nowacek et al., 2004; Wells and Scott, 1997). Understanding the physiological impacts of these changes and disturbances is essential to predicting the capacity of these animals to adapt and survive in the rapidly changing marine environment (Bejarano et al., 2017; Costa and Maresh, 2017; Costa et al., 2016; Doak et al., 2014; Gallagher et al., 2017; Maresh et al., 2014; McHuron et al., 2017; McHuron et al., 2018; Otani et al., 2001; Pirotta et al., 2018a; Pirotta et al., 2018b; Villegas-Amtmann et al., 2015; Williams et al., 2017b; Williams et al., 2017a). This dissertation represents important steps in increasing our knowledge of swimming and diving

physiology in marine mammals as well as our ability to continue studying these animals in the wild.

Examining a species' energetics relative to other marine and terrestrial mammals, as was done in **Chapters 1 and 2,** can help us understand the adaptations that determine fitness of a population (Williams, 1999; Williams et al., 2004b). The low maintenance costs exhibited by both the West Indian manatee and Hawaiian monk seal have allowed these species to persist in areas with low quality or patchy food resources (Baker et al., 2007; Bengston, 1983; Best, 1981; Parrish et al., 2005). However, the species' statuses as threatened and endangered, respectively, also shows the precarious nature of the advantages conferred by these adaptations. By demonstrating the costs associated with locomotion for these species are similar to other marine mammals and thus elevated relative to their typical maintenance costs, we can begin to understand the physiological stresses they are exposed to.

For example, manatees are particularly vulnerable to cold water temperatures due to their low metabolic rates and low insulation (Bossart et al., 2004; Laist et al., 2013). The population's habitat typically expands during warmer months to take advantage of dispersed food. Rapid changes in water temperature can leave the animals stranded in isolated warm water refugia or require relocation to warmer waters, necessitating increased locomotion and increased metabolic thermoregulation during transit. However, both would require increased energy expenditure despite the relatively low quality of the species' typical food source. For Hawaiian monk seals, decreased prey availability (Baker et al., 2007; Parrish et al., 2005) has required

increased energetic investment in foraging and disproportionately affects juvenile survival. Juvenile pinnipeds require time to build the physiological resources necessary for diving even in temperate and polar species (Noren et al., 2001; Somo et al., 2015). Given the patchy prey availability, juvenile monk seals would require additional time to build oxygen stores sufficient to provide for the cost of swimming. As such, it is little surprise that this group would be greater affected.

Unlike manatees and monk seals, beluga whales exhibit maintenance costs and locomotor costs similar to other cold-water marine mammals. Measurement of the species' resting and locomotor costs enables researchers to more accurately model the prey requirements for individuals and populations as well as the energetic costs of disturbances. For endangered populations such as the Cook Inlet beluga whale (NMFS, 2016), this information can be used to create bioenergetic models that allow researchers to elucidate the underlying causes of the group's continued decline in population size (Costa, 2012; Pirotta et al., 2018a; Pirotta et al., 2018b).

For the threatened and endangered species above, understanding how maintenance and locomotor costs interact helps us understand why these species are vulnerable and can enable more effective management and conservation practices. However, it is difficult to measure locomotor costs or apply energetic measurements to many marine mammal species in the wild (Hunt et al., 2013; NMFS, 2016; Williams et al., 2014). The locomotor metrics evaluated and calibrated in **Chapters 2 and 3**, along with the interactions described in **Chapters 1 and 2**, will allow researchers to begin bridging the gap between data collected in aquaria and applying that data to wild

animals. This will allow definition of transport costs to predict prey requirements, energetic costs of disturbance responses, and examination of species that are impossible to work with in managed care as a result of their size or cryptic behaviors (Halsey et al., 2009b; Jeanniard-du-Dot et al., 2016; Pagano and Williams, 2019; Wilson et al., 2006; Wilson et al., 2019). However, more work is still needed.

As shown in the chapters above, depth, dive response, surface drag, body condition, and instrument attachment are just some of the factors that can affect the energetic costs of both maintenance and locomotion in marine mammals. To increase the accuracy of energetic measurements in the wild, and thus ensure accurate bioenergetic modeling, continued work is needed to directly measure the impact of these energetic variables on a wider range of species. This must be done under controlled conditions that are usually only found in aquaria, rehabilitation, and research facilities, but it is essential to crafting effective management and conservation policies for wild marine mammals. This dissertation is just one more step forward in those continued efforts to better understand and protect these incredible, but vulnerable, species.

Bibliography

Alsenz, H., Regnery, J., Ashckenazi-Polivoda, S., Meilijson, A., Ron-Yankovich, L., Abramovich, S., Illner, P., Almogi-Labin, A., Feinstein, S., Berner, Z., et al. (2013). Sea surface temperature record of a Late Cretaceous tropical Southern Tethys upwelling system. *Palaeogeogr. Palaeoclimatol. Palaeoecol.* **392**, 350–358.

Baker, J. D., Polovina, J. J. and Howell, E. A. (2007). Effect of variable oceanic productivity on the survival of an upper trophic predator, the Hawaiian monk seal *Monachus schauinslandi*. *Mar. Ecol. Prog. Ser.* **346**, 277–283.

Bejarano, A. C., Wells, R. S. and Costa, D. P. (2017). Development of a bioenergetic model for estimating energy requirements and prey biomass consumption of the bottlenose dolphin *Tursiops truncatus*. *Ecol. Modell.* **356**, 162–172.

Bengston, J. L. (1983). Estimating Food Consumption of Free-Ranging Manatees in Florida. *J. Wildl. Manage.* **47**, 1186–1192.

Benoit-Bird, K. J. (2004). Prey caloric value and predator energy needs: Foraging predictions for wild spinner dolphins. *Mar. Biol.* **145**, 435–444.

Berman-Kowalewski, M., Gulland, F. M. D., Wilkin, S., Calambokidis, J., Mate, B., Cordaro, J., Rotstein, D., Leger, J. S., Collins, P., Fahy, K., et al. (2010). Association between blue whale (*Balaenoptera musculus*) mortality and ship strikes along the California coast. *Aquat. Mamm.* **36**, 59–66.

Berta, A., Sumich, J. L. and Kovacs, K. M. (2006). *Marine Mammals: Evolutionary Biology*. Second Edi. Burlington, MA: Elsevier Inc.

Best, R. C. (1981). Foods and feeding habits of captive and wild Sirenia. *Mamm. Rev.* **11**, 3–29.

Bidder, O. R., Qasem, L. A. and Wilson, R. P. (2012). On Higher Ground: How Well Can Dynamic Body Acceleration Determine Speed in Variable Terrain? *PLoS One* **7**, e50556.

Bidder, O. R., Goulding, C., Toledo, A., van Walsum, T. A., Siebert, U. and Halsey, L. G. (2017). Does the Treadmill Support Valid Energetics Estimates of Field Locomotion? *Integr. Comp. Biol.* **57**, 301–319.

Bossart, G. D., Meisner, R. a., Rommel, S. a., Lightsey, J. D., Varela, R. a. and Defran, R. H. (2004). Pathologic Findings in Florida Manatees (*Trichechus manatus latirostris*). *Aquat. Mamm.* **30**, 434–440.

Breton-Honeyman, K., Hammill, M. O., Furgal, C. M. and Hickie, B. (2016). Inuit Knowledge of Beluga Whale (*Delphinapterus leucas*) Foraging Ecology in

Nunavik (Arctic Quebec), Canada. *Can. J. Zool.* **94**, 713–726.

Brown, J. H., Gillooly, J. F., Allen, A. P., Savage, V. M. and West, G. B. (2004). Toward a metabolic theory of ecology. *Ecology* **85**, 1771–1789.

Cade, D. E., Barr, K. R., Calambokidis, J., Friedlaender, A. S. and Goldbogen, J. A. (2018). Determining forward speed from accelerometer jiggle in aquatic environments. *J. Exp. Biol.* **221**, jeb170449.

Castellini, M. (2009). Thermoregulation. In *Encyclopedia of marine mammals* (ed. Perrin, W. F., Wursig, B., and Thewissen, J. G. M.), pp. 1166–1171. Elsevier.

Castellini, M. A., Kooyman, G. L. and Ponganis, P. J. (1992). Metabolic Rates of Freely Diving Weddell Seals: Correlations with Oxygen Stores, Swim Velocity and Diving Duration. *J. Exp. Biol.* **165**, 181–194.

Caswell, H., Fujiwara, M. and Braulti, S. (1999). Declining Survival Probability Threatens the North Atlantic Right Whale. *PNAS* **96**, 3308–3313.

Costa, D. P. (1991). Reproductive and foraging energetics of high latitude penguins, albatrosses and pinnipeds: Implications for life history patterns. *Am. Zool.* **31**, 111–130.

Costa, D. P. (2012). A Bioenergetics Approach to Developing a Population Consequences of Acoustic Disturbance Model. In *The effects of noise on aquatic life* (ed. Popper, A. N. and Hawkins, A.), pp. 423–426. New York, NY: Springer.

Costa, D. P. and Kooyman, G. L. (1984). Contribution of Specific Dynamic Action to Heat Balance and Thermoregulation in the Sea Otter *Enhydra lutris*. *Physiol. Zool.* **57**, 199–203.

Costa, D. P. and Maresh, J. L. (2017). Energetics. In *Encyclopedia of Marine Mammals* (ed. Würsig, B., Thewissen, J. G. M., and Kovacs, K.), pp. 329–335. Academic Press.

Costa, D. P., Le Boeuf, B. J., Huntley, A. C. and Ortiz, C. L. (1986). The energetics of lactation in the Northern elephant seal, Mirounga angustirostris. *J. Zool.* **209**, 21–33.

Costa, D. P., Schwarz, L., Robinson, P., Schick, R. S., Morris, P. A., Condit, R., Crocker, D. E. and Kilpatrick, A. M. (2016). A Bioenergetics Approach to Understanding the Population Consequences of Disturbance: Elephant seals as a model system. In *The effects of noise on aquatic life II* (ed. Popper, A. N. and Hawkins, A.), pp. 161–169. New York, NY: Springer.

Davis, R. W. (2014). A review of the multi-level adaptations for maximizing aerobic dive duration in marine mammals: From biochemistry to behavior. *J. Comp. Physiol. B* **184**, 23–53.

Davis, R. W. (2019). *Marine mammals: Adaptations for an aquatic life*. 1st ed. Galveston, TX: Springer Nature Switzerland.

Davis, R. W. and Williams, T. M. (2012). The marine mammal dive response is exercise modulated to maximize aerobic dive duration. *J. Comp. Physiol. A* **198**, 583–591.

Davis, R. W., Williams, T. M. and Kooyman, G. L. (1985). Swimming Metabolism of Yearling and Adult Harbor Seals *Phoca vitulina*. *Physiol. Zool.* **58**, 590–596.

Davis, R. W., Fuiman, L. a., Madden, K. M. and Williams, T. M. (2013). Classification and behavior of free-ranging Weddell seal dives based on three-dimensional movements and video-recorded observations. *Deep Sea Res. Part II Top. Stud. Oceanogr.* **88**–**89**, 65–77.

de Muizon, C. (1982). Phocid phylogeny and dispersal. *Ann. South African Museum* **89**, 175–213.

Doak, D. F., Bakker, V. J., Goldstein, B. E. and Hale, B. (2014). What is the future of conservation? *Trends Ecol. Evol.* **29**, 77–81.

Domning, D. P. (1982). Evolution of Manatees: A Speculative History. *J. Paleontol.* **56**, 599–619.

Fedak, M. A., Rome, L. and Seeherman, H. J. (1981). One-step N2-dilution technique for calibrating open-circuit $V0_2$ measuring systems. *J. Appl. Physiol.* **51**, 772–776.

Feldkamp, S. D. (1987). Swimming in the California sea lion: morphometrics, drag and energetics. *J. Exp. Biol.* **131**, 117–135.

Fish, F. E. (1994). Influence of Hydrodynamic-Design and Propulsive Mode on Mammalian Swimming Energetics. *Aust. J. Zool.* **42**, 79–101.

Fish, F. E. (1996). Transitions from Drag-based to Lift-based Propulsion in Mammalian Swimming. *Am. Zool.* **36**, 628–641.

Fish, F. E. (1998). Comparative kinematics and hydrodynamics of odontocete cetaceans: morphological and ecological correlates with swimming performance. *J. Exp. Biol.* **201**, 2867–2877.

Fish, F. E., Innes, S. and Ronald, K. (1988). Kinematics and estimated thrust production of swimming harp and ringed seals. *J. Exp. Biol.* **137**, 157–173.

Fish, F. E., Howle, L. E. and Murray, M. M. (2008). Hydrodynamic flow control in marine mammals. *Integr. Comp. Biol.* **48**, 788–800.

Fyler, C. A., Reeder, T. W., Berta, A., Antonelis, G., Aguilar, A. and Androukaki, E. (2005). Historical biogeography and phylogeny of monachine seals (Pinnipedia: Phocidae) based on mitochondrial and nuclear DNA data. *J.*

Biogeogr. **32**, 1267–1279.

Gallagher, A. J., Creel, S., Wilson, R. P. and Cooke, S. J. (2017). Energy Landscapes and the Landscape of Fear. *Trends Ecol. Evol.* **32**, 88–96.

Gallivan, G. J. and Best, R. C. (1986). The Influence of Feeding and Fasting on the Metabolic Rate and Ventilation of the Amazonian Manatee (*Trichechus inunguis*). *Physiol. Zool.* **59**, 552–557.

Gallivan, G. J., Best, R. C. and Kanwisher, J. W. (1983). Temperature Regulation in the Amazonian Manatee *Trichechus inunguis*. *Physiol. Zool.* **56**, 255–262.

George, E. M. and Noonan, M. (2014). Respiration rates in captive beluga whales (*Delphinapterus leucas*): Effects of season, sex, age, and body size. *Aquat. Mamm.* **40**, 350–356.

Gillis, G. B. and Blob, R. W. (2001). How muscles accommodate movement in different physical environments: Aquatic vs. terrestrial locomotion in vertebrates. *Comp. Biochem. Physiol. Part A Mol. Integr. Physiol.* **131**, 61–75.

Goetz, K. T., Robinson, P. W., Hobbs, R. C., Laidre, K. L., Hückstädt, L. A. and Shelden, K. E. W. (2012). *Movement and dive behavior of beluga whales in Cook Inlet, Alaska.* AFSC Processed Rep. 2012-03, 40 p. Alaska Fish. Sci. Cent., NOAA, Natl. Mar. Fish. Serv., 7600 Sand Point Way NE, Seattle WA 98115.

Halsey, L. G., Green, J. a, Wilson, R. P. and Frappell, P. B. (2009a). Accelerometry to Estimate Energy Expenditure during Activity: Best Practice with Data Loggers. *Physiol. Biochem. Zool.* **82**, 396–404.

Halsey, L. G., Shepard, E. L. C., Quintana, F., Gomez Laich, A., Green, J. A. and Wilson, R. P. (2009b). The relationship between oxygen consumption and body acceleration in a range of species. *Comp. Biochem. Physiol. A. Mol. Integr. Physiol.* **152**, 197–202.

Halsey, L. G., White, C. R., Enstipp, M. R., Wilson, R. P., Butler, P. J., Martin, G. R., Grémillet, D. and Jones, D. R. (2011a). Assessing the validity of the accelerometry technique for estimating the energy expenditure of diving double-crested cormorants phalacrocorax auritus. *Physiol. Biochem. Zool.* **84**, 230–237.

Halsey, L. G., Shepard, E. L. C. and Wilson, R. P. (2011b). Assessing the development and application of the accelerometry technique for estimating energy expenditure. *Comp. Biochem. Physiol. Part A* **158**, 305–314.

Hays, G. C., Bailey, H., Bograd, S. J., Bowen, W. D., Campagna, C., Carmichael, R. H., Casale, P., Chiaradia, A., Costa, D. P., Cuevas, E., et al. (2019). Translating Marine Animal Tracking Data into Conservation Policy and Management. *Trends Ecol. Evol.* **34**, 459–473.

Hertel, H. (1966). *Structure, form, movement*. New York, NY: Reinhold.

Hill, R. D., Schneider, R. C., Liggins, G. C., Schuette, A. H., Elliott, R. L., Guppy, M., Hochachka, P. W., Qvist, J., Falke, K. J. and Zapol, W. M. (1987). Heart rate and body temperature during free diving of Weddell seals. *Am. J. Physiol. - Regul. Integr. Comp. Physiol.* **253**, 344–351.

Hindle, A. G., Allen, K. N., Batten, A. J., Hückstädt, L. A., Turner-Maier, J., Schulberg, S. A., Johnson, J., Karlsson, E., Lindblad-Toh, K., Costa, D. P., et al. (2019). Low guanylyl cyclase activity in Weddell seals: implications for peripheral vasoconstriction and perfusion of the brain during diving. *Am. J. Physiol. Regul. Integr. Comp. Physiol.* **316**, R704–R715.

Holt, M. M., Noren, D. P., Dunkin, R. C. and Williams, T. M. (2015). Vocal performance affects metabolic rate in dolphins: Implications for animals communicating in noisy environments. *J. Exp. Biol.* **218**, 1647–1654.

Hunt, K. E., Moore, M. J., Rolland, R. M., Kellar, N. M., Hall, A. J., Kershaw, J., Raverty, S. A., Davis, C. E., Yeates, L. C., Fauquier, D. A., et al. (2013). Overcoming the challenges of studying conservation physiology in large whales: a review of available methods. *Conserv. Physiol.* **1**.

Hurley, J. A. and Costa, D. P. (2001). Standard metabolic rate at the surface and during trained submersions in adult California sea lions (*Zalophus californianus*). *J. Exp. Biol.* **204**, 3273–3281.

Innes, H. S. (1984). Swimming energetics, metabolic rates and hind limb muscle anatomy of some phocid seals, *PhD Thesis*, University of Guelph, Guelph, ON.

IUCN (2020). The IUCN Red List of Threatened Species™ . Version 2020-2. *https://www.iucnredlist.org*.

Jeanniard-du-Dot, T., Trites, A. W., Arnould, J. P. Y., Speakman, J. R. and Guinet, C. (2016). Flipper strokes can predict energy expenditure and locomotion costs in free-ranging northern and Antarctic fur seals. *Sci. Rep.* **6**, 33912.

Kaczmarek, J., Reichmuth, C., McDonald, B. I., Kristensen, J. H., Larson, J., Johansson, F., Sullivan, J. L. and Madsen, P. T. (2018). Drivers of the dive response in pinnipeds; apnea, submergence or temperature? *J. Exp. Biol.* **221**, jeb176545.

Kanwisher, J. and Sundnes, G. (1965). Physiology of a small cetacean. *Hvalrad. Skr.* **48**, 45–53.

Kaschner, K., Tittensor, D. P., Ready, J., Gerrodette, T. and Worm, B. (2011). Current and Future Patterns of Global Marine Mammal Biodiversity. *PLoS One* **6**, e19653.

Kasting, N. W., Adderley, S. A. L., Safford, T. and Hewlett, K. G. (1989). Thermoregulation in Beluga (*Delphinapterus leucas*) and Killer (*Orcinus orca*) Whales. *Physiol. Zool.* **62**, 687–701.

Kendall, L. S., Sĭrović, A. and Roth, E. H. (2013). Effects of construction noise on the cook inlet beluga whale (*Delphinapterus leucas*) vocal behavior. *Can. Acoust. - Acoust. Can.* **41**, 3–14.

Kleiber, M. (1975). Metabolic turnover rate: A physiological meaning of the metabolic rate per unit body weight. *J. Theor. Biol.* **53**, 199–204.

Kojeszewski, T. and Fish, F. E. (2007). Swimming kinematics of the Florida manatee (*Trichechus manatus latirostris*): hydrodynamic analysis of an undulatory mammalian swimmer. *J. Exp. Biol.* **210**, 2411–2418.

Kooyman, G. L., Wahrenbrock, E. A., Castellini, M. A., Davis, R. W. and Sinnett, E. E. (1980). Aerobic and Anaerobic Metabolism During Voluntary Diving in Weddell Seals: Evidence of Preferred Pathways from Blood Chemistry and Behavior. *J. Comp. Physiol. B* **138**, 335–346.

Kriete, B. (1995). Bioenergetics in the killer whale, *Orcinus orca*, *PhD Thesis*, University of Brittish Columbia, Vancouver, BC.

Ladds, M. A., Rosen, D. A. S., Slip, D. J. and Harcourt, R. G. (2017). Proxies of energy expenditure for marine mammals: an experimental test of "the time trap." *Sci. Rep.* **7**, 11815.

Laist, D. W., Taylor, C. and Reynolds, J. E. (2013). Winter Habitat Preferences for Florida Manatees and Vulnerability to Cold. *PLoS One* **8**, e58978.

Learmonth, J. A., MacLeod, C. D., Santos, M. B., Pierce, G. J., Crick, H. Q. P. and Robinson, R. A. (2006). Potential effects of climate change on marine mammals. *Oceanogr. Mar. Biol. An Annu. Rev.* **44**, 431–464.

Liao, J. Å. (1990). An investigation of the effect of water temperature on the metabolic rate of the California sea lion *(Zalophus californianus)*, *PhD Thesis,* University of California, Santa Cruz.

Lockyer, C. (2007). All creatures great and smaller: A study in cetacean life history energetics. *J. Mar. Biol. Assoc. United Kingdom* **87**, 1035–1045.

Lotze, H. K., Mills Flemming, J. and Magera, A. M. (2017). Critical factors for the recovery of marine mammals. *Conserv. Biol.* **31**, 1301–1311.

Lovegrove, B. G. (2005). Seasonal thermoregulatory responses in mammals. *J. Comp. Physiol. B Biochem. Syst. Environ. Physiol.* **175**, 231–247.

Maresh, J. L., Simmons, S. E., Crocker, D. E., McDonald, B. I., Williams, T. M. and Costa, D. P. (2014). Free-swimming northern elephant seals have low field

metabolic rates that are sensitive to an increased cost of transport. *J. Exp. Biol.* **217**, 1485–1495.

Maresh, J. L., Adachi, T., Takahashi, A., Naito, Y., Crocker, D. E., Horning, M., Williams, T. M. and Costa, D. P. (2015). Summing the strokes: Energy economy in northern elephant seals during large-scale foraging migrations. *Mov. Ecol.* **3**, 22.

Martin, J., Sabatier, Q., Gowan, T. A., Giraud, C., Gurarie, E., Calleson, C. S., Ortega-Ortiz, J. G., Deutsch, C. J., Rycyk, A. and Koslovsky, S. M. (2016). A quantitative framework for investigating risk of deadly collisions between marine wildlife and boats. *Methods Ecol. Evol.* **7**, 42–50.

McDonald, B. I., Johnson, M. and Madsen, P. T. (2017). Dive heart rate in harbour porpoises is influenced by exercise and expectations. *J. Exp. Biol.* **221**, jeb168740.

McHuron, E. A., Costa, D. P., Schwarz, L. and Mangel, M. (2017). State-dependent behavioural theory for assessing the fitness consequences of anthropogenic disturbance on capital and income breeders. *Methods Ecol. Evol.* **8**, 552–560.

McHuron, E. A., Peterson, S. H., Hückstädt, L. A., Melin, S. R., Harris, J. D. and Costa, D. P. (2018). The energetic consequences of behavioral variation in a marine carnivore. *Ecol. Evol.* **8**, 4340–4351.

Merchant, N. D., Pirotta, E., Barton, T. R. and Thompson, P. M. (2014). Monitoring ship noise to assess the impact of coastal developments on marine mammals. *Mar. Pollut. Bull.* **78**, 85–95.

Miedler, S., Fahlman, A., Torres, M. V., Álvarez, T. Á. and Garcia-Parraga, D. (2015). Evaluating cardiac physiology through echocardiography in bottlenose dolphins: Using stroke volume and cardiac output to estimate systolic left ventricular function during rest and following exercise. *J. Exp. Biol.* **218**, 3604–3610.

Nagy, K. A. (2001). Food requirements of wild animals: predictive equations for free-living mammals, reptiles, and birds. *Nutr. Abstr. Rev. Ser. B* **71**, 21R-31R.

Nagy, K. A., Girard, I. A. and Brown, T. K. (1999). Energetics of Free-Ranging Mammals, Reptiles, and Birds. *Annu. Rev. Nutr.* **19**, 247–277.

New, L. F., Moretti, D. J., Hooker, S. K., Costa, D. P. and Simmons, S. E. (2013a). Using Energetic Models to Investigate the Survival and Reproduction of Beaked Whales (family Ziphiidae). *PLoS One* **8**, e68725.

New, L. F., Harwood, J., Thomas, L., Donovan, C., Clark, J. S., Hastie, G., Thompson, P. M., Cheney, B., Scott-Hayward, L. and Lusseau, D. (2013b).

Modelling the biological significance of behavioural change in coastal bottlenose dolphins in response to disturbance. *Funct. Ecol.* **27**, 314–322.

NMFS (2016). *Recovery Plan for the Cook Inlet Beluga Whale (Delphinapterus leucas)*. National Marine Fisheries Service, Alaska Region, Protected Resources Division, Juneau, AK.

Noren, D. P. (2010). Estimated field metabolic rates and prey requirements of resident killer whales. *Mar. Mammal Sci.* **27**, 60–77.

Noren, D. P., Williams, T. M., Berry, P. and Butler, E. (1999). Thermoregulation during swimming and diving in bottlenose dolphins, *Tursiops truncatus*. *J. Comp. Physiol. B* **169**, 93–99.

Noren, S. R., Williams, T. M., Pabst, D. A., McLellan, W. A. and Dearolf, J. L. (2001). The development of diving in marine endotherms: Preparing the skeletal muscles of dolphins, penguins, and seals for activity during submergence. *J. Comp. Physiol. B* **171**, 127–134.

Nowacek, S. M., Wells, R. S., Owen, E. C. G., Speakman, T. R., Flamm, R. O. and Nowacek, D. P. (2004). Florida manatees, *Trichechus manatus latirostris*, respond to approaching vessels. *Biol. Conserv.* **119**, 517–523.

Ortiz, R. M., Worthy, G. A. J. and Byers, F. M. (1999). Estimation of water turnover rates of captive West Indian manatees (*Trichechus manatus*) held in fresh and salt water. *J. Exp. Biol.* **202**, 33–38.

Otani, S., Naito, Y., Kato, A. and Kawamura, A. (2001). Oxygen consumption and swim speed of the harbor porpoise *Phocoena phocoena*. *Fish. Sci.* **67**, 894–898.

Pabst, D. A., McLellan, W. A., Meagher, E. M. and Westgate, A. J. (2002). *Measuring Temperatures and Heat Flux from Dolphins in the Eastern Tropical Pacific : Is Thermal Stress Associated With Chase and Capture in the ETP-Tuna Purse Seine Fishery?* Final Report on the Chase Encirclement Stress Study, CIE-S04 to the US National Marine Fisheries Service, La Jolla, CA, USA (2002).

Pagano, A. M. and Williams, T. M. (2019). Estimating the energy expenditure of free-ranging polar bears using tri-axial accelerometers: A validation with doubly labeled water. *Ecol. Evol.* **9**, 4210–4219.

Pagano, A. M., Durner, G. M., Rode, K. D., Atwood, T. C., Atkinson, S. N., Peacock, E., Costa, D. P., Owen, M. A. and Williams, T. M. (2018). High-energy, high-fat lifestyle challenges an Arctic apex predator, the polar bear. *Science.* **359**, 568–572.

Parrish, F. A., Marshall, G. J., Littnan, C. L., Heithaus, M., Canja, S., Becker, B., Braun, R. and Antonelis, G. A. (2005). Foraging of juvenile monk seals at French Frigate Shoals, Hawaii. *Mar. Mammal Sci.* **21**, 93–107.

Peddemors, V. M. (1990). Respiratory development in a captive-born bottlenose dolphin *Tursiops truncatus* calf. *South African J. Zool.* **25**, 178–184.

Pirotta, E., Booth, C. G., Costa, D. P., Fleishman, E., Kraus, S. D., Lusseau, D., Moretti, D., New, L. F., Schick, R. S., Schwarz, L. K., et al. (2018a). Understanding the population consequences of disturbance. *Ecol. Evol.* **8**, 9934–9946.

Pirotta, E., Mangel, M., Costa, D. P., Mate, B., Goldbogen, J. A., Palacios, D. M., Hückstädt, L. A., McHuron, E. A., Schwarz, L. and New, L. (2018b). A Dynamic State Model of Migratory Behavior and Physiology to Assess the Consequences of Environmental Variation and Anthropogenic Disturbance on Marine Vertebrates. *Am. Nat.* **191**, E40–E56.

Pirotta, E., Mangel, M., Costa, D. P., Goldbogen, J., Harwood, J., Hin, V., Irvine, L. M., Mate, B. R., McHuron, E. A., Palacios, D. M., et al. (2019). Anthropogenic disturbance in a changing environment: modelling lifetime reproductive success to predict the consequences of multiple stressors on a migratory population. *Oikos* **128**, 1340–1357.

Pompa, S., Ehrlich, P. R. and Ceballos, G. (2011). Global distribution and conservation of marine mammals. *Proc. Natl. Acad. Sci.* **108**, 13600–13605.

Ponganis, P. J. (2015). *Diving physiology of marine mammals and seabirds*. 1st ed. Cambridge, United Kingdom: Cambridge University Press.

Qasem, L., Cardew, A., Wilson, A., Griffiths, I., Halsey, L. G., Shepard, E. L. C., Gleiss, A. C. and Wilson, R. (2012). Tri-Axial Dynamic Acceleration as a Proxy for Animal Energy Expenditure; Should We Be Summing Values or Calculating the Vector? *PLoS One* **7**, e31187.

Rea, L. D. and Costa, D. P. (1992). Changes in Standard Metabolism during Long-Term Fasting in Northern Elephant Seal Pups (*Mirounga angustirostris*). *Physiol. Zool.* **65**, 97–111.

Rechsteiner, E. U., Rosen, D. A. S. and Trites, A. W. (2013). Seasonal resting metabolic rate and food intake of captive Pacific white-sided dolphins (*Lagenorhynchus obliquidens*). *Aquat. Mamm.* **39**, 241–252.

Reynolds, J. E. (1981). Behavior patterns in the West Indian manatee, with emphasis on feeding and diving. *Florida Sci.* **44**, 233–242.

Richard, P. R., Heide-Jørgensen, M. P. and Aubin, D. S. (1998). Fall movements of belugas (Delphinapterus leucas) with satellite-linked transmitters in Lancaster sound, Jones Sound, and Northern Baffin Bay. *Arctic* **51**, 5–16.

Rojano-Doñate, L., McDonald, B. I., Wisniewska, D. M., Johnson, M., Teilmann, J., Wahlberg, M., Hojer-Kristensen, J. and Madsen, P. T. (2018). High field

metabolic rates of wild harbour porpoises. *J. Exp. Biol.* **221**, jeb185827.

Roos, M. M. H., Wu, G.-M. and Miller, P. J. O. (2016). The significance of respiration timing in the energetics estimates of free-ranging killer whales (*Orcinus orca*). *J. Exp. Biol.* **219**, 2066–2077.

Rosen, D. A. S. and Trites, A. W. (1999). Metabolic effects of low-energy diet on Steller sea lions, *Eumetopias jubatus*. *Physiol. Biochem. Zool.* **72**, 723–731.

Rosen, D. A. S. and Trites, A. W. (2013). Resting Metabolic Rate of a Mature Male Beluga Whale (*Delphinapterus leucas*). *Aquat. Mamm.* **39**, 85–88.

Rosen, D. A. S., Winship, A. J. and Hoopes, L. A. (2007). Thermal and digestive constraints to foraging behaviour in marine mammals. *Philos. Trans. R. Soc. B* **362**, 2151–2168.

Scheel, D.-M., Slater, G. J., Kolokotronis, S. O., Potter, C. W., Rotstein, D. S., Tsangaras, K., Greenwood, A. D. and Helgen, K. M. (2014). Biogeography and taxonomy of extinct and endangered monk seals illuminated by ancient DNA and skull morphology. *Zookeys* **409**, 1–33.

Scheffer, V. B. (1972). The Weight of the Steller Sea Cow. *J. Mammal.* **53**, 912–914.

Schmidt-Nielsen, K. (1984). *Scaling: why is animal size so important?* Cambridge, UK: Cambridge University Press.

Scholander, P. F., Hock, R., Walters, V. and Irving, L. (1950). Adaptation to cold in arctic and tropical mammals and birds in relation to body temperature, insulation, and basal metabolic rate. *Biol. Bull.* **99**, 259–271.

Shaffer, S. A., Costa, D. P., Williams, T. M. and Ridgway, S. H. (1997). Diving and swimming performance of white whales, Delphinapterus leucas: an assessment of plasma lactate and blood gas levels and respiratory rates. *J. Exp. Biol.* **200**, 3091–3099.

Shepard, E. L. C., Wilson, R. P., Rees, W. G., Grundy, E., Lambertucci, S. A. and Vosper, S. B. (2013). Energy Landscapes Shape Animal Movement Ecology. *Am. Nat.* **182**, 298–312.

Somo, D. A., Ensminger, D. C., Sharick, J. T., Kanatous, S. B. and Crocker, D. E. (2015). Development of Dive Capacity in Northern Elephant Seals (*Mirounga angustirostris*): Reduced Body Reserves at Weaning Are Associated with Elevated Body Oxygen Stores during the Postweaning Fast. *Physiol. Biochem. Zool.* **88**, 471–482.

Speakman, J. (1997). Factors influencing the daily energy expenditure of small mammals. *Proc. Nutr. Soc.* **56**, 1119–1136.

Thometz, N. M., Kendall, T. L., Richter, B. P. and Williams, T. M. (2015).

Physiological capacity for diving in the critically endangered Hawaiian monk seal. In *The Society for Integrative & Comparative Biology*, p. 323. West Palm Beach, FL.

Tittensor, D. P., Mora, C., Jetz, W., Lotze, H. K., Ricard, D., Berghe, E. Vanden and Worm, B. (2010). Global patterns and predictors of marine biodiversity across taxa. *Nature* **466**, 1098–1101.

Tyack, P. L. (2008). Implications for marine mammals of large-scale changes in the marine acoustic environment. *J. Mammal.* **89**, 549–558.

Villegas-Amtmann, S., Schwarz, L. K., Sumich, J. L. and Costa, D. P. (2015). A bioenergetics model to evaluate demographic consequences of disturbance in marine mammals applied to gray whales. *Ecosphere* **6**, 183.

Volpov, B. L., Rosen, D. A. S., Trites, A. W. and Arnould, J. P. Y. (2015). Validating the relationship between 3-dimensional body acceleration and oxygen consumption in trained Steller sea lions. *J. Comp. Physiol. B* **185**, 695–708.

Wells, R. S. and Scott, M. D. (1997). Seasonal incidence of boat strikes on bottlenose dolphins near Sarasota, Florida. *Mar. Mammal Sci.* **13**, 475–480.

Whittow, G. C. (1987). Thermoregulatory Adaptations in Marine Mammals: Interacting Effects of Exercise and Body Mass. A Review. *Mar. Mammal Sci.* **3**, 220–241.

Wikelski, M. and Cooke, S. J. (2006). Conservation physiology. *Trends Ecol. Evol.* **21**, 38–46.

Williams, T. M. (1989). Swimming by sea otters: adaptations for low energetic cost locomotion. *J. Comp. Physiol. A* **164**, 815–824.

Williams, T. M. (1999). The Evolution of Cost Efficient Swimming in Marine Mammals: Limits to Energetic Optimization. *Philos. Trans. Biol. Sci.* **354**, 193–201.

Williams, T. M., Noren, D., Berry, P., Estes, J. A., Allison, C. and Kirtland, J. (1999a). The diving physiology of bottlenose dolphins (*Tursiops truncatus*) III. Thermoregulation at depth. *J. Exp. Biol.* **202**, 2763–2769.

Williams, T. M., Haun, J. E. and Friedl, W. A. (1999b). The Diving Physiology of Bottlenose Dolphins (*Tursiops Truncatus*), I. Balancing the demands of exercise for energy conservation at depth. *J. Exp. Biol.* **202**, 2739–2748.

Williams, T. M., Haun, J., Davis, R. W., Fuiman, L. A. and Kohin, S. (2001). A killer appetite: Metabolic consequences of carnivory in marine mammals. *Comp. Biochem. Physiol. Part A Mol. Integr. Physiol.* **129**, 785–796.

Williams, T. M., Estes, J. A., Doak, D. F. and Springer, A. M. (2004a). Killer

Appetites : Assessing the Role of Predators in Ecological Communities. *Ecology* **85**, 3373–3384.

Williams, T. M., Fuiman, L. A., Horning, M. and Davis, R. W. (2004b). The cost of foraging by a marine predator, the Weddell seal *Leptonychotes weddellii*: pricing by the stroke. *J. Exp. Biol.* **207**, 973–982.

Williams, R., Lusseau, D. and Hammond, P. S. (2006). Estimating relative energetic costs of human disturbance to killer whales (*Orcinus orca*). *Biol. Conserv.* **133**, 301–311.

Williams, T. M., Richter, B., Kendall, T. and Dunkin, R. (2011a). Metabolic Demands of a Tropical Marine Carnivore, the Hawaiian Monk Seal (*Monachus schauinslandi*): Implications for Fisheries Competition. *Aquat. Mamm.* **37**, 372–376.

Williams, T. M., Noren, S. R. and Glenn, M. (2011b). Extreme physiological adaptations as predictors of climate-change sensitivity in the narwhal, *Monodon monoceros*. *Mar. Mammal Sci.* **27**, 334–349.

Williams, R., Ashe, E., Blight, L., Jasny, M. and Nowlan, L. (2014). Marine mammals and ocean noise: Future directions and information needs with respect to science, policy and law in Canada. *Mar. Pollut. Bull.* **86**, 29–38.

Williams, T. M., Fuiman, L. A. and Davis, R. W. (2015). Locomotion and the Cost of Hunting in Large, Stealthy Marine Carnivores. *Integr. Comp. Biol.* **55**, 673–682.

Williams, T. M., Blackwell, S. B., Richter, B., Sinding, M.-H. S. and Heide-Jørgensen, M. P. (2017a). Paradoxical escape responses by narwhals (*Monodon monoceros*). *Science.* **358**, 1328–1331.

Williams, T. M., Kendall, T. L., Richter, B. P., Ribeiro-French, C. R., John, J. S., Odell, K. L., Losch, B. A., Feuerbach, D. A. and Stamper, M. A. (2017b). Swimming and Diving Energetics in Dolphins: A stroke-by-stroke analysis for predicting the cost of flight responses in wild odontocetes. *J. Exp. Biol.* **220**, 1135–1145.

Wilson, R. P., White, C. R., Quintana, F., Halsey, L. G., Liebsch, N., Martin, G. R. and Butler, P. J. (2006). Moving towards acceleration for estimates of activity-specific metabolic rate in free-living animals: The case of the cormorant. *J. Anim. Ecol.* **75**, 1081–1090.

Wilson, R. P., Griffiths, I. W., Legg, P. A., Friswell, M. I., Bidder, O. R., Halsey, L. G., Lambertucci, S. A. and Shepard, E. L. C. (2013a). Turn costs change the value of animal search paths. *Ecol. Lett.* **16**, 1145–1150.

Wilson, J. W., Mills, M. G., Wilson, R. P., Peters, G., Mills, M. E. J., Speakman,

J. R., Durant, S. M., Bennett, N. C., Marks, N. J. and Scantlebury, M. (2013b). Cheetahs, *Acinonyx jubatus*, balance turn capacity with pace when chasing prey. *Biol. Lett.* **9**, 20130620.

Wilson, K., Littnan, C., Halpin, P. and Read, A. (2017). Integrating Multiple Technologies to Understand the Foraging Behavior of Hawaiian monk seals. *R. Soc. Open Sci.* **4**, 160703.

Wilson, R. P., Börger, L., Holton, M. D., Scantlebury, D. M., Gómez-Laich, A., Quintana, F., Rosell, F., Graf, P. M., Williams, H., Gunner, R., et al. (2019). Estimates for energy expenditure in free-living animals using acceleration proxies: A reappraisal. *J. Anim. Ecol.* **89**, 161–172.

Withers, P. C. (1977). Measurement of VO_2, VCO_2, and evaporative water loss with a flow through mask. *J. Appl. Physiol.* **42**, 120–123.

Worthy, G. A. J., Innes, S., Braune, B. M. and Stewart, R. E. A. (1987). Rapid acclimation of cetaceans to an open-system respirometer. *Approaches to Mar. mammal Energ.* **1**, 115–126.

Worthy, G. A. J., Worthy, T. A. M., Yochem, P. K. and Dold, C. (2014). Basal metabolism of an adult male killer whale (*Orcinus orca*). *Mar. Mammal Sci.* **30**, 1229–1237.

Wright, A. J., Deak, T. and Parsons, E. C. M. (2011). Size matters: Management of stress responses and chronic stress in beaked whales and other marine mammals may require larger exclusion zones. *Mar. Pollut. Bull.* **63**, 5–9.

Yazdi, P., Kilian, A. and MCulik, B. M. (1999). Energy expenditure of swimming bottlenose dolphins (*Tursiops truncatus*). *Mar. Biol.* **134**, 601–607.

Yoda, K., Sato, K., Niizuma, Y., Kurita, M., Bost, C. A., Le Maho, Y. and Naito, Y. (1999). Precise monitoring of porpoising behaviour of Adelie penguins determined using acceleration data loggers. *J. Exp. Biol.* **202**, 3121–3126.

Yoda, K., Naito, Y., Sato, K., Takahashi, A., Nishikawa, J., Ropert-Coudert, Y., Kurita, M. and Le Maho, Y. (2001). A new technique for monitoring the behaviour of free-ranging Adélie penguins. *J. Exp. Biol.* **204**, 685–690.

Zapol, W. M., Liggins, G. C., Schneider, R. C., Qvist, J., Snider, M. T., Creasy, R. K. and Hochachka, P. W. (1979). Regional blood flow during simulated diving in the conscious Weddell seal. *J. Appl. Physiol.* **47**, 968–973.